DRAFT 16 February 1988 CDF/CALORIMETRY/DOC/PUBLIC/502*

Phototube Testing for CDF

by

T. Devlin, J. Cruz,[a] U. Joshi, K. Kazlauskis,

C. Muehleisen, T.-S. Yang[c]

Department of Physics and Astronomy, Rutgers - The State University

P. O. Box 849, Piscataway, New Jersey 08855-0849

J. Elias, H. Jensen,

Fermilab, P. O. Box 500, Batavia, Illinois 60510

L. Nodulman

Argonne National Laboratory, Argonne, Illinois 60431

ABSTRACT

Photomultiplier tubes for the Collider Detector at Fermilab were subjected to pre-installation testing for stability, linearity and other properties. This report is an archival description of the apparatus which provided computer control of light sources, monitoring of environmental conditions and data logging of responses from up to 48 photomultiplier simultaneously. Statistical summaries of the test results are included for 1041 tubes for the central electro-magnetic calorimeter and 687 tubes for the endwall hadron calorimeter.

*abstract for distribution; full document may be seen or copied on request

Phototube Testing for CDF

by

T. Devlin, J. Cruz,[a] U. Joshi, K. Kazlauskis,
C. Muehleisen, T.-S. Yang[c]
Department of Physics and Astronomy, Rutgers - The State University
P. O. Box 849, Piscataway, New Jersey 08855-0849

J. Elias, H. Jensen,
Fermilab, P. O. Box 500, Batavia, Illinois 60510

L. Nodulman
Argonne National Laboratory, Argonne, Illinois 60431

ABSTRACT

Photomultiplier tubes for the Collider Detector at Fermilab were subjected to pre-installation testing for stability, linearity and other properties. This report is an archival description of the apparatus which provided computer control of light sources, monitoring of environmental conditions and data logging of responses from up to 48 photomultiplier simultaneously. Statistical summaries of the test results are included for 1041 tubes for the central electro-magnetic calorimeter and 687 tubes for the endwall hadron calorimeter.

OUTLINE

I. INTRODUCTION

The central electromagnetic calorimeter system for the Collider Detector at Fermilab was designed to detect and measure the energy of photons, electrons and positrons emerging from proton-antiproton collisions at 2 TeV. The system, described in detail elsewhere [1], consists of 480 towers surrounding the intersection region in a projective geometry. Each tower consists of 30 layers of 0.32-cm-thick lead and 31 layers of 0.50-cm-thick scintillation plastic, a total of 18 radiation lengths. Light from the scintillators is brought out each end by Y7 doped UVA acrylic wavelength shifters (wavebars) to two photomultiplier tubes (PMT's) per tower.

This system has an energy resolution $\Delta E/E = 14\%/\sqrt{E}$, where the energy, E, is expressed in GeV. Since interesting physics is expected in the region where E is 100 GeV or more, it is necessary for this system to operate at a level of 1% accuracy. The problems of calibration, stability, linearity and uniformity are formidable.

To minimize potential problems, the phototubes and bases in this system were subjected to extensive pre-installation testing to ensure that each of them met specifications, to establish operating characteristics and to exercise each for approximately one week to monitor stability and detect early failures.

A total of 1041 tubes (Hamamatsu Model R580B) and bases were tested for the central EM calorimeter. In addition, another 687 tubes (Thorn-EMI Model 9902KB06) and bases for the end wall hadron calorimeter [2] were subjected to similar, but briefer tests in the same apparatus.

This paper is intended as an archival description of the apparatus and procedures used for these tests and summarizes the results. It is not intended for general distribution.

A shorter version of this report has been published.[3]

II. PHOTOTUBE SPECIFICATIONS FOR CENTRAL ELECTROMAGNETIC CALORIMETER

The apparatus used in this work was designed to test most of the specifications in the Request for Quotation (RFQ) for the Central EM phototube. The specifications were:

1. Geometry: head-on, ≈1.5-inch ceramic based, consistent with Phillips XP2012B or Hammamatsu R580. See Fig. 2.1.
2. Gain/Operating Voltage: The tube should operate at a current gain of 4×10^5. The required high voltage to obtain this gain should be within ±100 V of the average voltage.
3. Quantum Efficiency: the tubes will be viewing the spectrum shown in Fig. 2.2. A QE averaged over this spectrum must be at least 8% or at least 75% of the QE of the average tube provided, whichever is greater.
4. Dark current: less than 5 nA at a current gain of 4×10^5.
5. Linearity: for a triangular pulse of base 60 ns, the tube must be linear within ±1% up to a peak current of 40 mA.
6. Stability: for fixed high voltage and temperature, the gain times QE, after burn-in at 5 μA for 40 hours, must be stable to less than 1.5% for an average anode current of 2 μA over a period of 100 hours. In addition, the gain should be stable to within ±2% over 1000 hours at an average anode current of 50 nA.
7. Rate effects: The change in gain resulting from changing average anode current between 50 nA and 2 μA must be less than 5%.

8. Pulse recovery: the tube current gain must recover to within 2% of its previous value within 1 ms after a full scale pulse (40 mA peak).
9. Temperature Dependence: The absolute gains times QE of the tubes must change by no more than 0.5%/^{o}C.
10. Useful lifetime: the tubes should be expected to remain within specifications for 50,000 hours of operation at an average anode current of 30 nA. For purposes of testing, a subset of tubes will be subjected to 5 μA average anode current for 300 hours, and 90% of the tested tubes must pass this test.

For each tube, the manufacturer was required to provide measurements of the high voltage, pulse height resolution and dark current at a current gain of $4X10^{5}$ and the QE.

The geometry (Spec 1) was trivially satisfied by the R580B. The measurement of absolute QE is fairly difficult, and it was decided to accept the manufacturer's data for Spec 3. (Our tests yield a relative QE for our light sources which correlates fairly well with the manufacturer's data.) Specs 8 and 10 were tested for a subsample of tubes.

The remaining Specs (2, 4-7, 9) were tested for every tube with some variation from the original RFQ specs as described in the following sections.

III. APPARATUS AND PROCEDURES

A. Test Overview

The basic requirements for the Central EM testing program dictated 40 hours of burn-in and 100 hours of stability/linearity testing at GQE = $1.2X0^4$. To this, we added 20 hours of stability/linearity testing at GQE = $2.4X10^4$. There were 1100 tubes to be tested in a period of approximately one year. This clearly required computer-controlled test procedures and data acquisition for many tubes simultaneously.

The overall structure of the testing program is displayed in Fig. 3.1. Upon receipt of tubes from the manufacturer in monthly batches of 100, some preliminary, semi-automated tests, requiring roughly 15 minutes per tube were performed in a small, single-tube test chamber. At this point, the data base for a group of forty tubes plus eight controls was started with the manufacturer's data and the small-chamber tests results. The main test facility described below was capable of handling a total of 48 tubes. The first half-hour of testing required some operator intervention, but thereafter the conduct of the tests and data logging was fully automatic.

B. Small Test Chamber

The initial testing was performed in a small, single-tube chamber. The objectives of this testing were to establish operating voltages at each of three gain settings, and to measure dark current.

Figure 3.2 shows this apparatus schematically. The light-tight test chamber contained a single LED and a sleeve-and-stop assembly which guided

each PMT photocathode into a fixed position relative to the LED. An S-100 based, Z80 microcomputer (μC) provided operator guidance through various steps in the test and logged the results on floppy disks for use in subsequent tests and the PMT database. The μC was equipped with an interface to a CAMAC crate where the analog-to-digital converter (ADC) and some control circuitry were located.

Clock-driven NIM logic modules provided pulses with fixed charge to drive the LED, and a gate signal for the ADC. The output of the PMT could be plugged into the ADC for pulse-height measurements, or into a pico-ammeter for dark current measurements.

The voltage for each tube was manually adjusted to yield a standard pulse response to the test chamber LED. The amplitude was chosen in the following manner. The earliest tubes delivered were measured by the manufacturer to have QE's from 8% to 16% with an average of 12%. The voltage dependence of the absolute current gain of a number of these was established by the method described below. These tubes were used to measure the brightness of the LED in the small chamber, i.e. the number of photons hitting the photocathode in a fixed position relative to the LED. Thereafter, the voltage for every tube was adjusted to give a fixed pulse height corresponding to a GQE product of 1.2×10^4, i.e. a gain of 10^5 for a QE of 12%. Two other voltage settings were also determined for GQE's of 2.4×10^4 and 4.8×10^4.

The first step in testing a batch of 48 PMT's was to initialize a data file with the properties of the eight control PMT's which were retained as part of every batch. Then individual PMT's were subjected to the following procedures in the small chamber until 40 had successfully passed the preliminary tests. The procedures were:

1. Fit the tube with a base. (See Ref. [4] and Appendix A.)
2. Enter into the μC the PMT identification number, QE, and other data supplied by the manufacturer;
3. Adjust PMT voltage to produce the pulse height corresponding to GQE = 1.2×10^4. The μC program provided guidance for the operator by extrapolations based on the voltage and pulse height readings;
4. Measure and record the dark current at the resulting voltage setting;
5. Repeat steps 3 and 4 for GQE = 2.4×10^4 and 4.8×10^4.
6. If the tube-base combination met specifications, label the base with the tube ID number to make the combination permanent.
7. If the tube-base combination failed to meet specifications, repeat the tests with each in other tube-base combinations before rejecting either.

C. Large Test Chambers

A diagram of the major features of the main test facility is given in Fig. 3.3. A second Z80 μC in an S-100 bus system was used as a front end controller interfaced to CAMAC. It was connected by an asynchronous line to a VAX 780 for data logging. The Z80 controlled the sequence of DC and pulsed light source tests, and the PMT high voltage. It recorded data from the ADC's which read pulsed response of the tubes, anode currents, power supply voltages and temperatures. The two test chambers described below were capable of handling a combined total of 48 tubes, 40 under test and 8 long term controls. We followed a weekly cycle of 160 hours testing plus 8 hours for exchanging tubes for the next cycle. Various features of the apparatus and procedures are listed below.

1. Test Duration

-- 40 hours burn-in at a typical anode current of 5 μA

-- 100 hours stability/linearity testing at GQE = 1.2×10^4

-- 10 to 20 hours stability/linearity testing at GQE = 2.4×10^4

2. Test Chamber

The principal geometric features of the test chambers are shown in Fig. 3.4. Two such chambers were built. Twenty-four tubes under test are supported in a 5X5 lattice (central position empty). Each position in the lattice contained a magnetic shield, plastic leaf springs and a stop to position the photocathode in a reproducible fashion.

The main bank of light sources for light levels 1 - 5 (see below) was located on the wall of the chamber 70 cm from the photocathodes. The sources were mounted on four identical printed circuit boards placed symmetrically on that wall to smooth the illumination profile at the bank of photocathodes. Each individual phototube was illuminated by four additional LED's placed on the support lattice approximately 3 cm from each photocathode to provide high amplitude pulsed signals.

A light map (Fig. 3.5) of illumination of the photocathode positions for one of the test chambers was measured with light level 5, which provided about 3000 photoelectrons (pe^-) at the center of the photocathode lattice. One position in one chamber received 54% of the peak illumination and all others received 70% or more. A "bootstrap calculation based on the main test data yielded similar results.

3. Pulsed Light Sources

The test objectives required a dynamic range from ~30 to ~80,000 pe^- pulses for each of 24 tubes in each of two test chambers. This was achieved with an array of pulsed green LED's (wavelength = 560 nm) organized into nine groups, each with a fixed illumination levels as indicated in Table 3.1. The control circuitry for the LED's is given in Appendix A. The LED's were flashed at a rate of ~10 Hz which never varied during a test, even during the "off" condition for a particular level. "On" and "off" states were achieved by phase selection, i.e. changing the timing of the pulse by ~2 μsec relative to the ADC gate as shown in Fig. 3.6. This was done to maintain maintain short term stability.

Green LED's have a fairly slow response. The typical pulse was only roughly triangular and had a width of ~150 ns at 10% of full amplitude. Thus, the width and peak pulse amplitude of Specification 5 were not achieved. The maximum amplitude with combined light levels 6 through 9 was typically 20 to 25 mA.

Early tests of the light sources showed crosstalk among the nine levels. The light output for a given level was not independent of which other levels were "on" or "off". This crosstalk was eliminated by providing unregulated DC power to the circuit board and using an independent regulator for the drivers for each light level.

4. Steady Light Sources

Small tungsten filament lamps driven by digital-to-analog converters (DAC's) were used as variable-intensity steady light sources to produce anode

currents ranging from 20 nA to 5 μA. The driver circuit and a typical intensity curve are shown in Fig. 3.7. These sources were not intended for precise illumination or good time response.

Sixteen LED's driven by a μC-controlled TTL logic level were used as a step-function source which could be rapidly switched from off to a steady level of ~100 nA.

5. Analog-to-Digital Converters for Pulsed Signals

The ADC used for pulse height measurements was the LeCroy 2285A, a 15-bit ADC with a least count of about 0.03 pC, corresponding to 1 pe^- and a full range of >20,000 pe^-. This covered the operating range expected in the detector, 0.032 pC to 640 pC at a gain of $2X10^5$. The tests at ~25 mA peak pulsed current corresponded to a full range of ~2000 pC, and were done with a X5 attenuator at the ADC input.

Two calibration methods were used to determine the counts/picocoulomb for each of the 48 channels in the ADC system. One is described in the 2285 operating manual. An example is shown in Fig. 3.8. The other was to provide a NIM logic pulse of known charge (957 pC) at the input. Both methods agreed at the 1% level, and the first showed a linearity of better than 1%. The typical response was 28 counts/pC.

6. Gain Estimates and Photoelectron Statistics

The absolute gain for pulsed signals in each phototube is the ratio of the charge collected at the anode to the charge created at the photocathode. The anode charge was measured by the absolute calibration of the ADC's described briefly above. At our gain settings, roughly two photoelectrons

yield an anode output corresponding to a single ADC count. Thus, gain estimates based on single pe^- pulse-height measurements were impractical. Instead, the cathode charge was determined from the statistical width of the pulse-height distribution.

We expect the mean, H, and standard deviation, σ, of a pulse height distribution to be related to the number of pe^-, P, as follows:

$$\left[\frac{\sigma}{H}\right]^2 = \frac{1}{P} + b \qquad (4.2)$$

where the first term, 1/P, accounts for pe^- statistics, and b represents non-statistical contributions to the width of the pulse-height distribution. A test of this relationship was performed with a fixed phototube and light source combination by imposing a series of neutral-density filters between them to vary the number of pe^-. This provided a series of measurements with $P_i = f_i P_o$ where f_i (i = 1,4) are the known attenuation factors and P_o is the (unknown) number of photoelectrons in the absence of any filter. The results, plotted in Fig. 3.9, indicate that $b \approx 10^{-5}$ or less. Since gain measurements discussed below are based on pulsed light levels yielding no more than 20,000 pe^- ($1/P > 5 \times 10^{-5}$), the procedure can be valid at the 20% level or better for a stable system.

Any small, time-dependent drifts in gain or pulsed-light-source intensity during the measurement of a pulse-height distribution will cause errors in one direction only. They broaden the distribution and make σ larger, P smaller, and the gain larger. For this reason, data sets for this purpose were collected in less than five minutes, and were repeated many times and averaged to minimize the effects of drifts. Our experience with the full body of test

data tended to support the validity of this procedure. However two successive runs of the test chambers (out of thirty), while satisfactory in all other respects, show spuriously large gains for all tubes including the controls. These are omitted from any distributions in the following sections which involve this calculation.

7. Relative Quantum Efficiency Measurement

Since the absolute number of photons incident on the photocathodes was unknown, we were unable to measure the absolute quantum efficiency of the tubes under test, but values relative to the sample average were calculable, and correlations between this and the manufacturer's value were made. The procedure consisted in correcting the pulse height for the "light map", the relative light intensity at each position or "slot" in the test chambers, and for time dependent drifts in light intensity. The latter is expressed in terms of the batch numbers accumulated over more than a year. (We discuss this in terms of the Central EM testing; an identical, independent analysis was made for the Endwall Hadron tests.) The pulse height (in pC) for any tube can be expressed as:

$$H_{ij} = e\, Q_{ij}\, G_{ij}\, L_{ij} ,$$

where i=1,30 is the batch number, j=1,48 is the slot, Q_{ij} is the quantum efficiency, G_{ij} is the gain, L_{ij} is the number of incident photons per pulse, e is 1.6×10^{-7} pC. The number of photo-electrons, P_{ij}, can be calculated as described in the previous section, and is expressed

$$P_{ij} = Q_{ij} L_{ij} .$$

The gain is:

$$G_{ij} = H_{ij}/(e P_{ij}) .$$

For each of these quantities, it is convenient to form averages over batches or slots. Our notations are illustrated by the examples: $\langle H_{ij} \rangle_i = H_{0j}$ for the pulse height in the j^{th} slot averaged over all batches, or $\langle P_{ij} \rangle_j = P_{i0}$ for the i^{th} batch averaged over all slots. Normalizing to these averages cancels fixed, uninteresting quantities and isolates relative variations with position and time.

The product, $G_{ij}Q_{ij}$, should be the same for all tubes because the voltage setting was chosen to yield a fixed pulse height in the small-box tests. This assumption is most reliable from slot-to-slot within a given batch since all tubes in a given batch passed through the small-box tests in a short interval over which drifts were unlikely. Any time dependent drift in this product (other than for controls) reveals a drift in the small-box light source. No significant drift was observed.

Our goal is to isolate the dependence of the light intensity, L_{ij}, on position (slot number) and time (batch number). We make the assumption that these two dependences factorize, i.e. that

$$L_{ij} = L_{00}(1 + b_i) (1 + s_j).$$

(This is defined so that the appropriate averages of b_i and s_j are zero.) Evidence from the control tubes supports the factorization assumption if the two test chambers are treated separately. Each has its own time dependence, arising from different repair history, but within each chamber the four control tubes show similar patterns of small drifts (about 10%). By normalizing to appropriate averages it was possible to isolate and correct for variations of L_{ij} with position and time.

Any common drift in P_{ij} for the control tubes is a measure of a drift in the large-chamber light intensity. (We assume that Q_{ij} remains constant for these tubes.) It is given by

$$\frac{P_{ij}}{P_{0j}} = \frac{L_{ij}}{L_{0j}} = (1 + b_i) \text{ (control tubes only).}$$

As noted above a drift was observed at the 10% level, was different for the two test chambers, and correlated with moves or other physical interference with the chambers. The average of this quantity for the four control tubes in each chamber gave the time drift of the light intensity.

The light map, $(1 + s_j)$ was measured prior to the tests, but can be determined from the data by noting that, over the short time period to assemble a single batch of tubes, the small-chamber light intensity used to set the high voltages can safely be assumed constant. Thus, $Q_{ij}G_{ij}$ is constant for all tubes in a batch. Normalizing the pulse heights to the average over all slots within a batch,

$$\frac{H_{ij}}{H_{i0}} = \frac{Q_{ij}\, G_{ij}L_{ij}}{\langle Q_{ij}\, G_{ij}L_{ij}\rangle_j} = \frac{L_{ij}}{L_{i0}} = (1 + s_j) \, .$$

The average of this quantity over all batches was used to correct for the position dependence of the illumination.

Another quantity can be formed for the tubes under test (which change with each batch) so that

$$\frac{P_{ij}}{P_{00}} = \frac{Q_{ij}\, L_{ij}}{\langle Q_{ij}\, L_{ij}\rangle_{ij}} = \frac{Q_{ij}\, L_{ij}}{Q_{00}\, L_{00}} = \frac{Q_{ij}}{Q_{00}}(1 + b_i)(1 + s_j) \ .$$

Here, it is assumed that, since Q and L are uncorrelated, the average of their product is the product of their averages. It is clear that the relative, tube-to-tube variation in quantum efficiency can be obtained correcting this for the variation in light intensity obtained in the previous equations.

For the eight control tubes, a time drift in G_{ij} was observe over the thirty-month duration of the tests, most likely from the integrated anode current which reached over 50 Coulombs for these tubes. (It was assumed that Q_{ij} was constant for the controls, i.e., independent of i.) This is discussed in Section IV-D-3.

8. Analog-to-Digital Converter for DC Signals

A Dual Systems Model AIM-12 ADC residing on the S-100 bus was used to make measurements of the following DC signals:

-- average anode currents over a range from 1 nA to 5 μA. Each phototube output was sent to a computer-controlled reed-relay which could direct the anode signal to the LeCroy ADC or to a current-to-voltage amplifier with computer-controlled auto-ranging. At various periods during the test cycle, the tubes were swiched, one at a time, to the amplifier and

its output was digitized by the Dual Systems ADC. Under computer control, the amplifier was switched between two ranges. The calibration curves for these ranges are shown in Fig. 3.10.

-- Various low-level DC power supply voltages,

-- output voltages from temperature sensors.

9. Temperature Sensing

Temperature sensors incorporating the National Semiconductor LM234 were placed near the light sources and near the photomultiplier bases. The sensitivity of these devices was about 23 mV/^{o}C (about 10 ADC counts). We were primarily interested in correcting for gain and light source brightness changes with temperature fluctuations during a test. The calibration data for one of the sensors is shown in Fig. 3.11.

In normal testing, the entire test chamber, including LED's and PMTs's stayed the ambient room temperature which varied diurnally by a few degrees. This environmental variation supplied the bulk of the data on temperature sensitivity. In order to unfold the temperature coefficients of the PMT's and the LED's a special test was done with eight tubes. A transparent barrier was placed in the large test chamber between the tubes and light sources, and a heater was installed to allow independent variation of the temperature in the two chamber segments. This allowed us to separate the effects of tube response and LED output. The pulsed LED output was found to vary by (-0.66 ± 0.03)%/deg-C. This value was used in correcting the data for the full set of PMT's as presented in Sec. IV.

10. High Voltage Control and Readout

High voltage, including regulation and readout, for the 48 phototubes under test was supplied by a LeCroy 1440 system controlled by the μC through Camac. At each stage of the test procedure, values were automatically set to those specified in the database by the small chamber tests.

IV. RESULTS: CENTRAL EM TUBES

A. Manufacturing Data

The values of the quantum efficiency (QE) measured by the manufacturer are shown in the histogram of Fig. 4.1. The average value for the entire set of tubes was 0.141. The relative QE, measured as described in the previous section, was found to have a 71% correlation with this. The difference from 100% correlation is consistent with the statistical flucutations of the measurement, about 0.02.

B. Results From Small Test Chamber

1. High Voltage Settings

The average voltage settings for the gain x quantum efficiency values tested are: 1059 V for GQE = 1.2×10^4, 1165 V for GQE = 2.4×10^4, and 1283 V for GQE = 4.8×10^4. The distributions for the tubes tested are shown in Fig. 4.2.

For purposes of interpolation between measured points, the dependence of gain on voltage was parametrized as follows:

$$(G_2/G_1) = (V_2/V_1)^N. \qquad (4.1)$$

The distribution of the values of N determined from the two lower settings is shown in Fig. 4.3

2. Dark Current

The dark currents measured at the three gain settings are shown in the histograms of Fig. 4.4. Note the log scale on the current axis.

C. Results from Large Test Chambers

Figure 4.5 shows the time dependence of a part of the data for one of the tests. It helps to illustrate some features of the topics discussed below. In Fig. 4.5(a) the ADC response to Level 5 of the pulsed light sources is plotted as a function of time. The tungsten light source was cycled through four different levels during the tests. The change in pulsed response between the lowest and highest level is clearly seen in the ~0.5% displacement between the two sets of points. Fig. 4.5(b) shows the output of the temperature sensors which varied diurnally by about 4° C. The phototube shows a clear change in output which is about -0.3% per degree-C, and is a combination of the change in LED output and the PMT response. Approximately 12 hours of data were lost by an overnight interruption in the asynchronous connection between the μC and the VAX, but the testing continued uninterrupted during this period. A few times a test was interrupted by a power failure which disabled the μC. In such cases, depending on the amount of data collected at the time, the test was either re-started or terminated early.

1. Dependence on Time, Temperature and Anode Current

Data on 40 tubes and 8 controls were collected for approximately 160 hours during which test parameters went through the test cycle many times. When the data in Fig. 4.5(a) are corrected for temperature dependence, the output signal is stable with time to about 1%. The data for each tube and pulsed light source were fit to a time-dependent function with the following form:

$$H(t) = a_1 + a_2 t + a_3 t^2 + a_4[T(t) - T(0)] \qquad (4.2)$$

where the a's are fitted parameters, t is the time (starting with t = 0 at the end of the 40-hour burn-in period), T(t) is the measured temperature as a function of time. This was done for each pulse level and DAC setting for the tungsten lamp which controls the anode current. The displacements in pulse height caused by the anode currents are clearly seen in Fig. 4.5(a).

The stability criterion was met if, after unfolding the temperature dependence, the minimum-to-maximum variation of the residual time dependence was less than 2%. A small number of tubes (<1%) marginally exceeded this criterion. They were re-cycled through the entire test, including a second burn-in period, and none was ultimately rejected for this reason.

2. Current Gain

Figure 4.6 shows the distribution of gains obtained by the method described in Sec. III-C-6. A small number of anomalously high, non-statistical widths of the pulse height distributions appear as high gains. The mean value of the gain is 1.02×10^5 and the R.M.S. deviation of the distribution is 0.25×10^5. Figure 4.7 shows a similar distribution for the product of measured gain and the manufacturer's value for the quantum efficiency. The mean and R.M.S. deviation are 1.34×10^4 and 0.29×10^4, respectively, for a nominal setting of 1.2×10^4. This distribution is fairly broad. A more realistic estimate of the scatter in the data is obtained by plotting the values of a_1 form Eq. 4.2, corrected for position and time variation as described in Sec. III-C-7. The pulse heights, thus corrected, are

shown in Fig. 4.8, and the distribution is considerably narrower than that of Fig. 4.7.

3. Short Term Stability

The typical test yielded data over 140 hours of operation with the tubes held at a fixed high voltage. The first forty hours were a burn-in period with an anode current of about 5 μA induced by the tungsten lamp. The stability criteria were based on the remaining 100 hours of data where the average anode current was cycled between 10 nA (tungsten lamp off) and 2 μA. Data for the lowest anode current setting for pulsed light level 5 were fit to Eq. (4.2) and the temperature dependence removed to yield a corrected pulse height

$$H' = a_1 + a_2 t + a_3 t^2 \qquad (4.3)$$

This was examined for minimum and maximum values over the test interval, and the quantity $\Delta H = H'(\max) - H'(\min)$ was computed and plotted in Fig. 4.9 as a percentage of pulse height. The time interval used was 80 hours, centered in the 100-hour testing period after burn-in, during which the tube GQE was maintained at nominal 1.2×10^4.

4. Temperature Dependence

The normal test procedure did not include any systematic variation of temperature. However, environmental temperature variations were observed, and it was possible to measure the combined temperature dependence of tube response and LED output, viz. a_4 in Eq. (4.2). This was corrected for the

known LED temperature dependence (Sec. III-C-7) to yield the histogram plotted in Fig. 4.10. The accuracy of individual measurements varied greatly, depending on the magnitude of temperature fluctuations, and the more accurate results are highlighted in the figure.

5. Rate Effects

The rate dependence was tested by observing the change in pulse height as a function of average anode current. The latter was controlled by the tungsten lamp discussed previously. An apparent interaction between the lamp driver and the LED's was discovered after all testing was complete. The pulse heights were about 0.9% higher with the lamp selected even at extremely low settings. The data have corrected for this effect. Figure 4.11 shows a scatter plot of the percentage change in pulse height vs. anode current. It is quite stable from a the 10 nA level arising from the LED's up to about 3 μA where it abruptly rises. The stable region covers all normal conditions expected in CDF operation.

6. Linearity

The technique used for linearity testing was chosen to avoid any dependence on the long term stability of light sources or filters at the 1% level. The PMT response was measured for each of fifteen different combinations of up to three pulsed LED's levels 1 through 6. The combinations were: 1, 1+2, 1+2+3, 2, 2+3, 2+3+4, 3, 3+4, 3+4+5, 4, 4+5, 4+5+6, 5, 5+6, and 6. (See Table 3.1.) These combinations covered a dynamic range from typically 30 to 20,000 pe^-, with 10% to 30% increments about the largest single level in each combination. If the response is linear, the measured pulse heights should be

well-represented by the appropriate linear combinations of six parameters, one amplitude for each of the six LED levels used. A χ^2 test with nine degrees of freedom can be made for such a fit.

One hundred samples were taken for each pulse height level in this test, and the average pulse height, H, and r.m.s. deviation, σ, were computed. The statistical uncertainty on H was taken to be $\Delta H = \sigma/\sqrt{N}$, where N = 100. For the higher pulse heights, ΔH was typically well below 0.1% of H. Therefore, since the specifications called for 1% linearity, a lower limit of 1% of H was placed on ΔH for purposes of the χ^2 test.

Data for the fifteen different combinations of LED's required about seven minutes to collect, and the test was repeated about twice per hour for the duration of the testing period. All χ^2's were averaged to give a single value for each PMT, and these values are given in the histogram of Fig. 4.12. If the linearity is 1% or better, one expects $\chi^2 \leq 9$. Figure 4.12 shows this to be true.

D. Subsample Tests

Specifications 8 and 10 (See Sec. II) were tested for only a subsample of PMT's as described below.

1. Pulse Recovery

Pulse recovery was defined to be satisfactory if the tube current gain recovered to within 2% of its previous value within 1 ms after a full-scale pulse (40 mA peak). An argon flash lamp was set up to provide this large pulse followed, with variable delay, by a smaller pulse from an LED. A change in the tube output pulse height for this delayed pulse was assumed to be due

to a change in tube gain because of the large preceding pulse. With a 10 μsec delay, a 4% rise in pulse height was observed, but at 100 μsec or greater, there was no detectable effect on the pulse height.

2. Differential Linearity (Flash Lamp Tests)

The flash lamp, LED setup described in the previous section was operated with zero delay to test differential linearity at large amplitude. The output signal was attenuated by X11.3 to bring it into the ADC range, and pulse heights were measured for the combination, LF, and each source individually L and F. A measure of percentage differential non-linearity is

$$D = \{\frac{LF - F}{L} - 1\}X100\%. \qquad (4.3)$$

The flash lamp yielded F = 500,000 pe^- and the four highest amplitude LED's provided L = 80,000 pe^-. This tested amplitudes well beyond the expected operating range of CDF. Eighteen tubes were tested in this manner. Half yielded D < 1%, and the worst case was 5%. Data for four of these are given in Fig. 4.13 which shows a plot of the difference in pulse heights, $H(Q+\Delta) - H(Q)$ as a function of Q. It is fairly easy to show that, if the non-linearity is a low order term in a power series (e.g. a quadratic term), even the worst case implies non-linearities well under 1% in the range of interest.

3. Long Term Stability

Eight tubes and bases, including four R580B's remained in the test chambers as controls throughout the duration of the testing program, about one year. The total integrated current passing through these tubes reached about

fifty coulombs. Conditions were far from stable because the high voltage was switched off every time a new batch of forty tubes was installed, and the entire test setup was moved to a new location three times. Nevertheless, a simple plot of the tube response to one of the pulse light levels (Fig. 4.13) shows a tendency for the output to diminish by up to 10% over the period.

V. ENDWALL CALORIMETER TUBES

The EMI phototubes for the endwall hadron calorimeter where subjected to tests similar to those described above. The tests differed in two respects: after 40 hours of burn in, the subsequent testing period was reduced to about 40 hours instead of 120; the tubes were operated at gains of approximately 10^6 instead of 10^5. We chose not to change any characteristics of the test fixtures, e.g. the ADC conversion gains. As a result, the pulse response for light level 6 was often off scale for the EMI tubes.

The data analysis yielded the results summarized in Table 5.1, and in Figs. 5.1 to 5.7. The most significant effect of the absence of data for light level 6 for most tubes is that the linearity tests for the EMI sample were done over a narrower dynamic range (typically 70:1) than for the R580B-'s (typically 250:1). Thus, the smaller χ^2 values should not be interpreted as evidence for better performance.

The duration of the test period (less than two diurnal temperature cycles) yielded large measurement uncertainties and strong correlations between parameters for tests of stability and temperature dependence. The results are omitted from Table 5.1, but they are consistent with no drift and zero temperature coefficient with an uncertainty of about 2%. The variation of gain with anode current for the EMI tubes was quantitatively very similar to that for the Hamamatsu tubes as shown in Fig. 4.11. Note that, because the EMI tubes were operated at higher gain, the tungsten lamp light levels were lowered to produce anode currents similar to those for the Hamamatsu tests.

VI. ACKNOWLEDGEMENTS

We would like to thank the following people for valuable contributions and suggestions: Robert Darling, Mark Devlin, Ted Devlin, Robert Plano, Lee Scott, Bob Stone, Alvin Tollestrup and Debbie Weiss. This work was supported in part by the National Science Foundation and the Department of Energy.

APPENDIX A. CIRCUIT DIAGRAMS

Fig. A-1 shows the circuit diagram for the base used to power the R580B tubes. Figs. A-2 to A-7 show the control circuitry, cable pinouts for the light sources, and details of the LED drivers. The temperature sensor circuitry is given in Fig. A-8. The "anode MUX" and nano-ammeter circuitry used for online measurement of phototube anode currents are shown in Figs. A-9 and A-10.

FOOTNOTES AND REFERENCES

(a) Present address: I.T.T. Avionics, 390 Washington Av., Nutley, NJ 07011

(b) Present address: Room 2B108, AT&T Bell Labs, 555 Union Blvd., Allentown, PA 18103

[1] L. Balka et al., "The CDF Central Electromagnetic Calorimeter", (submitted to Nuclear Instruments and Methods).

[2] S. Bertolucci et al., "The CDF Central and End Wall Hadron Calorimeters" (submitted to Nuclear Instruments and Methods).

[3] T. Devlin et al., "Phototube Testing for CDF" (submitted to Nuclear Instruments and Methods).

[4] The bases for the R580B photomultiplier tubes were designed and build at the University of Pennsylvania under the supervision of J. Cook and R. Van Berg. A circuit diagram can be found in Ref. 1.

FIGURE CAPTIONS

Fig. 2.1 (A) Spectral sensitivity for the R580B phototube. (B) Output spectrum of Y7 waveshifters. (C) Output spectrum of the light source used by the manufacturer in quantum efficiency measurements. The peak in the overlap of (A) and (C) is at 510 nm indicated by arrow (D). The wavelength of the green LED's used in the present tests is 560 nm, indicated by arrow (E).

Fig. 2.2 Small test chamber for measuring operating points and dark currents.

Fig. 3.1 Overall test procedure, showing stage at which various specifications were tested.

Fig. 3.2 Small test chamber for measuring operating points and dark current.

Fig. 3.3 Large test chamber block diagram. The clock pulsed all the LED light sources at 10 Hz. The microcomputer selected which sources were "on" (within the ADC gate) or "off" (delayed beyond the ADC gate), and the steady light levels. The phototube outputs were normally all connected to the LeCroy ADC for pulse height measurements. Periodically, they were switched, one at a time, to an amplifier/ADC system which measured the average anode current. The same ADC also monitored low-level DC voltages for the light sources and the temperature in the test chambers. The photomultiplier high voltage supply was controlled by the microcomputer through CAMAC.

Fig. 3.4 The geometry of the large test chambers. The shaded areas of Section AA contained the the timing circuitry (located in the center) and four driver boards, each containing identical sets of circuitry for all pulsed light levels, 1-5, and a tungsten lamp. Section BB contained 24 circular holes to pass light through to the photocathodes, approximately 3 cm to the right on this diagram. The shaded areas in BB supported driver circuitry for light levels 6-10 and the associated LED's which protrude into the apertures for each tube.

Fig. 3.5 A "light map" of one of the test chamber. The central position in the 5X5 lattice is not used. Each of the 24 positions is labelled by its position number and the relative light intensity averaged over the area of an R580B photocathode. The scale is arbitrary.

Fig. 3.6 Timing of the ADC gate and phototube responses to "On" and "Off" pulsed light sources.

Fig. 3.7 Photomultiplier anode current as a function of DAC input to tungsten lamp. At low DAC input values the upper curve has a lower bound determined by the average current from the pulsed LED's. The lower curve was taken with the LED's off and its lower bound is fixed by small light leaks in the test chamber.

Fig. 3.8 Calibration data for the LeCroy ADC. The built-in test mode injects a charge proportional to the applied voltage into the ADC. The resultant ADC output is plotted against this voltage and is linear to better than 1%.

Fig. 3.9 Relationship between the square of the fractional statistical width of the pulse height $(\sigma/H)^2$ and the inverse of the optical attenuation. Data shown were taken at different times with different phototubes, bases and light levels. The agreement of these results with the unit-slope lines demonstrates that the width of the pulse height distribution is almost entirely determined by photoelectron statistics. Thus, the width can be used to determine the number of photoelectrons which is subsequently used to compute the absolute gain of the photomultiplier tube.

Fig. 3.10 Calibration data for the (a) low gain and (b) high gain settings of the current-to-voltage amplifier which monitored the phototube anode currents. Amplifier output, which was fed to the Dual Systems ADC, is plotted in terms of ADC counts. The current was generated by a power supply which drove a precisely known high resistance in series with the amplifier input.

Fig. 3.11 Calibration data for one of the four temperature sensors.

Fig. 4.1 Distribution of quantum efficiencies reported by the manufacturer.

Fig. 4.2 Distribution of high voltage settings required to achieve a gain-quantum efficiency product of (a) 1.2×10^4; (b) 2.4×10^4; (c) 4.8×10^4.

Fig. 4.3 Distribution of the exponent, n, characterizing the gain vs. voltage relationship, $(G_i/G_j) = (V_i/V_j)^n$ for (a) i=1, j=2 and (b) i=2, j=3, where 1,2 and 3 characterize the low, intermediate and high gain settings as in Fig. 4.2.

Fig. 4.4 Distribution of dark current for gain-quantum efficiency products of (a) 1.2×10^4, (b) 2.4×10^4 and (c) 4.8×10^4. Note the logarithmic scale on the current axis.

Fig. 4.5 A sample of data taken over a period of about four days which shows the dependence of the pulse area response of one of the photomultipliers on time, temperature and average anode current. The upper graph (a) shows the time dependence for a specific pulsed light source (yielding about 3500 photoelectrons per pulse). Data are shown for two different settings of the tungsten lamp which induced a DC current in the phototube (approximately 0 and 2 μAmps). The tube gain increases about 0.5% for the higher current. The lower graph (b) shows the temperature in the test chamber during the same period. A clear negative correlation between pulse height and temperature is seen - about $0.3\%/^{\circ}C$.

Fig. 4.6 A histogram of phototube gains measured by the procedure described in the text.

Fig. 4.7 A histogram of the products of gain (See Fig. 4.6) and quantum efficiency (manufacturer's value) for 510 nm green light.

Fig. 4.8 Histogram of the pulse height (in pC) corrected for position and time dependence of the light source. It shows the uniformity of the gain^{X}QE product as set in the small box. Some part of the width can be attributed to variations in the starting phase of the diurnal temperature variations in both the small box setting and the large box tests.

Fig. 4.9 Histogram of the percentage difference in the minimum and maximum pulse heights (temperature corrected) during an 80-hour period centered in the test interval.

Fig. 4.10 A histogram of phototube temperature coefficients. In cases where the changes in ambient temperature were small, measurement uncertainties were large. The solid bars represent data in which the measurement uncertainty was less than 0.1%/deg-C.

Fig. 4.11 A scatter plot of the percentage change in pulse height as a function of anode current. The reference pulse height is that with the tungsten lamp off. Note the logarithmic scale on the current axis.

Fig. 4.12 A histogram of the values of χ^2 for the linearity tests described in the text. A lower limit of 1% was placed on the uncertainty of each of the fifteen pieces of data in the fit to six LED pulse amplitudes. A typical $\chi^2 = 9.0$ or less indicates that non-linearities are 1% or better. The dynamic range for this measurement was typically about 250:1.

Fig. 4.13 The pulse height response of four R580B phototubes which remained in the test chambers as controls for the duration of the testing program. Values are plotted as functions of the total integrated anode current in coulombs.

Fig. 5.1 Distribution of quantum efficiencies reported by the manufacturer for the EMI tubes.

Fig. 5.2 Distribution of high voltage settings required to achieve a nominal gain of (a) 1.0×10^6; (b) 2.0×10^6; (c) 4.0×10^6.

Fig. 5.3 Distribution of the exponent, n, characterizing the gain vs. voltage relationship, $(G_i/G_j) = (V_i/V_j)^n$ for (a) i=1, j=2 and (b) i=2, j=3, where 1,2 and 3 characterize the low, intermediate and high gain settings as in Fig. 5.2.

Fig. 5.4 Distribution of dark current for gain-quantum efficiency products of (a) 1.0×10^6, (b) 2.0×10^6 and (c) 4.0×10^6. Note the logarithmic scale on the current axis.

Fig. 5.5 A histogram of phototube gains measured by the procedure described in the text.

Fig. 5.6 Histogram of the pulse height (in pC) corrected for position and time dependence of the light source.

Fig. 5.7 A histogram of the values of χ^2 for the linearity tests described in the text. A lower limit of 1% was placed on the uncertainty of each of the fifteen pieces of data in the fit to six LED pulse amplitudes. A typical $\chi^2 = 8.0$ or less indicates that non-linearities are 1% or better. Since light level 6 was off scale for this gain setting, the dynamic range for this measurement is about 70:1.

Fig. A-1 (a) Circuit diagram and PC board layout for base used to power the Hamamatsu R580B phototubes used in the Central EM calorimeters. (b) Socket wiring diagram.

Fig. A-2 (a) Cabling diagram for light source controls, power and temperature monitoring of a large test chambers. Two such assemblies were used. The clock was a 2-μsec-long, positive-going, TTL pulse operated at about 10 Hz. The temperature sensors and (not shown) sense lines from each of the DC voltages in the power supply were connected to the Dual Systems ADC for periodic monitoring. Temperatures were monitored in the vicinity of light sources 1-5, and just behind the phototube bases. (b) Pinout diagrams for cables A, B and C. (c) Pinout diagram for Cable D.

Fig. A-3 Control Board (mounted at center in Section A-A of Fig. 3.4) for light sources in the main test chambers: (a) circuit diagram; (b) component layout and connector locations; (c) details of phase selection circuitry for pulsed LED's; (d) DAC circuit and driver for tungsten lamps. (e) Manufacturer's data sheet for DAC use in (a).

Fig. A-4 Layout for boards containing light sources. These are the four symmetrically placed boards in Section A-A of Fig. 3.4.

Fig. A-5 Circuit diagram for LED drivers.

Fig. A-6 Layout and circuitry for pulse-forming and control board used for pulsed LED levels 6-9. This board was mounted at the center of Section B-B of Fig. 3.4, and the four fanout legs served each of the boards displayed in Fig. A-7.

Fig. A-7 Physical layout and circuitry of LED's and drivers for Levels 6-9. Four such boards were mounted at Section B-B of Fig. 3.4, each serving six phototube positions.

Fig. A-8 (a) Circuit diagram for temperature sensors. (b) Manufacturer's data sheet for temperature sensor.

Fig. A-9 (a) Circuit diagram for the "Anode MUX", the switching circuit which switched the phototube anodes, one at a time, to the amplifier/ADC circuitry used as a nano-ammeter. Two such circuits were built, one for each of the test chambers. (b) Details of the control circuitry which selected the reed relays for switching. Selection was done on a row-and-column code with control bits S_0, S_1 and S_2 selecting the row, bits S_3 and S_4 selecting the column. In addition, S_5 and S_6 were used as a box select code in which 0 meant all channels off. A final bit, S_7, was used as to select high or low amplifier range for the circuit described in Fig. A-10. (c) Details of the relay wiring.

Fig. A-10 Two range amplifier circuitry used for current-to-voltage conversion in measurements of phototube anode currents. The two outputs went to two channels of the Dual Systems ADC where they were accessible by the microcomputer which controlled the system. Range selection was done by the computer through the CAMAC-based Jorway Model 40.

Table 3.1

Characteristics of Light Sources in Large Test Chambers

Level Number	Type	# of sources	Distance to PMT (cm)	Nominal Pulse[c] (photoelectrons)	Anode Current (nA)
1	Pulsed[a]	4	70	30	(b)
2	"	4	70	100	"
3	"	4	70	300	"
4	"	8	70	1,000	"
5	"	24	70	3,000	"
6	"	1[d]	3	20,000	"
7	"	1[d]	3	20,000	"
8	"	1[d]	3	20,000	"
9	"	1[d]	3	20,000	"
	Step-Function[a]	16	70	--	0-100
	Tungsten Lamps (e)	4	70	--	0-10,000

Note: (a) Green LED's with wavelength of 560 nm.
(b) The average anode current from all nine pulsed light sources was about 10 nA.
(c) Actual numbers varied downward by as much as 50% depending on tube location and quantum efficiency.
(d) One LEDF for each phototube position.
(e) The tungsten filament lamps were set to yield 5μA anode current during burn-in, and were cycled through four different settings for the stability tests: off, 20 nA, 200 nA, and 2μA.

Table 4.1

Characteristics of R580B Phototubes for Central EM Calorimeter

Quantity	Units	Sample Size	Distribution Mean	Distribution Std. Dev.	Min. Value	Max. Value
Quantum Eff.	%	1041	14.1	1.6	8.0	19.0
HV1 (a)	Volts	1041	1057	55	920	1200
HV2 (a)	Volts	1041	1163	62	1020	1340
HV3 (a)	Volts	1041	1282	71	1120	1480
Gain-Voltage Exponent (N in Eq. 2.1)						
HV2/HV1	--	1041	7.25	0.18	6.4	7.8
HV3/HV2	--	1041	7.15	0.22	6.1	7.7
$\text{Log}_{10}(I_d/1\text{ nA})$ (b)						
@ HV1	--	1041	-1.02	0.51	-2.4	0.4
@ HV2	--	1041	-0.83	0.51	-2.2	0.6
@ HV3	--	1041	-0.58	0.53	-1.8	0.8
Quantities below are for the HV1 setting						
Corrected Pulse Area (c)	pC	963	26.9	1.5		
Gain (d)	($\times 10^5$)	849	1.00	0.24		
χ^2(9 d.f.) for Linearity Test (σ > 1%)	--	1041	9.8	4.1		
Temp. Coeff. (e)	%/°C	1041	0.4	0.6		
Peak-to-Peak Drift in Pulse Area (f)	%	865	-0.4	1.3		

Notes:

(a) HV1 is the high-voltage setting for a nominal gain of 1.0×10^5. HV2 and HV3 are the settings for twice and four times that value, respectively.

(b) On a linear scale histograms for dark currents, I_d, were strongly skewed and peaked near zero. On a logarithmic scale, they were roughly Gaussian with the parameters given here.

(c) Value for light level 5. The absolute pulse area is of no significance. The standard deviation of the distribution is a measure of our ability to correct for position and time variations of the pulsed light sources.

(d) Average value which required at least two consistent measurements from light levels 4, 5 and 6. For this sample, the uncertainty on the average for an individual phototube was required to be $<0.1\times10^5$.

(e) Corrected for -0.66%/^{o}C variation of LED's.

(f) Measured over ~80 hours and corrected for temperature dependence. For each test chamber, several runs were omitted from this sample because they had large statistical uncertainties for three or more tubes (of 24). The uncertainties on individual measurements varied from 0.3% to 2%. The distribution width is consistent with measurement uncertainties, and there is no evidence for drifts at this level.

Table 5.1

Characteristics of EMI Phototubes for Endwall Hadron Calorimeter

Quantity	Units	Sample Size	Distribution Mean	Distribution Std. Dev.	Min. Value	Max. Value
Quantum Eff.	%	687	18.9	2.3	10.0	23.0
HV1 (a)	Volts	687	962	136	700	1280
HV2 (a)	Volts	687	1054	158	740	1420
HV3 (a)	Volts	687	1158	184	800	1580
Gain-Voltage Exponent (N in Eq. 2.1)						
HV2/HV1	--	687	7.74	0.71	5.4	9.4
HV3/HV2	--	687	7.59	0.78	5.6	9.8
$\text{Log}_{10}(I_d/1\text{ nA})$ (b)						
@ HV1	--	687	-0.16	0.43	-2.2	0.8
@ HV2	--	687	0.07	0.42	-2.0	1.0
@ HV3	--	687	0.34	0.42	-1.0	1.2
Quantities below are for the HV1 setting						
Corrected Pulse Area (c)	pC	687	191	34		
Gain (d)	($\times 10^5$)	550	9.54	3.58		
χ^2(8 d.f.) for Linearity Test (σ > 1%)	--	687	3.8	1.0		

Notes:

(a) HV1 is the high-voltage setting for a nominal gain of 1.0×10^6. HV2 and HV3 are the settings for twice and four times that value, respectively.

(b) On a linear scale the dark current histograms were strongly skewed and peaked near zero. On a logarithmic scale, they were roughly Gaussian with the parameters given here.

(c) Value for light level 5. The absolute pulse area is of no significance. The spread is a measure of our ability to correct for position and time variations of the pulsed light sources.

(d) Average value which required at least two consistent measurements from light levels 4, 5 and, when available, 6. For this sample, the uncertainty on the average for an individual phototube was required to be $< 2X10^{5}$.

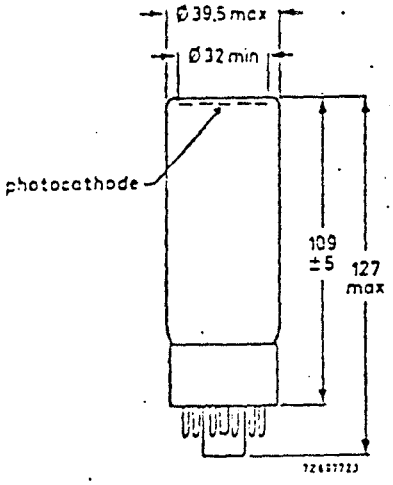

Figure 2.1 (dimension in mm)

FIG. 2.1

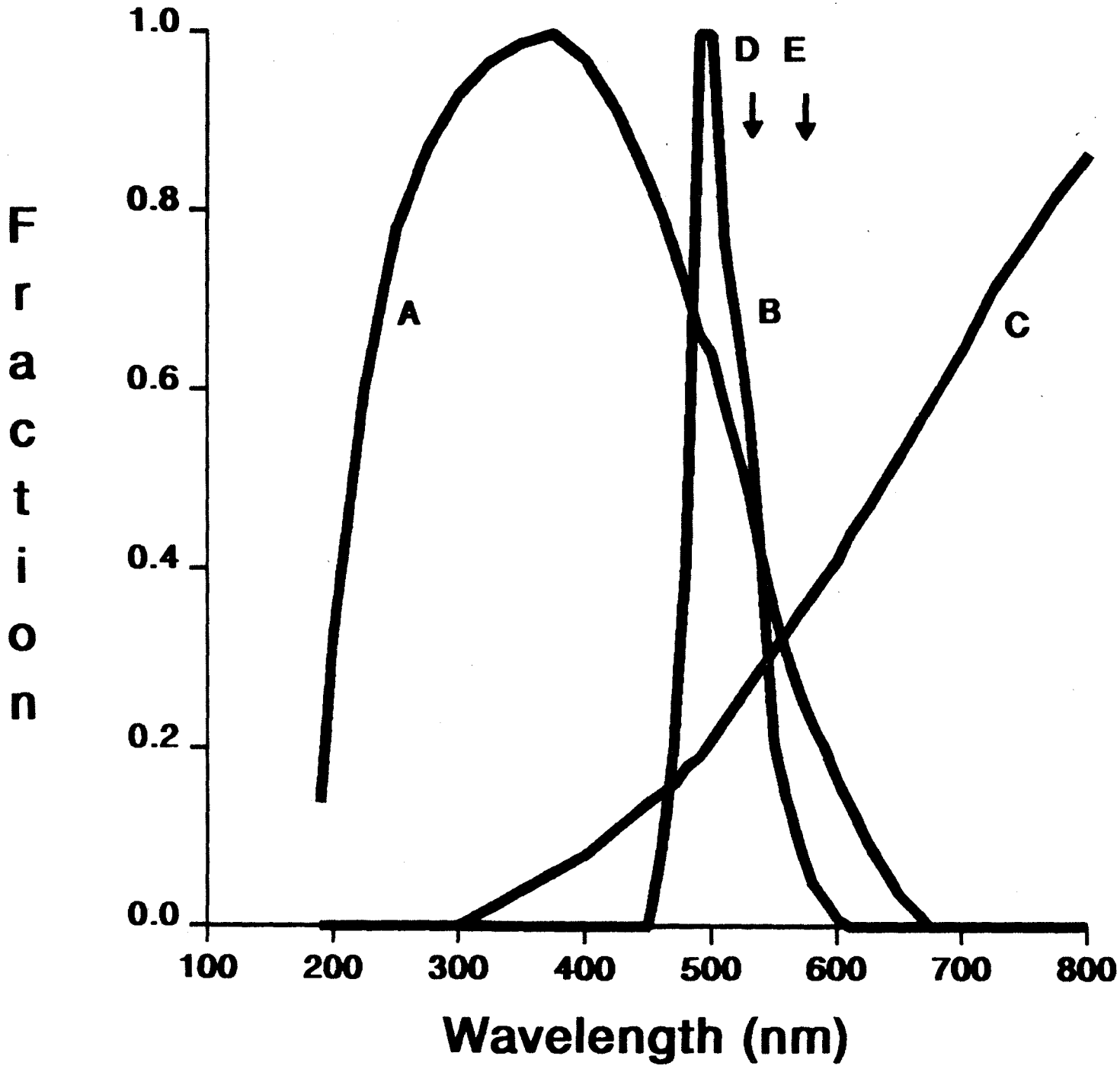
1.0
0.8
0.6
0.4
0.2
0.0
Fraction
A
B
C
D
E
100
200
300
400
500
600
700
800
Wavelength (nm)

FIG. 2.2

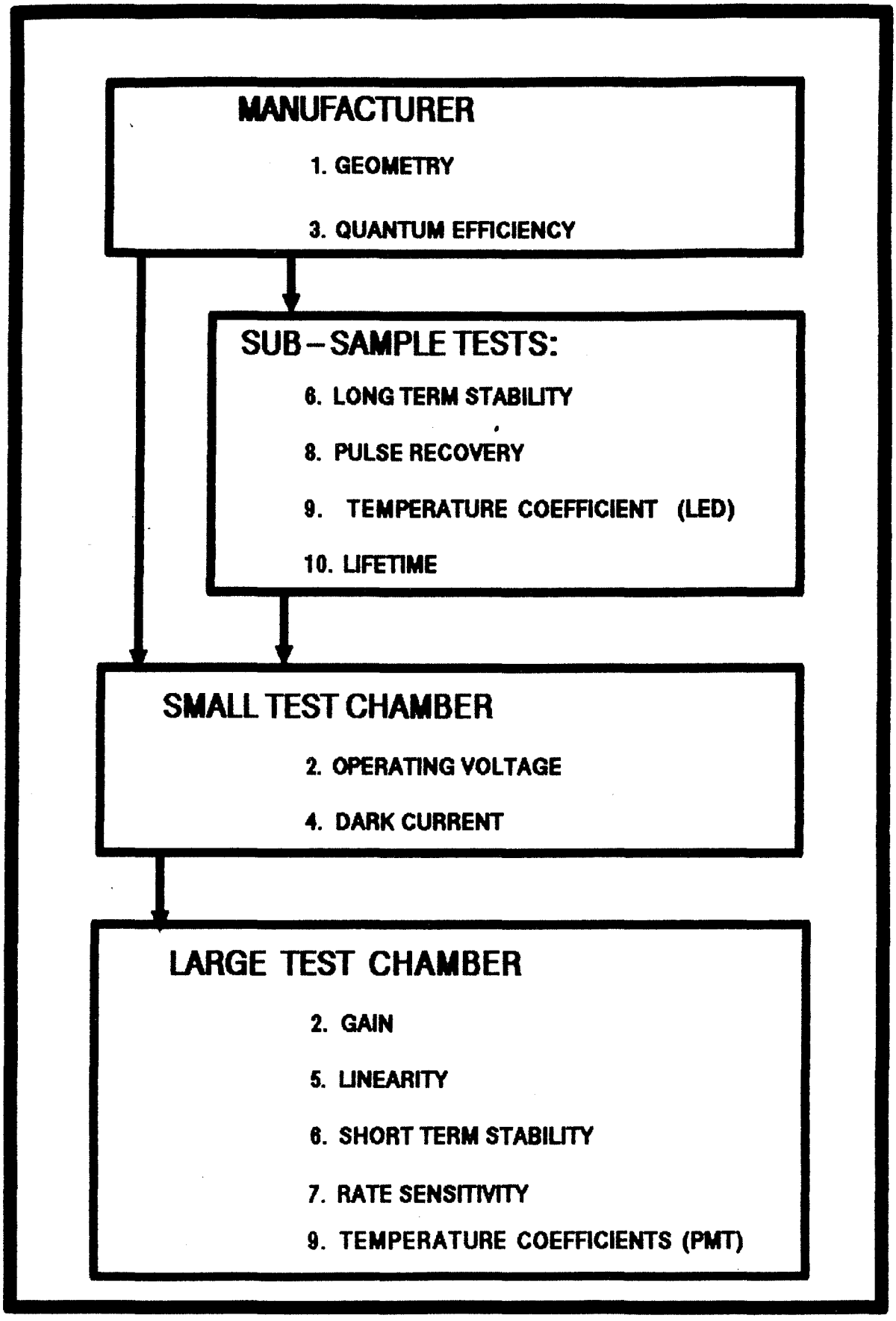
MANUFACTURER
1. GEOMETRY
3. QUANTUM EFFICIENCY
SUB – SAMPLE TESTS:
6. LONG TERM STABILITY
8. PULSE RECOVERY
9. TEMPERATURE COEFFICIENT (LED)
10. LIFETIME
SMALL TEST CHAMBER
2. OPERATING VOLTAGE
4. DARK CURRENT
LARGE TEST CHAMBER
2. GAIN
5. LINEARITY
6. SHORT TERM STABILITY
7. RATE SENSITIVITY
9. TEMPERATURE COEFFICIENTS (PMT)

Fig. 3.1

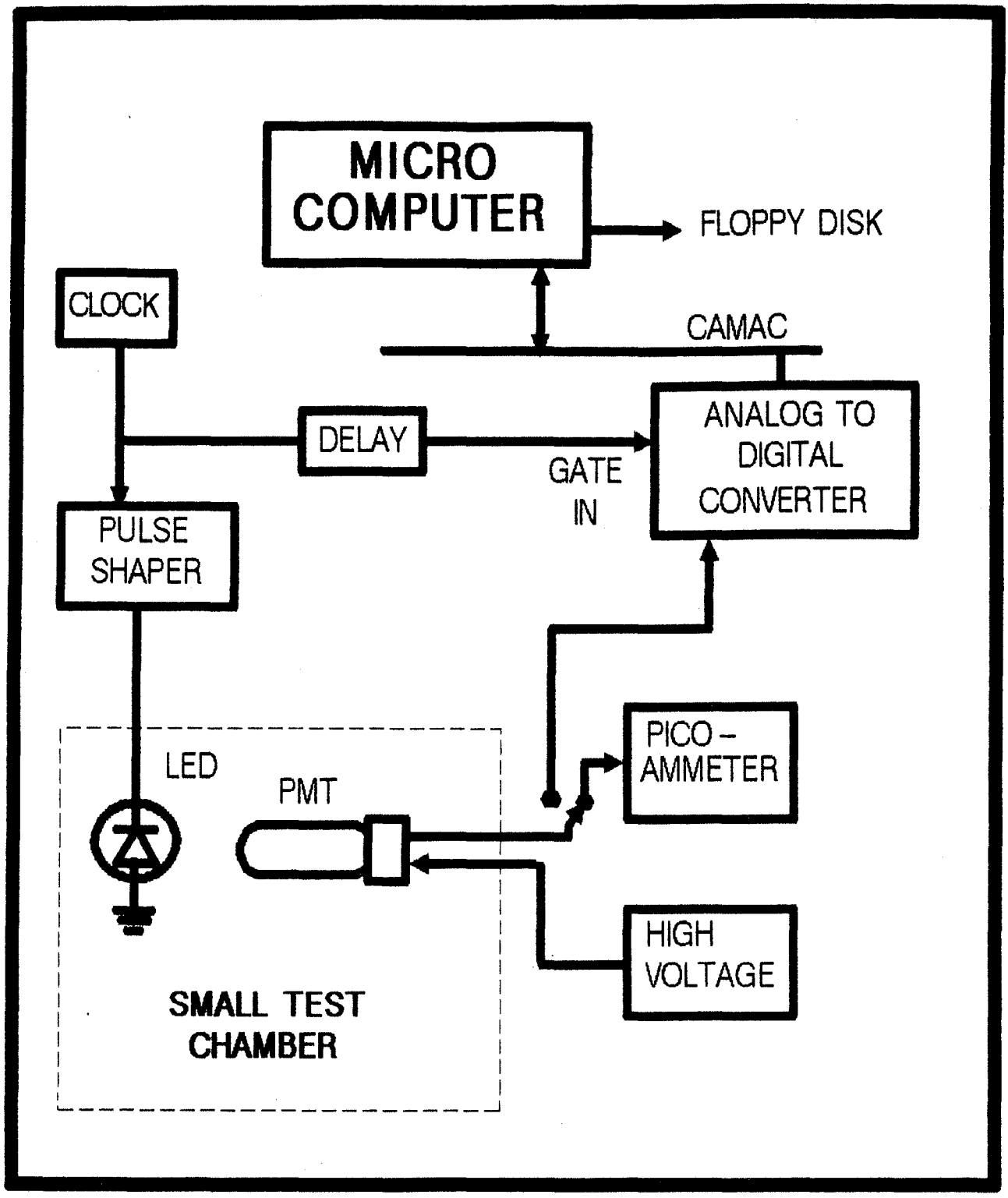
MICRO COMPUTER
FLOPPY DISK
CLOCK
CAMAC
DELAY
ANALOG TO DIGITAL CONVERTER
GATE IN
PULSE SHAPER
LED
PMT
PICO – AMMETER
HIGH VOLTAGE
SMALL TEST CHAMBER

Fig. 3.2

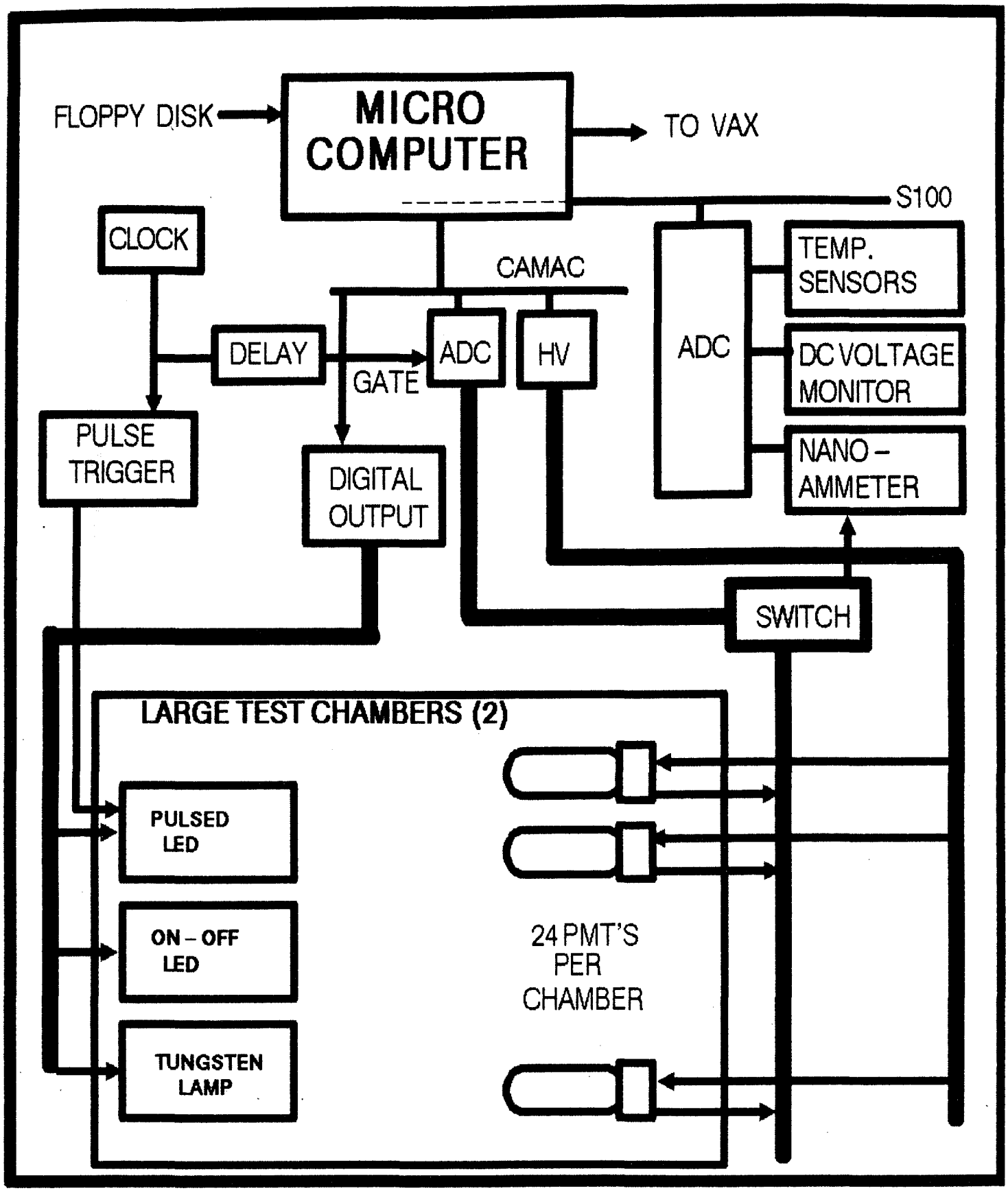
FLOPPY DISK
MICRO COMPUTER
TO VAX
S100
CLOCK
CAMAC
TEMP. SENSORS
DELAY
ADC
HV
ADC
DC VOLTAGE MONITOR
GATE
PULSE TRIGGER
DIGITAL OUTPUT
NANO – AMMETER
SWITCH
LARGE TEST CHAMBERS (2)
PULSED LED
ON – OFF LED
TUNGSTEN LAMP
24 PMT'S PER CHAMBER

Fig. 3.3

Fig. 3.4

1	2	3	4	5
0.54	0.70	0.75	0.75	0.65
6	7	8	9	10
0.70	0.84	0.89	0.90	0.80
11	12		13	14
0.75	0.91		0.98	0.85
15	16	17	18	19
0.76	0.92	0.99	0.97	0.85
20	21	22	23	24
0.70	0.82	0.90	0.90	0.70

POSITION	LIGHT LEVEL

FIG. 3.5

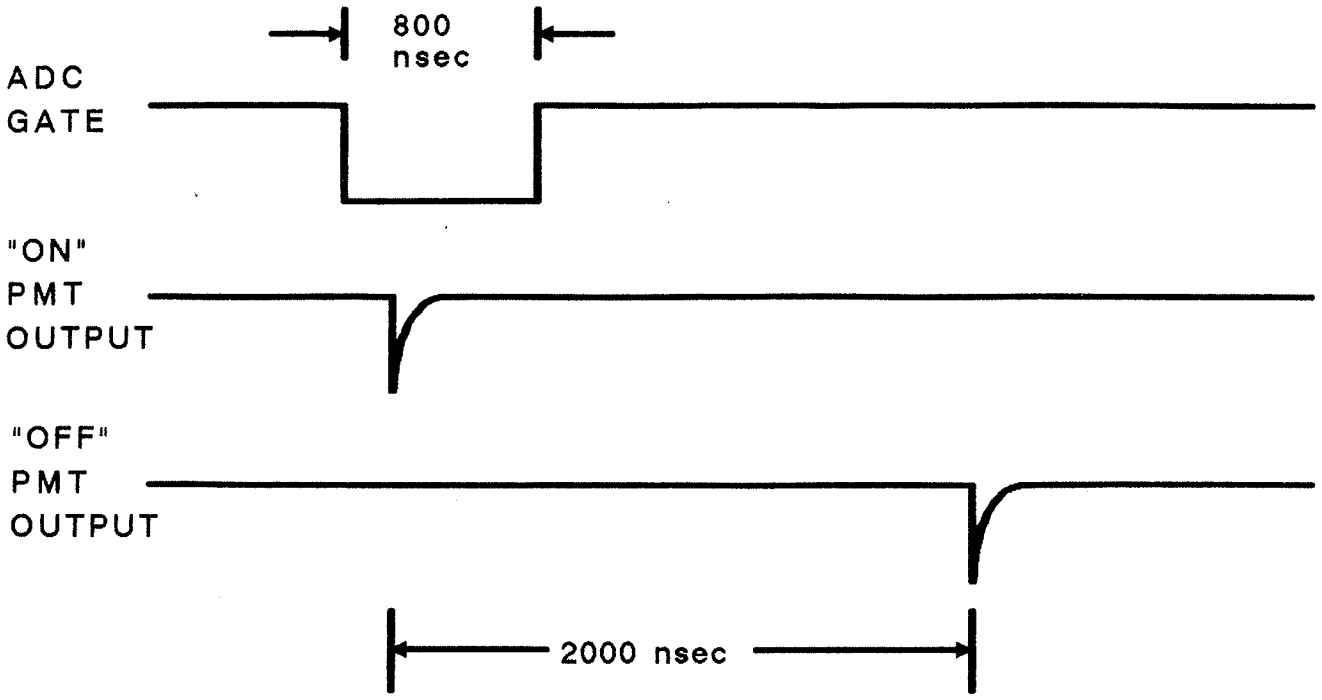

FIG. 3.6

FIG. 3.6

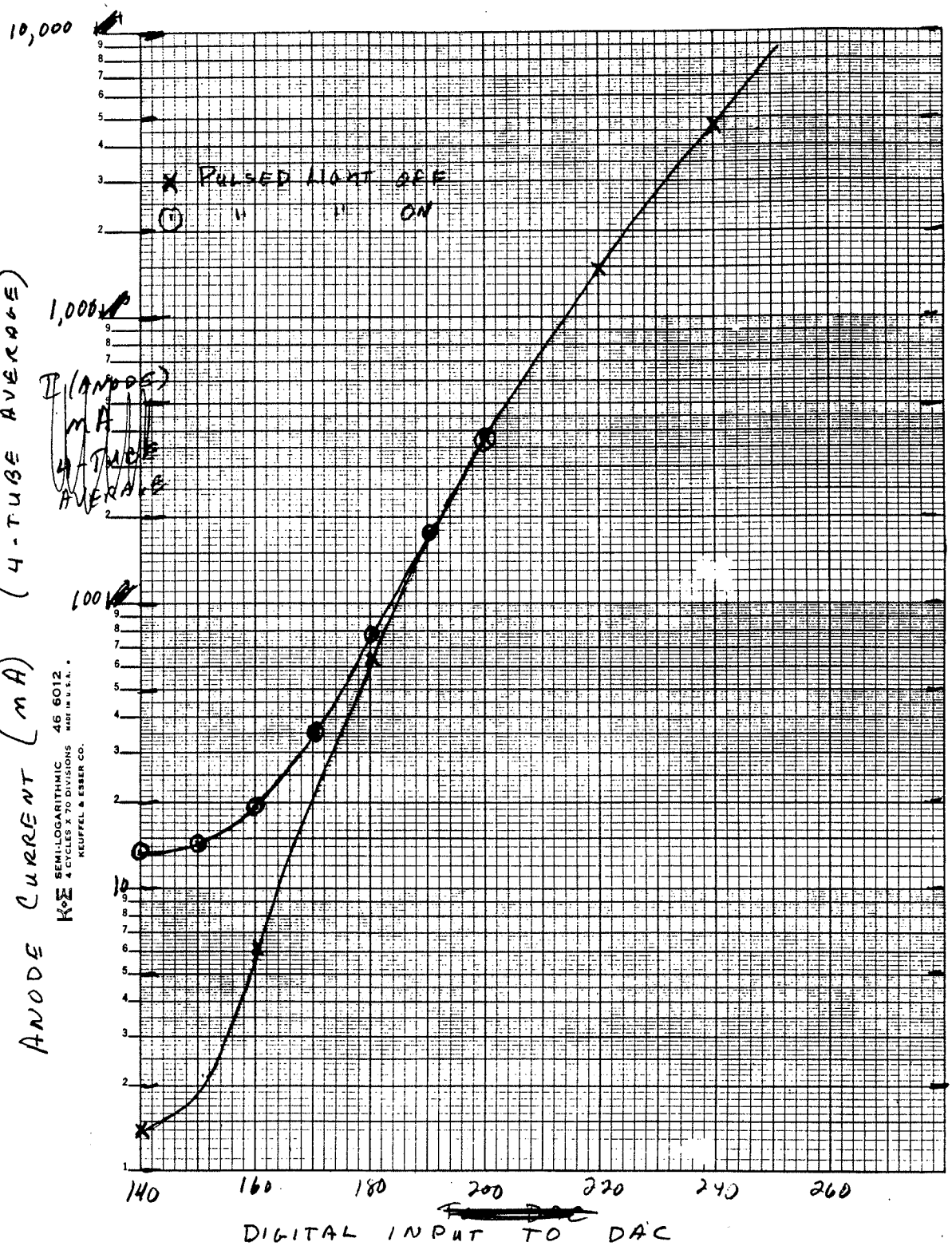
10,000
1,000
100
10
1
ANODE CURRENT (mA) (4-TUBE AVERAGE)
PULSED LIGHT OFF
" " ON
140
160
180
200
220
240
260
DIGITAL INPUT TO DAC
K&E SEMI-LOGARITHMIC 46 6012
4 CYCLES X 70 DIVISIONS
KEUFFEL & ESSER CO.

FIG. 37

Running C2285 with Test input
ch 48 is stuck @ 13208

Input level (Volts)	<PH>
0.83	3565
5.00	9942
10.00	17621
15.00	25325
18.00	29935 ? saturated

3.8

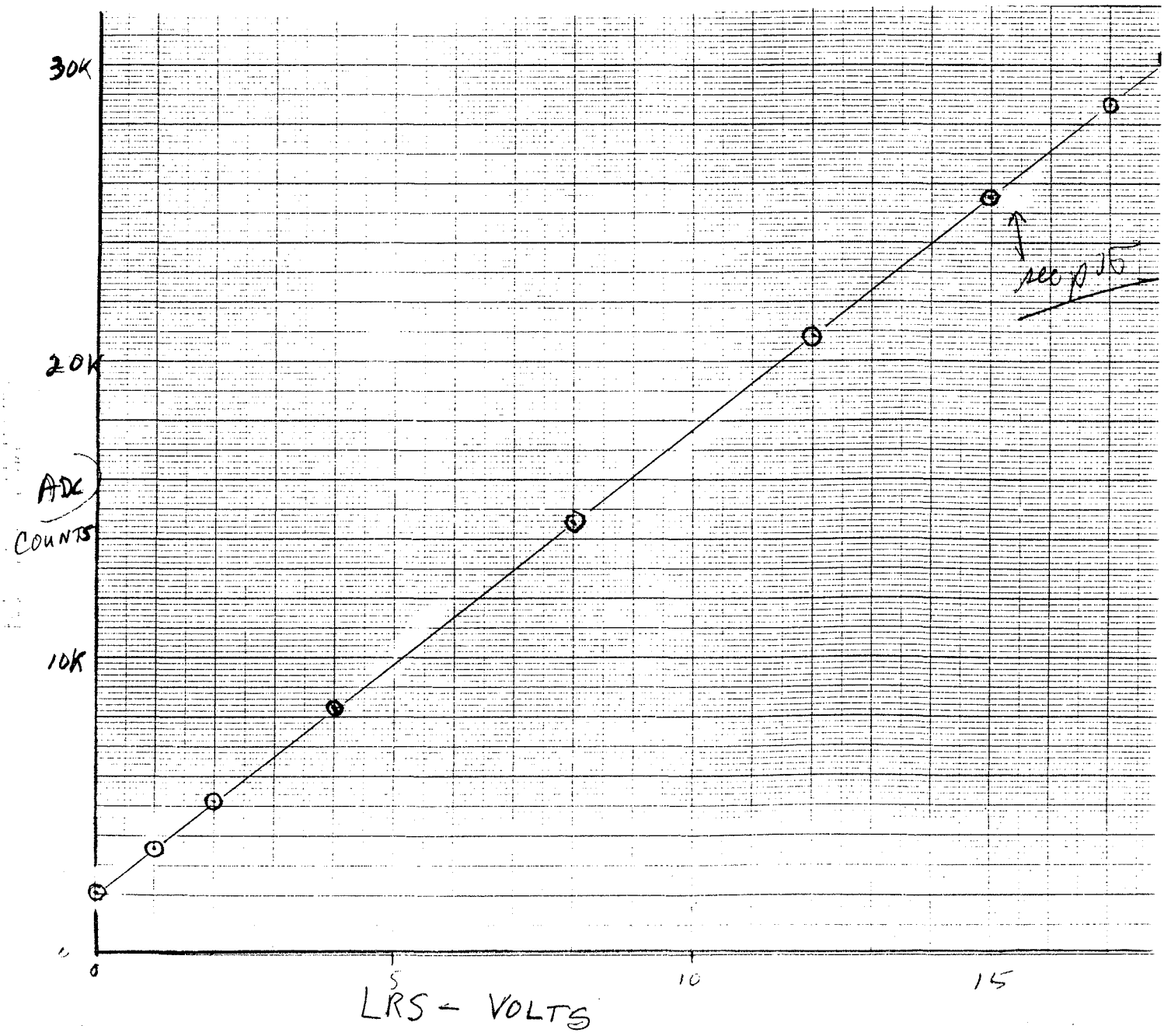

FIG. 38

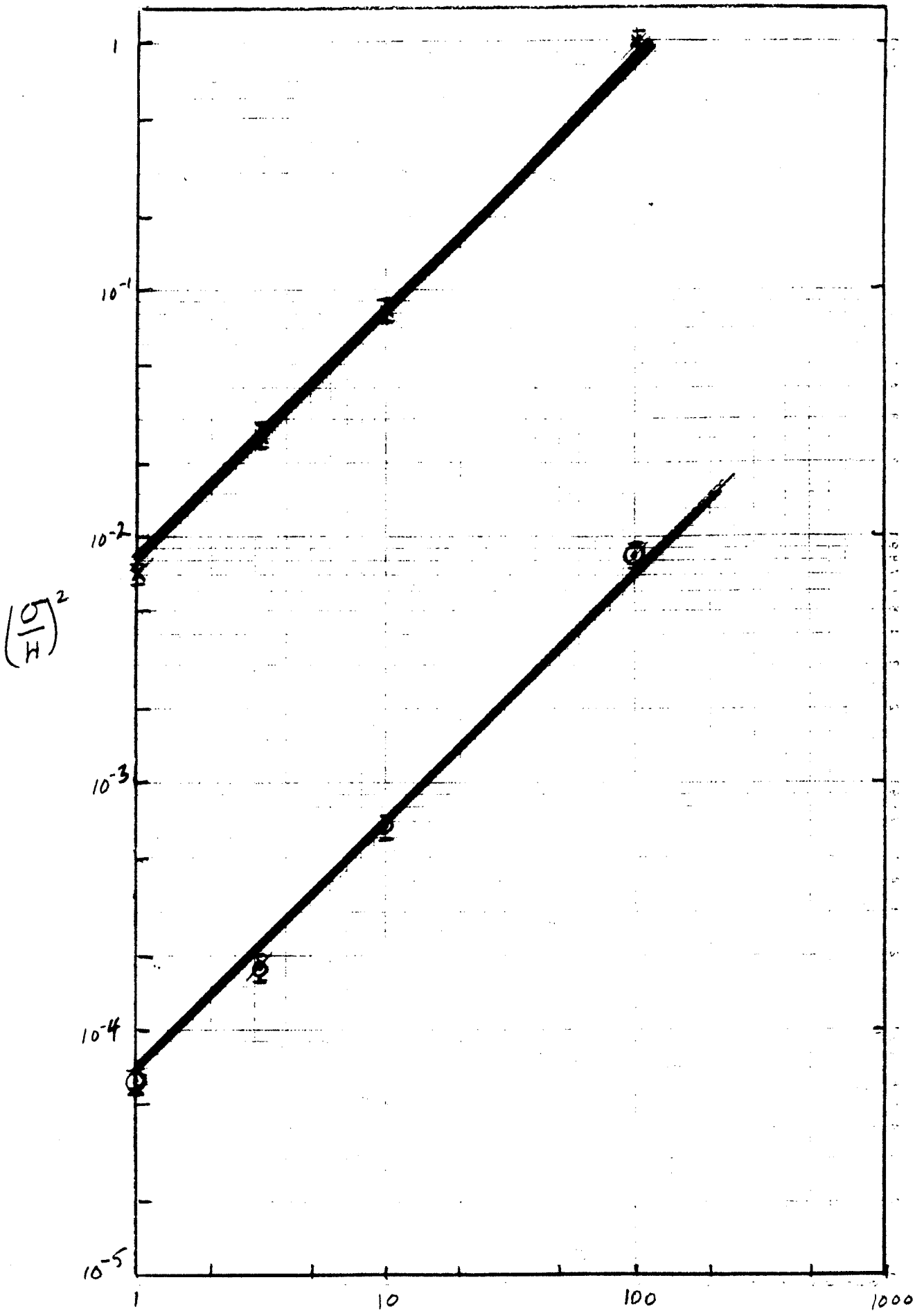

FIG. 3.9

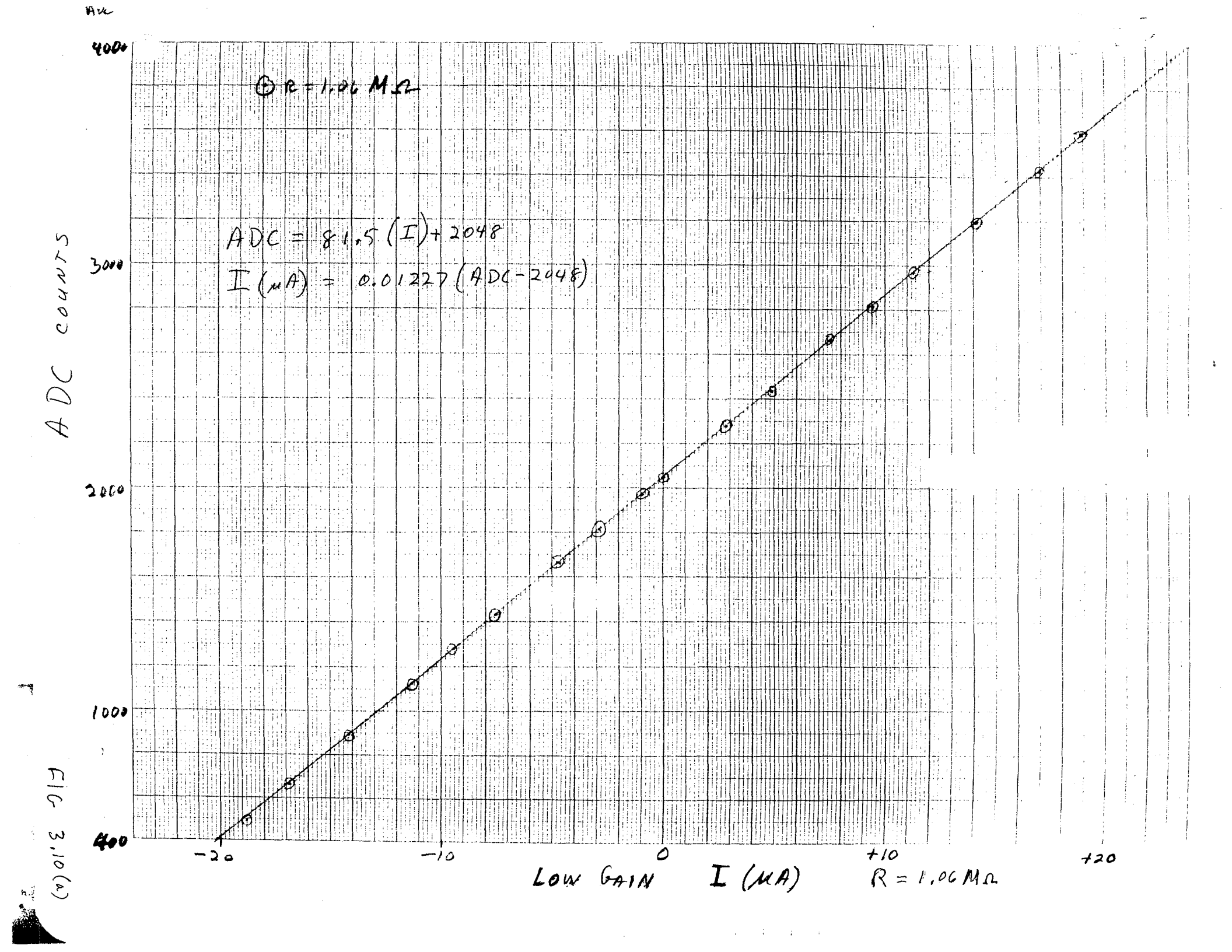
4000
3000
2000
1000
400
ADC counts
⊕ R = 1.06 MΩ
ADC = 81.5 (I) + 2048
I (μA) = 0.01227 (ADC - 2048)
-20
-10
0
+10
+20
LOW GAIN I (μA)
R = 1.06 MΩ

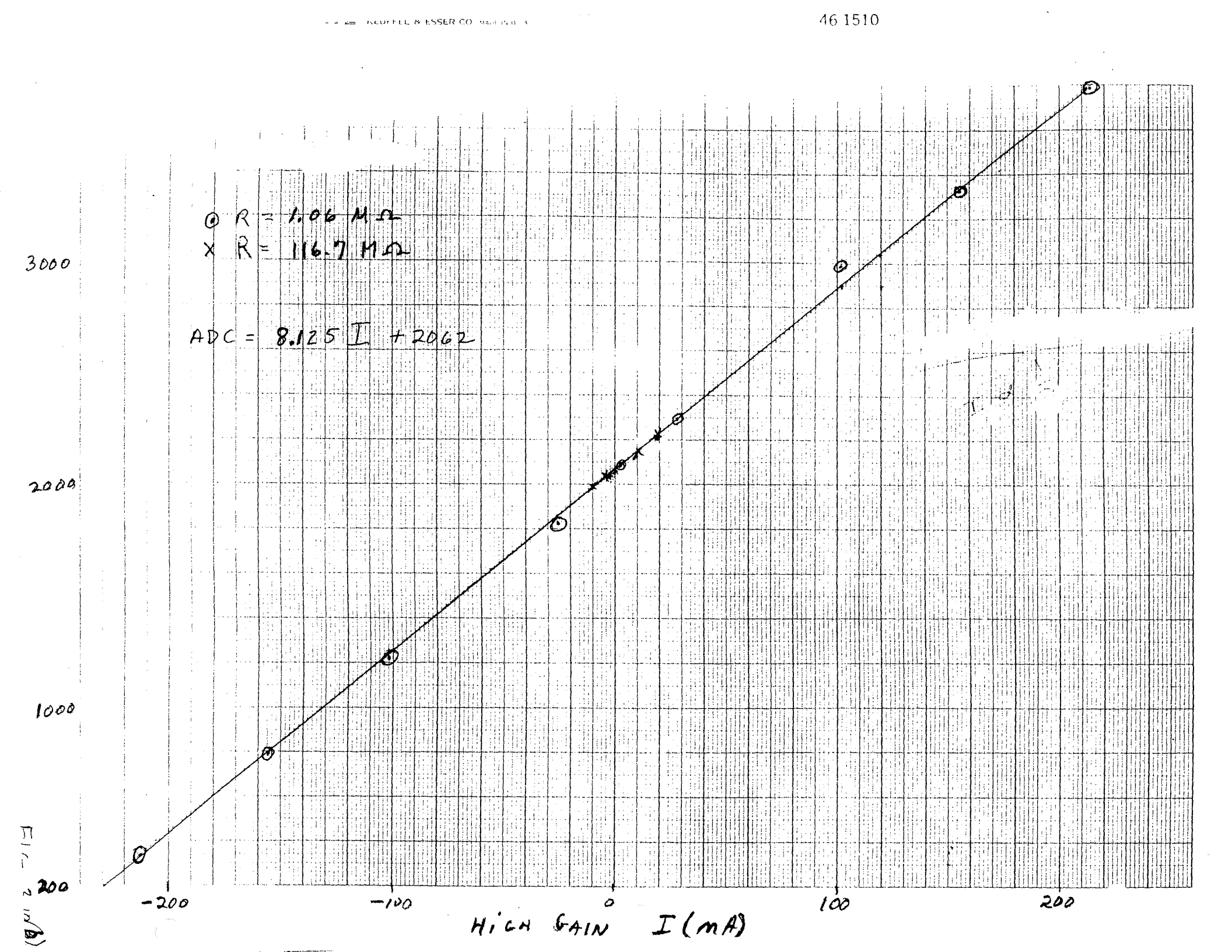
⊙ R = 1.06 MΩ
X R = 116.7 MΩ
ADC = 8.125 I + 2062
3000
2000
1000
200
-200
-100
0
100
200
HIGH GAIN I (mA)

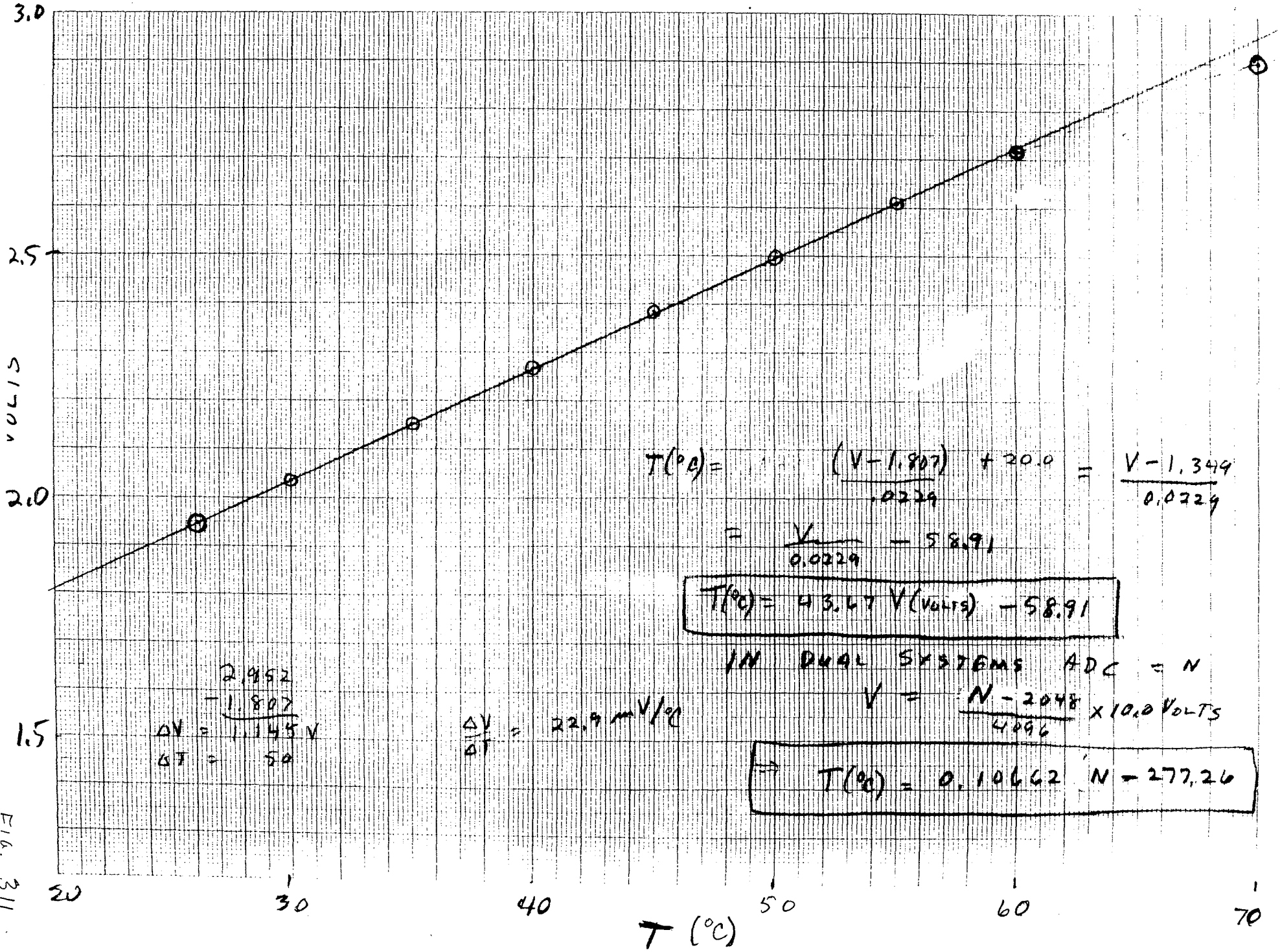

$$T(^\circ C) = \frac{(V - 1.807)}{.0229} + 20.0 = \frac{V - 1.349}{0.0229}$$

$$= \frac{V}{0.0229} - 58.91$$

$$T(^\circ C) = 43.67\ V(\text{VOLTS}) - 58.91$$

IN DUAL SYSTEMS ADC = N

$$V = \frac{N - 2048}{4096} \times 10.0\ \text{VOLTS}$$

$$\Rightarrow T(^\circ C) = 0.10662\ N - 277.26$$

$$\Delta V = 2.952 - 1.807 = 1.145\ V$$

$$\Delta T = 50$$

$$\frac{\Delta V}{\Delta T} = 22.9\ mV/^\circ C$$

FIG. 311

HISTOGRAMME 1 ARG(9)

1=TRUE. // 17=FALS, Corner Tube //

4.1: Mfr. Q.E. PAS DE 3

1	0.0000E+00	0	
2	0.5000	0	
3	1.000	0	
4	1.500	0	
5	2.000	0	
6	2.500	0	
7	3.000	0	
8	3.500	0	
9	4.000	0	
10	4.500	0	
11	5.000	0	
12	5.500	0	
13	6.000	0	
14	6.500	0	
15	7.000	0	
16	7.500	0	
17	8.000	1	
18	8.500	2	X
19	9.000	2	X
20	9.500	2	X
21	10.00	2	X
22	10.50	13	XXXX
23	11.00	19	XXXXXX
24	11.50	49	XXXXXXXXXXXXXXX
25	12.00	62	XXXXXXXXXXXXXXXXXXX
26	12.50	84	XXXXXXXXXXXXXXXXXXXXXXXXX
27	13.00	127	XXXXXXXXXXXXXXXXXXXXXXXXXXXXXXXXXXXXXXX
28	13.50	66	XXXXXXXXXXXXXXXXXXX
29	14.00	184	XXXXXXXXXXXXXXXXXXXXXXXXXXXXXXXXXXXXXXXXXXXXXXXXXXXXXX
30	14.50	112	XXXXXXXXXXXXXXXXXXXXXXXXXXXXXXXX
31	15.00	147	XXXXXXXXXXXXXXXXXXXXXXXXXXXXXXXXXXXXXXXXXX
32	15.50	56	XXXXXXXXXXXXXXXX
33	16.00	41	XXXXXXXXXXXXX
34	16.50	43	XXXXXXXXXXXXX
35	17.00	11	XXXX
36	17.50	13	XXXX
37	18.00	3	X
38	18.50	1	
39	19.00	1	
40	19.50	0	

QUANTUM EFFICIENCY (%)

1041 ENTRIES + 0 UNDERFLOW + 0 OVERFLOW = 1041 TOTAL ENTRIES

MEAN: 14.09 STANDARD DEVIATION: 1.554 PRECISION: 0.1103 (SANS LES DEBORDEMENTS)

Fig. 4.1

HISTOGRAMME ARG(10)

1=TRUE. // 17=FALS, Corner Tube //

4.2a: HV1 PAS DE 2

1	900.0	0	
2	920.0	1	X
3	940.0	15	XXXXXXXX
4	960.0	47	XXXXXXXXXXXXXXXXXXXXXXX
5	980.0	110	XXXXXXXXXXXXXXXXXXXXXXXXXXXXXXXXXXXXXXXXXXXXXXXXXX
6	1000.	127	XXXXXXXXXXXXXXXXXXXXXXXXXXXXXXXXXXXXXXXXXXXXXXXXXXXXXXXXXX
7	1020.	133	XXXXXXXXXXXXXXXXXXXXXXXXXXXXXXXXXXXXXXXXXXXXXXXXXXXXXXXXXXXXXXXX
8	1040.	134	XXXXXXXXXXXXXXXXXXXXXXXXXXXXXXXXXXXXXXXXXXXXXXXXXXXXXXXXXXXXXXXX
9	1060.	113	XXXXXXXXXXXXXXXXXXXXXXXXXXXXXXXXXXXXXXXXXXXXXXXXXXXXXX
10	1080.	104	XXXXXXXXXXXXXXXXXXXXXXXXXXXXXXXXXXXXXXXXXXXXXXXXXX
11	1100.	98	XXXXXXXXXXXXXXXXXXXXXXXXXXXXXXXXXXXXXXXXXX
12	1120.	76	XXXXXXXXXXXXXXXXXXXXXXXXXXXXXXXXXX
13	1140.	42	XXXXXXXXXXXXXXXXXXX
14	1160.	28	XXXXXXXXXXXXX
15	1180.	11	XXXXXX
16	1200.	2	X
17	1220.	0	
18	1240.	0	
19	1260.	0	
20	1280.	0	
21	1300.	0	
22	1320.	0	
23	1340.	0	
24	1360.	0	
25	1380.	0	
26	1400.	0	
27	1420.	0	
28	1440.	0	
29	1460.	0	
30	1480.	0	

VOLTS

1041 ENTRIES + 0 UNDERFLOW + 0 OVERFLOW = 1041 TOTAL ENTRIES

MEAN: 1057. STANDARD DEVIATION: 54.83 PRECISION: 0.5186E-01 (SANS LES DEBORDEMENTS)

FIG 4.2(a)

HISTOGRAMME 3 ARG(11)

1=TRUE. // 17=FALS. Corner Tube //

4.2b: HV2 PAS DE 2

1	900.0	0	
2	920.0	0	
3	940.0	0	
4	960.0	0	
5	980.0	0	
6	1000.	0	
7	1020.	4	XX
8	1040.	24	XXXXXXXXXXXX
9	1060.	46	XXXXXXXXXXXXXXXXXXXXXX
10	1080.	113	XXXXXXXXXXXXXXXXXXXXXXXXXXXXXXXXXXXXXXXXXXXXXXXXXXXXXX
11	1100.	110	XXXXXXXXXXXXXXXXXXXXXXXXXXXXXXXXXXXXXXXXXXXXXXXXXXXXX
12	1120.	109	XXXXXXXXXXXXXXXXXXXXXXXXXXXXXXXXXXXXXXXXXXXXXXXXXXXXX
13	1140.	126	XXXXXXXXXXXXXXXXXXXXXXXXXXXXXXXXXXXXXXXXXXXXXXXXXXXXXXXXXXXXXXXXX
14	1160.	96	XXXXXXXXXXXXXXXXXXXXXXXXXXXXXXXXXXXXXXXXXXXXXX
15	1180.	109	XXXXXXXXXXXXXXXXXXXXXXXXXXXXXXXXXXXXXXXXXXXXXXXXXXXXXX
16	1200.	84	XXXXXXXXXXXXXXXXXXXXXXXXXXXXXXXXXXXXXXXX
17	1220.	87	XXXXXXXXXXXXXXXXXXXXXXXXXXXXXXXXXXXXXXXXXXX
18	1240.	59	XXXXXXXXXXXXXXXXXXXXXXXXXXXX
19	1260.	35	XXXXXXXXXXXXXXXXX
20	1280.	25	XXXXXXXXXXXXX
21	1300.	10	XXXXX
22	1320.	2	X
23	1340.	2	X
24	1360.	0	
25	1380.	0	
26	1400.	0	
27	1420.	0	
28	1440.	0	
29	1460.	0	
30	1480.	0	

VOLTS

1041 ENTRIES + 0 UNDERFLOW + 0 OVERFLOW = 1041 TOTAL ENTRIES

MEAN: 1163. STANDARD DEVIATION: 62.25 PRECISION: 0.5351E-01 (SANS LES DEBORDEMENTS)

Fig. 4.2(b)

```
HISTOGRAMME      ARG( 12)

   1=TRUE.                        // 17=FALS.Corner Tube          //

   4.Sc: HV3                                                PAS DE    2

   1      900.0            0
   2      920.0            0
   3      940.0            0
   4      960.0            0
   5      980.0            0
   6      1000.            0
   7      1020.            0
   8      1040.            0
   9      1060.            0
  10      1080.            0
  11      1100.            0
  12      1120.            3   XX
  13      1140.           16   XXXXXXXX
  14      1160.           41   XXXXXXXXXXXXXXXXXXXX
  15      1180.           71   XXXXXXXXXXXXXXXXXXXXXXXXXXXXXXXXXX
  16      1200.          108   XXXXXXXXXXXXXXXXXXXXXXXXXXXXXXXXXXXXXXXXXXXXXXXXXX
  17      1220.           97   XXXXXXXXXXXXXXXXXXXXXXXXXXXXXXXXXXXXXXXXXXXXXX
  18      1240.           98   XXXXXXXXXXXXXXXXXXXXXXXXXXXXXXXXXXXXXXXXXXXXXX
  19      1260.          110   XXXXXXXXXXXXXXXXXXXXXXXXXXXXXXXXXXXXXXXXXXXXXXXXXX
  20      1280.           93   XXXXXXXXXXXXXXXXXXXXXXXXXXXXXXXXXXXXXX
  21      1300.           90   XXXXXXXXXXXXXXXXXXXXXXXXXXXXXXXXXXXXXX
  22      1320.           82   XXXXXXXXXXXXXXXXXXXXXXXXXXXXXXXXXXXX
  23      1340.           75   XXXXXXXXXXXXXXXXXXXXXXXXXXXXXXXXXX
  24      1360.           60   XXXXXXXXXXXXXXXXXXXXXXXXXXXX
  25      1380.           46   XXXXXXXXXXXXXXXXXXXX
  26      1400.           27   XXXXXXXXXXXXX
  27      1420.           19   XXXXXXXXXX
  28      1440.           11   XXXXXX
  29      1460.            2   X
  30      1480.            2   X

    1041 ENTRIES  +         0 UNDERFLOW  +         0 OVERFLOW   =        1041 TOTAL ENTRIES

     MEAN:    1282.        STANDARD DEVIATION:    71.34        PRECISION:   0.5565E-01        (SANS LES DEBORDEMENTS)
```

VOLTS

FIG. 4.2(C)

HISTOGRAMME 9 ARG(206)

1=TRUE, // 17=FALS,Corner Tube //

T2.1 N12 PAS DE 4

1	5.000	0	
2	5.100	0	
3	5.200	0	
4	5.300	0	
5	5.400	0	
6	5.500	0	
7	5.600	0	
8	5.700	1	
9	5.800	0	
10	5.900	0	
11	6.000	0	
12	6.100	0	
13	6.200	0	
14	6.300	0	
15	6.400	1	
16	6.500	0	
17	6.600	0	
18	6.700	5	X
19	6.800	20	XXXXX
20	6.900	68	XXXXXXXXXXXXXXXX
21	7.000	105	XXXXXXXXXXXXXXXXXXXXXXXXX
22	7.100	156	XXXXXXXXXXXXXXXXXXXXXXXXXXXXXXXXXXXX
23	7.200	264	XXXXXXXXXXXXXXXXXXXXXXXXXXXXXXXXXXXXXXXXXXXXXXXXXXXXXXXXXXXXXXXXXXXXXXX
24	7.300	222	XXXXXXXXXXXXXXXXXXXXXXXXXXXXXXXXXXXXXXXXXXXXXXXXXXXXXX
25	7.400	126	XXXXXXXXXXXXXXXXXXXXXXXXXXXXXX
26	7.500	46	XXXXXXXXXXX
27	7.600	21	XXXXX
28	7.700	5	X
29	7.800	1	
30	7.900	0	

1041 ENTRIES + 0 UNDERFLOW + 0 OVERFLOW = 1041 TOTAL ENTRIES

MEAN: 7.253 STANDARD DEVIATION: 0.1838 PRECISION: 0.2534E-01 (SANS LES DEBORDEMENTS)

Fig 4.3 (a)

HISTOGRAMME ARG(207)

1=TRUE, // 17=FALS,Corner Tube //

T2.1 N23 PAS DE 3

1	5.000	0	
2	5.100	0	
3	5.200	0	
4	5.300	0	
5	5.400	0	
6	5.500	0	
7	5.600	0	
8	5.700	0	
9	5.800	0	
10	5.900	0	
11	6.000	0	
12	6.100	1	
13	6.200	0	
14	6.300	0	
15	6.400	1	
16	6.500	4	X
17	6.600	15	XXXXX
18	6.700	35	XXXXXXXXXXX
19	6.800	71	XXXXXXXXXXXXXXXXXXXXXXX
20	6.900	135	XXXXXXXXXXXXXXXXXXXXXXXXXXXXXXXXXXXXXXXXXX
21	7.000	153	XXXXXXXXXXXXXXXXXXXXXXXXXXXXXXXXXXXXXXXXXXXXXXX
22	7.100	197	XXXXXXXXXXXXXXXXXXXXXXXXXXXXXXXXXXXXXXXXXXXXXXXXXXXXXXXXXXXXXXXXXXX
23	7.200	154	XXXXXXXXXXXXXXXXXXXXXXXXXXXXXXXXXXXXXXXXXXXXXXX
24	7.300	134	XXXXXXXXXXXXXXXXXXXXXXXXXXXXXXXXXXXXXXXX
25	7.400	90	XXXXXXXXXXXXXXXXXXXXXXXXXX
26	7.500	35	XXXXXXXXXXX
27	7.600	14	XXXXX
28	7.700	2	X
29	7.800	0	
30	7.900	0	

1041 ENTRIES + 0 UNDERFLOW + 0 OVERFLOW = 1041 TOTAL ENTRIES

MEAN: 7.153 STANDARD DEVIATION: 0.2182 PRECISION: 0.3050E-01 (SANS LES DEBORDEMENTS)

Fig. 4.3(b)

HISTOGRAMME 11 ARG(222)

1=TRUE, // 17=FALS,Corner Tube //

T2.1 ALOG10(DKI1) PAS DE 3

1	-3.000	0	
2	-2.800	0	
3	-2.600	0	
4	-2.400	0	
5	-2.200	0	
6	-2.000	56	XXXXXXXXXXXXXXXXX
7	-1.800	73	XXXXXXXXXXXXXXXXXXXXX
8	-1.600	76	XXXXXXXXXXXXXXXXXXXXX
9	-1.400	203	XXXXXXXXXXXXXXXXXXXXXXXXXXXXXXXXXXXXXXXXXXXXXXXXXXXXXXXXXXXXXXXXXXXXXX
10	-1.200	125	XXXXXXXXXXXXXXXXXXXXXXXXXXXXXXXXXXXXXXX
11	-1.000	152	XXXXXXXXXXXXXXXXXXXXXXXXXXXXXXXXXXXXXXXXXXXXXXXXX
12	-0.8000	143	XXXXXXXXXXXXXXXXXXXXXXXXXXXXXXXXXXXXXXXXXXXXXX
13	-0.6000	80	XXXXXXXXXXXXXXXXXXXXXXXXX
14	-0.4000	62	XXXXXXXXXXXXXXXXXXX
15	-0.2000	40	XXXXXXXXXXXX
16	0.0000E+00	18	XXXXXX
17	0.2000	4	X
18	0.4000	3	X
19	0.6000	0	
20	0.8000	0	

log (I_DARK)

1035 ENTRIES + 6 UNDERFLOW + 0 OVERFLOW = 1041 TOTAL ENTRIES

MEAN: -1.021 STANDARD DEVIATION: 0.5052 PRECISION: -0.4949 (SANS LES DEBORDEMENTS)

Fig 4.4(a)

HISTOGRAMME ARG(223)

1=TRUE, // 17=FALS,Corner Tube //

T2.1 ALOG10(DKI2) PAS DE 3

1	-3.000	0	
2	-2.800	0	
3	-2.600	0	
4	-2.400	0	
5	-2.200	0	
6	-2.000	19	XXXXXX
7	-1.800	44	XXXXXXXXXXXXXX
8	-1.600	50	XXXXXXXXXXXXXXXX
9	-1.400	158	XXXXXXXXXXXXXXXXXXXXXXXXXXXXXXXXXXXXXXXXXXXXXXXXXX
10	-1.200	120	XXXXXXXXXXXXXXXXXXXXXXXXXXXXXXXXXXXX
11	-1.000	160	XXXXXXXXXXXXXXXXXXXXXXXXXXXXXXXXXXXXXXXXXXXXXXXXXX
12	-0.8000	157	XXXXXXXXXXXXXXXXXXXXXXXXXXXXXXXXXXXXXXXXXXXXXXXXX
13	-0.6000	113	XXXXXXXXXXXXXXXXXXXXXXXXXXXXXXXXXX
14	-0.4000	98	XXXXXXXXXXXXXXXXXXXXXXXXXXXXXX
15	-0.2000	50	XXXXXXXXXXXXXXXX
16	0.0000E+00	47	XXXXXXXXXXXXXXX
17	0.2000	18	XXXXXX
18	0.4000	4	X
19	0.6000	2	X
20	0.8000	0	

log (I_{DREX})

1040 ENTRIES + 1 UNDERFLOW + 0 OVERFLOW = 1041 TOTAL ENTRIES

MEAN: -0.8328 STANDARD DEVIATION: 0.5118 PRECISION: -0.6145 (SANS LES DEBORDEMENTS)

FIG 4.4(b)

HISTOGRAMME 13 ARG(224)

1=TRUE, // 17=FALS,Corner Tube //

T2.1 ALOG10(DKI3) PAS DE 3

1	-3.000	0	
2	-2.800	0	
3	-2.600	0	
4	-2.400	0	
5	-2.200	0	
6	-2.000	0	
7	-1.800	22	XXXXXXX
8	-1.600	24	XXXXXXXX
9	-1.400	86	XXXXXXXXXXXXXXXXXXXXXXXXXXX
10	-1.200	96	XXXXXXXXXXXXXXXXXXXXXXXXXXXX
11	-1.000	142	XXXXXXXXXXXXXXXXXXXXXXXXXXXXXXXXXXXXXXXXXX
12	-0.8000	170	XXXXXXXXXXXXXXXXXXXXXXXXXXXXXXXXXXXXXXXXXXXXXXXXXXXXXX
13	-0.6000	123	XXXXXXXXXXXXXXXXXXXXXXXXXXXXXXXXXXXXX
14	-0.4000	131	XXXXXXXXXXXXXXXXXXXXXXXXXXXXXXXXXXXXXXXXX
15	-0.2000	86	XXXXXXXXXXXXXXXXXXXXXXXXXX
16	0.0000E+00	66	XXXXXXXXXXXXXXXXXXXX
17	0.2000	56	XXXXXXXXXXXXXXXXX
18	0.4000	24	XXXXXXXX
19	0.6000	14	XXXXX
20	0.8000	1	

log (I dark)

1041 ENTRIES + 0 UNDERFLOW + 0 OVERFLOW = 1041 TOTAL ENTRIES

MEAN: -0.5828 STANDARD DEVIATION: 0.5337 PRECISION: -0.9158 (SANS LES DEBORDEMENTS)

Fig 4.4 (c)

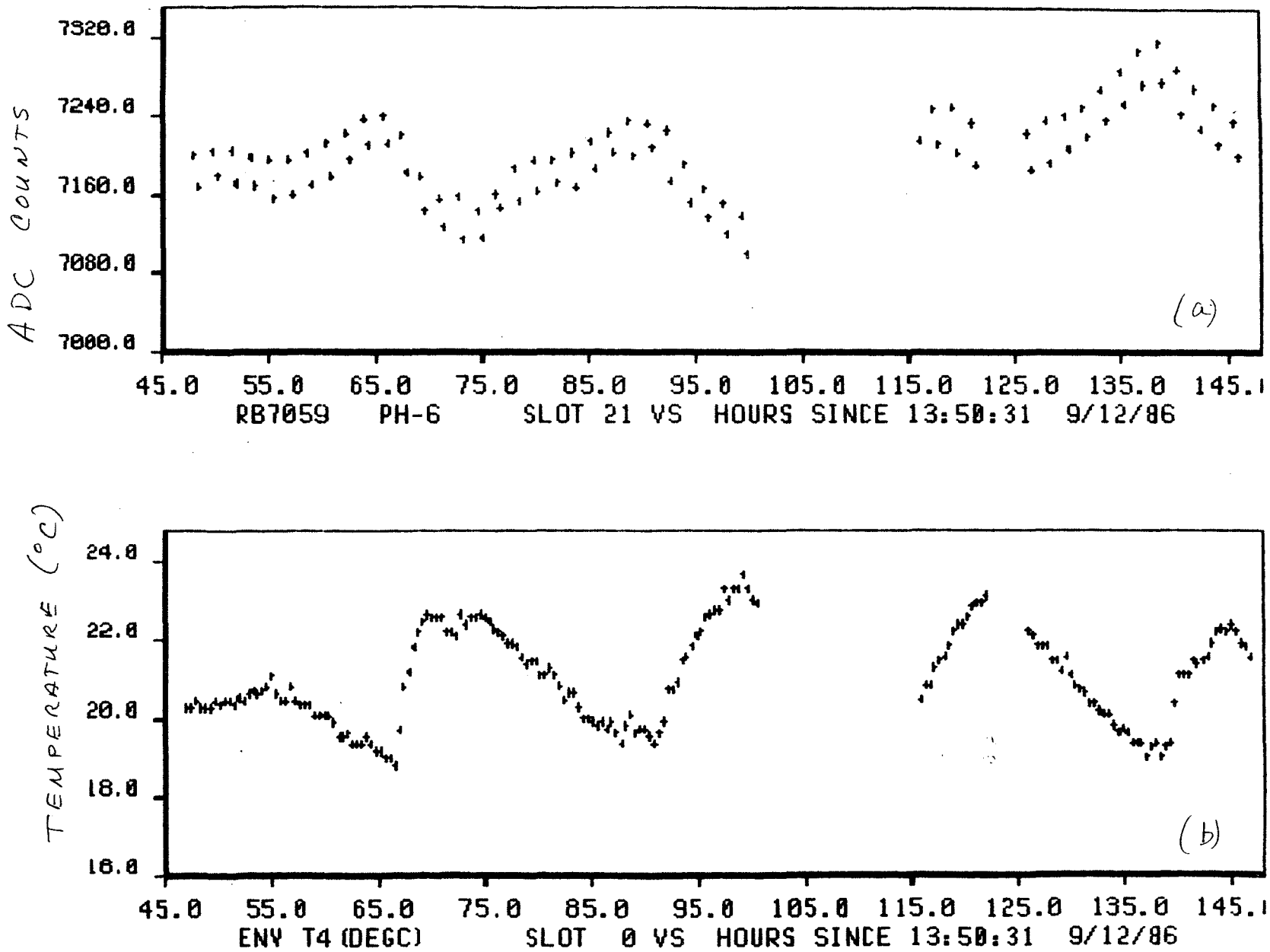
ADC COUNTS
7320.0
7240.0
7160.0
7080.0
7000.0
(a)
45.0 55.0 65.0 75.0 85.0 95.0 105.0 115.0 125.0 135.0 145.
RB7059 PH-6 SLOT 21 VS HOURS SINCE 13:50:31 9/12/86
TEMPERATURE (°C)
24.0
22.0
20.0
18.0
16.0
(b)
45.0 55.0 65.0 75.0 85.0 95.0 105.0 115.0 125.0 135.0 145.
ENV T4 (DEGC) SLOT 0 VS HOURS SINCE 13:50:31 9/12/86

FIG. 4.5

HISTOGRAMME 17 ARG(203)

1=TRUE, // 17=FALS,Corner Tube // 81=FALS,Big Gain Uncert. //

T2.1 Av. Gn. (*10E5) PAS DE 2

1	0.0000E+00	0	
2	0.1000	0	
3	0.2000	0	
4	0.3000	0	
5	0.4000	1	X
6	0.5000	4	XX
7	0.6000	35	XXXXXXXXXXXXXXXXX
8	0.7000	84	XXXXXXXXXXXXXXXXXXXXXXXXXXXXXXXXXXXXXXXX
9	0.8000	145	XXXXXXXXXXXXXXXXXXXXXXXXXXXXXXXXXXXXXXXXXXXXXXXXXXXXXXXXXXXXXXXXXXXXXXX
10	0.9000	142	XXXXXXXXXXXXXXXXXXXXXXXXXXXXXXXXXXXXXXXXXXXXXXXXXXXXXXXXXXXXXXXXXXXXX
11	1.000	102	XXXXXXXXXXXXXXXXXXXXXXXXXXXXXXXXXXXXXXXXXXXXXX
12	1.100	63	XXXXXXXXXXXXXXXXXXXXXXXXXXXXX
13	1.200	56	XXXXXXXXXXXXXXXXXXXXXXXXXX
14	1.300	35	XXXXXXXXXXXXXXXXX
15	1.400	38	XXXXXXXXXXXXXXXXXX
16	1.500	13	XXXXXXX
17	1.600	4	XX
18	1.700	6	XXX
19	1.800	3	XX
20	1.900	4	XX
21	2.000	2	X
22	2.100	1	X
23	2.200	0	
24	2.300	0	
25	2.400	0	
26	2.500	0	
27	2.600	0	
28	2.700	0	
29	2.800	0	
30	2.900	0	

GAIN (x10⁵)

738 ENTRIES + 9 UNDERFLOW + 0 OVERFLOW = 747 TOTAL ENTRIES

MEAN: 1.024 STANDARD DEVIATION: 0.2549 PRECISION: 0.2489 (SANS LES DEBORDEMENTS)

Fig. 4.6

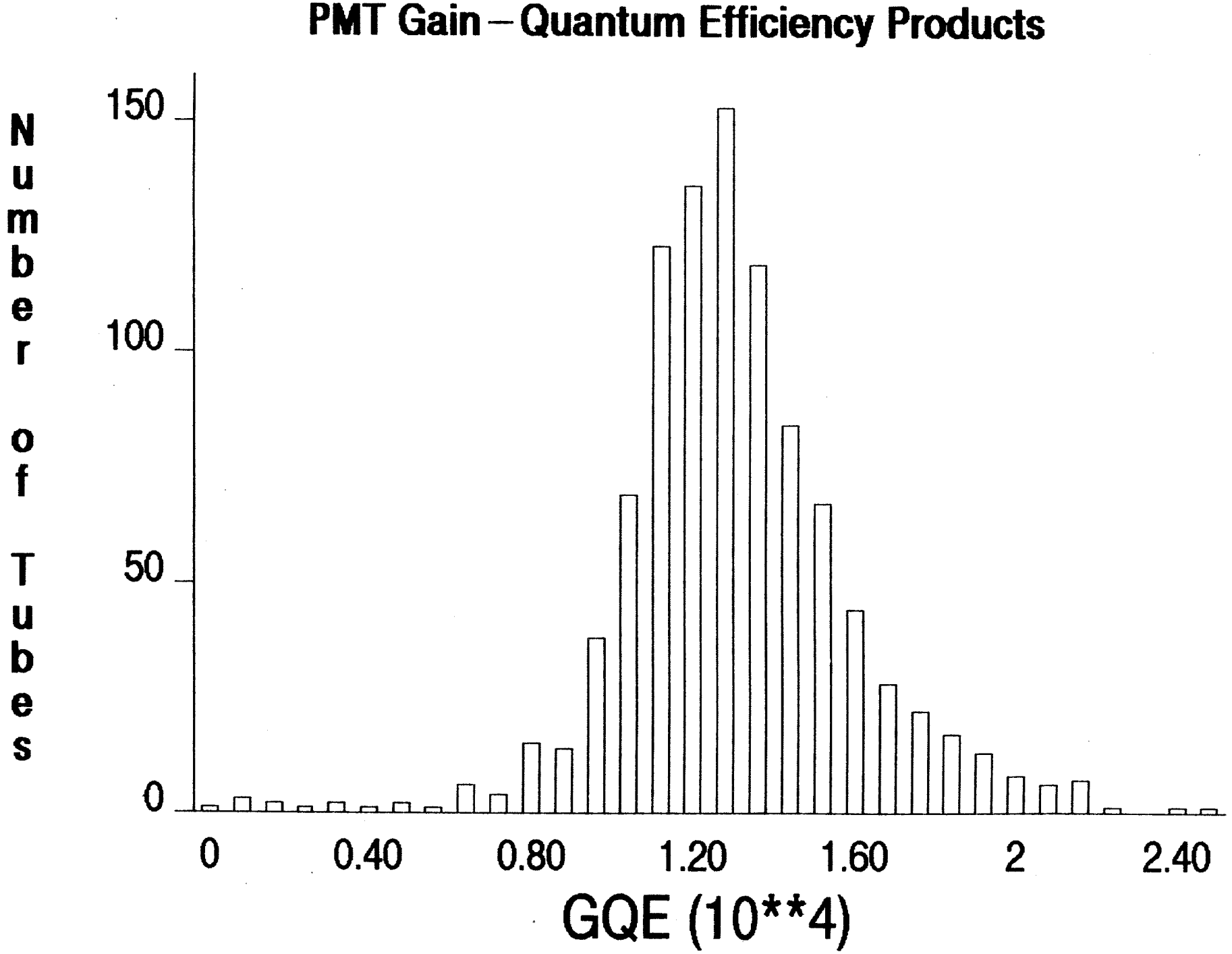
PMT Gain – Quantum Efficiency Products
Number of Tubes
150
100
50
0
0
0.40
0.80
1.20
1.60
2
2.40
GQE (10**4)

Fig. 4.7

```
HISTOGRAMME  14  ARG(332)

  1=TRUE,                // 17=FALS,Corner Tube        //  75=FALS,Batch 25          //  76=FALS,Batch 26        //

  T2.1 Corr. PH(5)                                  PAS DE    4

  1   0.0000E+00     0
  2    1.000         0
  3    2.000         0
  4    3.000         0
  5    4.000         0
  6    5.000         0
  7    6.000         0
  8    7.000         0
  9    8.000         0
 10    9.000         0
 11    10.00         0
 12    11.00         0
 13    12.00         0
 14    13.00         0
 15    14.00         0
 16    15.00         0
 17    16.00         0
 18    17.00         1
 19    18.00         0
 20    19.00         0
 21    20.00         3  X
 22    21.00         3  X
 23    22.00         4  X
 24    23.00        14  XXXX
 25    24.00        54  XXXXXXXXXXXXXX
 26    25.00       157  XXXXXXXXXXXXXXXXXXXXXXXXXXXXXXXXXXXXXXXX
 27    26.00       284  XXXXXXXXXXXXXXXXXXXXXXXXXXXXXXXXXXXXXXXXXXXXXXXXXXXXXXXXXXXXXXXXXXXXXXX
 28    27.00       251  XXXXXXXXXXXXXXXXXXXXXXXXXXXXXXXXXXXXXXXXXXXXXXXXXXXXXXXXXXXXXXX
 29    28.00       123  XXXXXXXXXXXXXXXXXXXXXXXXXXXXXXX
 30    29.00        53  XXXXXXXXXXXXXX
 31    30.00        12  XXX
 32    31.00         4  X
 33    32.00         0
 34    33.00         0
 35    34.00         0
 36    35.00         0
 37    36.00         0
 38    37.00         0
 39    38.00         0
 40    39.00         0

    963 ENTRIES  +      0 UNDERFLOW  +      0 OVERFLOW   =      963 TOTAL ENTRIES

    MEAN:   26.89    STANDARD DEVIATION:   1.494    PRECISION:  0.5555E-01     (SANS LES DEBORDEMENTS)
```

FIG. 4.8

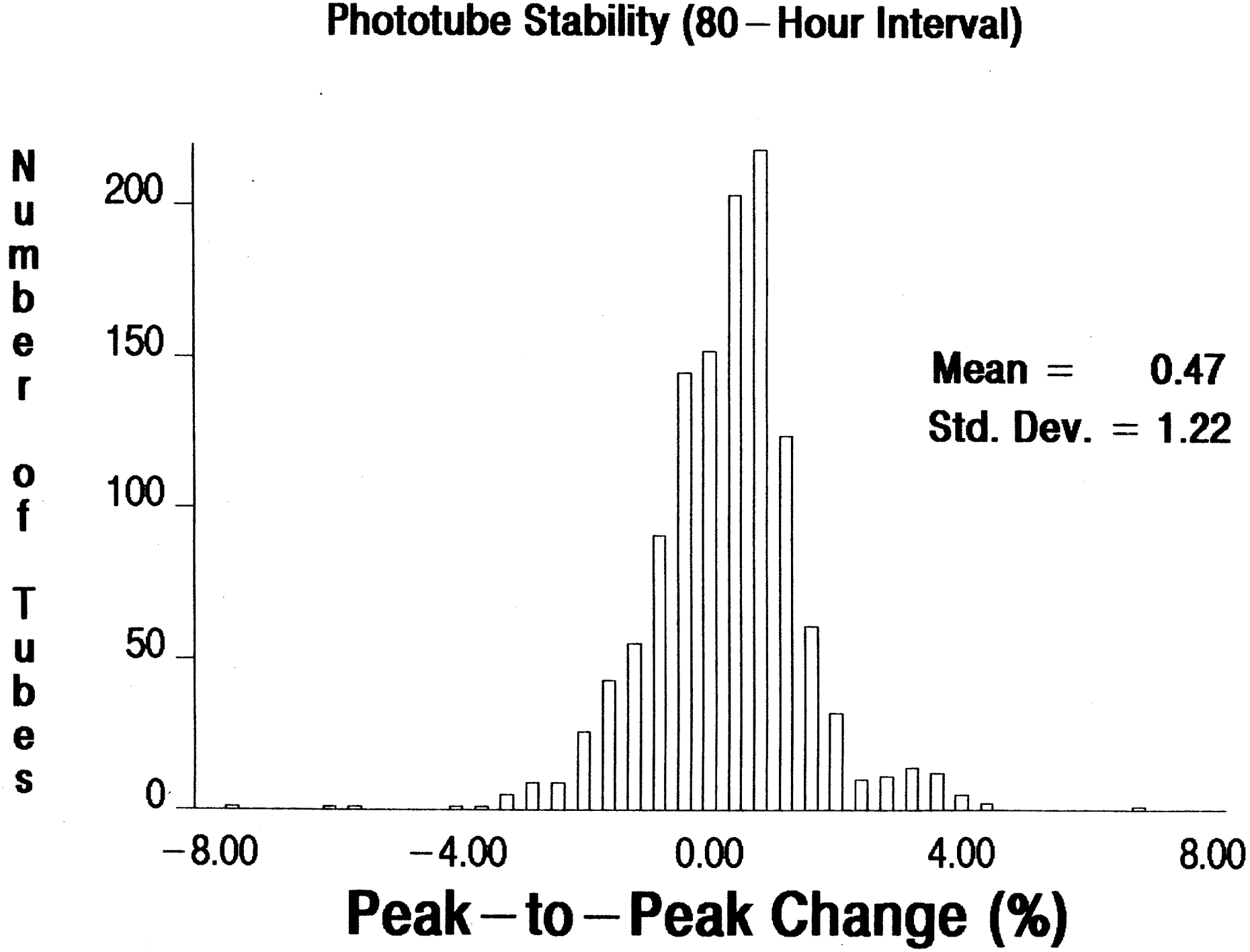
Phototube Stability (80 – Hour Interval)
Number of Tubes
200
150
100
50
0
Mean = 0.47
Std. Dev. = 1.22
–8.00
–4.00
0.00
4.00
8.00
Peak – to – Peak Change (%)

Fig. 4.9

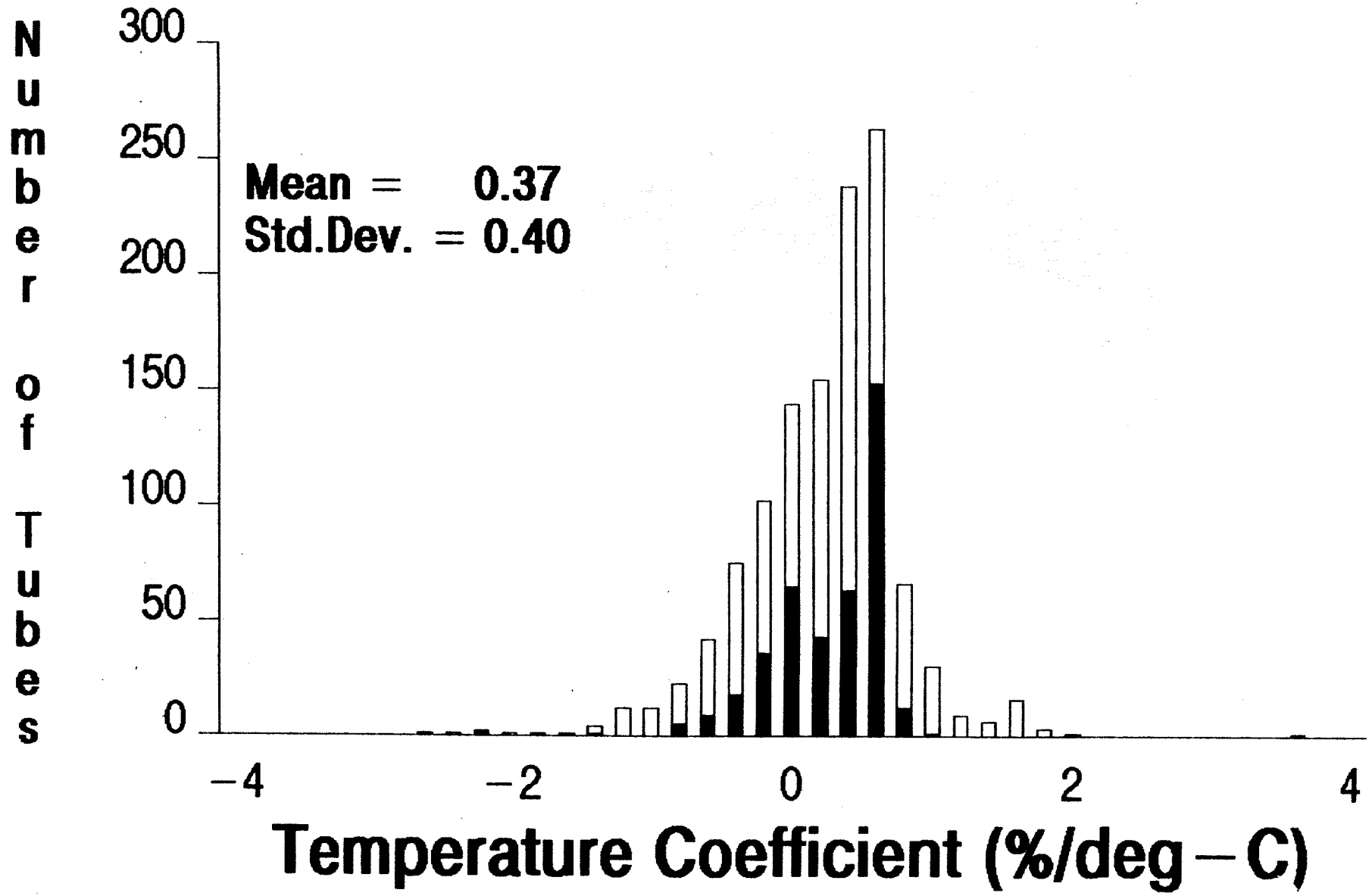
Number of Tubes
300
250
200
150
100
50
0
Mean = 0.37
Std.Dev. = 0.40
−4
−2
0
2
4
Temperature Coefficient (%/deg−C)

Fig. 4.1a

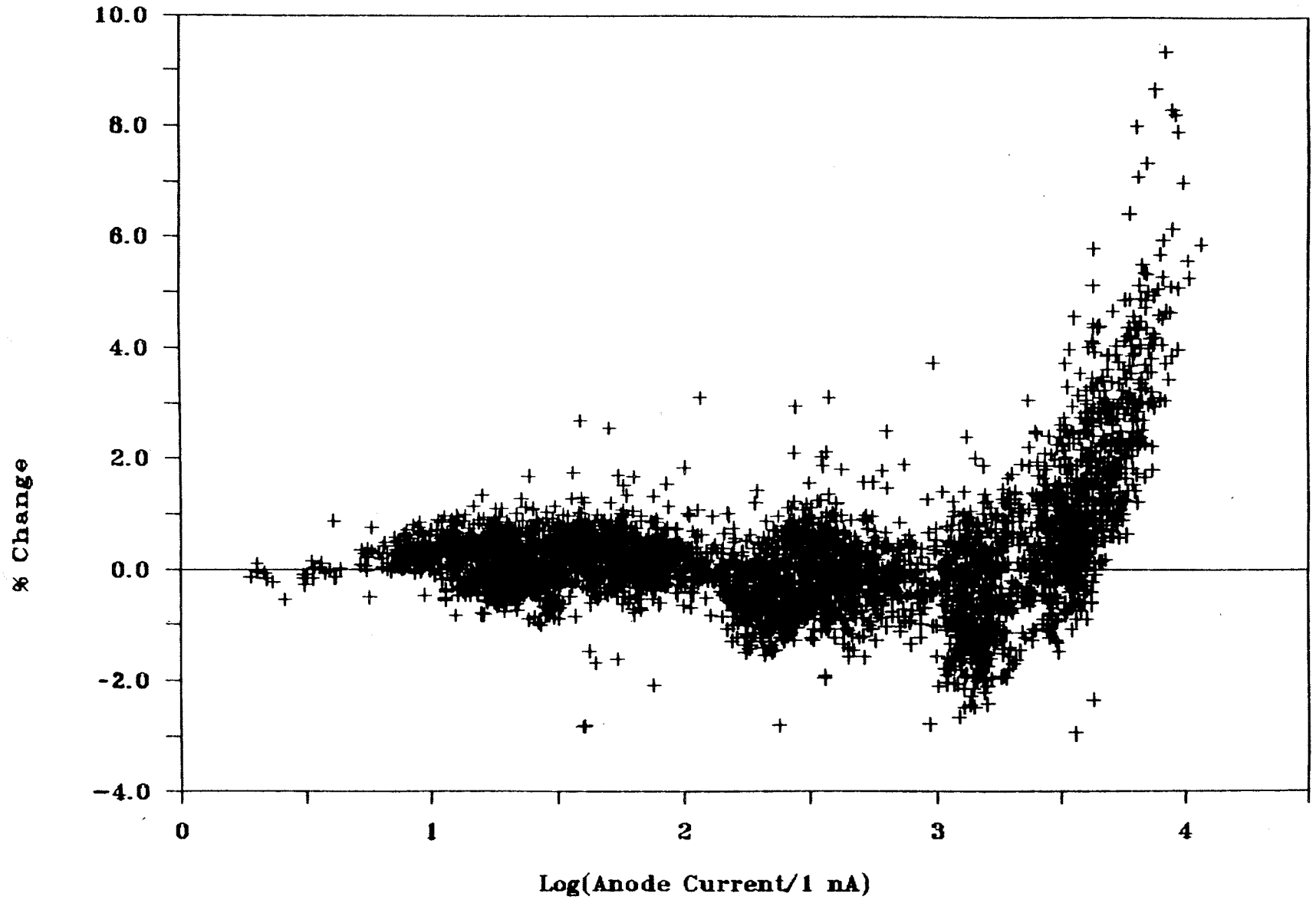

Fig. 4.11

HISTOGRAMME 27 ARG(149)

1=TRUE. // 17=FALS, Corner Tube //

4.11 Lin. chi sq. PAS DE 3

1	0.0000E+00	0	
2	1.000	0	
3	2.000	0	
4	3.000	1	
5	4.000	11	XXXX
6	5.000	169	XXXXXXXXXXXXXXXXXXXXXXXXXXXXXXXXXXXXXXXXXXXXXXXXXXXXXXXXX
7	6.000	177	XXXXXXXXXXXXXXXXXXXXXXXXXXXXXXXXXXXXXXXXXXXXXXXXXXXXXXXXXXXXXXXX
8	7.000	84	XXXXXXXXXXXXXXXXXXXXXXXXXXXX
9	8.000	84	XXXXXXXXXXXXXXXXXXXXXXXXXXXX
10	9.000	87	XXXXXXXXXXXXXXXXXXXXXXXXXXXXX
11	10.00	91	XXXXXXXXXXXXXXXXXXXXXXXXXXXXXXX
12	11.00	79	XXXXXXXXXXXXXXXXXXXXXXXXXXX
13	12.00	45	XXXXXXXXXXXXXXX
14	13.00	46	XXXXXXXXXXXXXXX
15	14.00	45	XXXXXXXXXXXXXXX
16	15.00	38	XXXXXXXXXXXXX
17	16.00	23	XXXXXXXX
18	17.00	15	XXXXX
19	18.00	5	XX
20	19.00	11	XXXX
21	20.00	9	XXX
22	21.00	5	XX
23	22.00	5	XX
24	23.00	2	X
25	24.00	3	X
26	25.00	2	X
27	26.00	2	X
28	27.00	2	X
29	28.00	0	
30	29.00	0	

χ^2

1041 ENTRIES + 0 UNDERFLOW + 0 OVERFLOW = 1041 TOTAL ENTRIES

MEAN: 9.834 STANDARD DEVIATION: 4.145 PRECISION: 0.4215 (SANS LES DEBORDEMENTS)

Fig 4.12

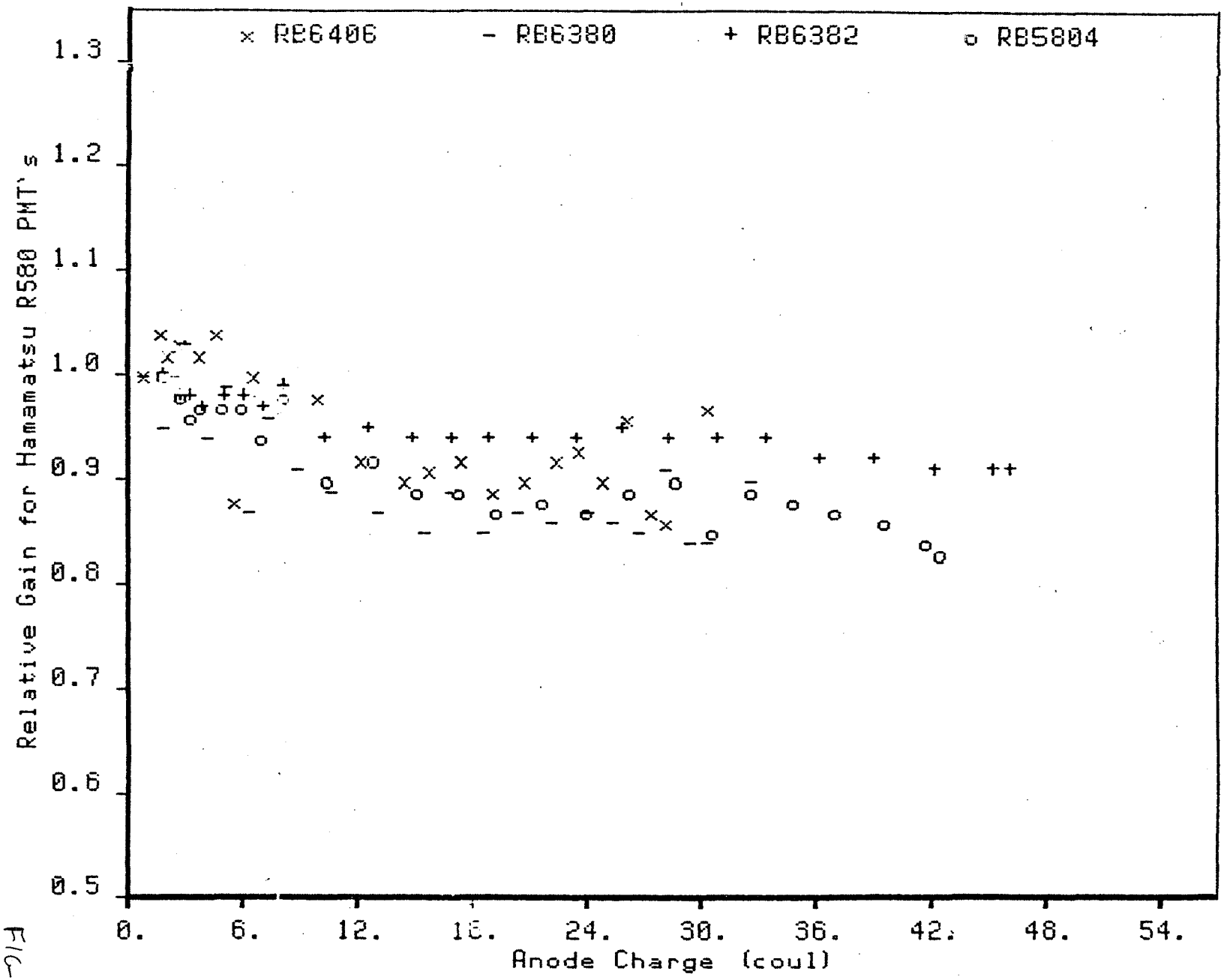
× RB6406
- RB6380
+ RB6382
o RB5804
Relative Gain for Hamamatsu R580 PMT's
1.3
1.2
1.1
1.0
0.9
0.8
0.7
0.6
0.5
0.
6.
12.
18.
24.
30.
36.
42.
48.
54.
Anode Charge (coul)

Fig 4.13

HISTOGRAMME 5 ARG(7)

1=TRUE, // 17=FALS,Corner Tube //

T4.1 Mfr. Q.E. PAS DE 3

1	0.0000E+00	0	
2	1.000	0	
3	2.000	0	
4	3.000	0	
5	4.000	0	
6	5.000	0	
7	6.000	0	
8	7.000	0	
9	8.000	0	
10	9.000	0	
11	10.00	2	X
12	11.00	5	XX
13	12.00	6	XX
14	13.00	7	XX
15	14.00	15	XXXXX
16	15.00	23	XXXXXXXX
17	16.00	42	XXXXXXXXXXXXX
18	17.00	36	XXXXXXXXXXX
19	18.00	105	XXXXXXXXXXXXXXXXXXXXXXXXXXXXXXXXX
20	19.00	104	XXXXXXXXXXXXXXXXXXXXXXXXXXXXXXXX
21	20.00	179	XXXXXXXXXXXXXXXXXXXXXXXXXXXXXXXXXXXXXXXXXXXXXXXXXXXXXXXXXXXXXXX
22	21.00	116	XXXXXXXXXXXXXXXXXXXXXXXXXXXXXXXXXX
23	22.00	43	XXXXXXXXXXXXX
24	23.00	4	X
25	24.00	0	

687 ENTRIES + 0 UNDERFLOW + 0 OVERFLOW = 687 TOTAL ENTRIES

MEAN: 18.92 STANDARD DEVIATION: 2.253 PRECISION: 0.1191 (SANS LES DEBORDEMENTS)

Q.E. (%)

Fig. 5.1

HISTOGRAMME 6 ARG(10)

1=TRUE // 17=FALSE Corner Tube //

T4.1 HV1 PAS DE 1

1	700.0	2	XX
2	720.0	16	XXXXXXXXXXXXXXX
3	740.0	21	XXXXXXXXXXXXXXXXXXXXX
4	760.0	28	XXXXXXXXXXXXXXXXXXXXXXXXXXXX
5	780.0	30	XXXXXXXXXXXXXXXXXXXXXXXXXXXXXX
6	800.0	22	XXXXXXXXXXXXXXXXXXXXXX
7	820.0	33	XXXXXXXXXXXXXXXXXXXXXXXXXXXXXXXXX
8	840.0	32	XXXXXXXXXXXXXXXXXXXXXXXXXXXXXXXX
9	860.0	27	XXXXXXXXXXXXXXXXXXXXXXXXXXX
10	880.0	35	XXXXXXXXXXXXXXXXXXXXXXXXXXXXXXXXXXX
11	700.0	33	XXXXXXXXXXXXXXXXXXXXXXXXXXXXXXXXX
12	720.0	39	XXXXXXXXXXXXXXXXXXXXXXXXXXXXXXXXXXXXXXX
13	740.0	33	XXXXXXXXXXXXXXXXXXXXXXXXXXXXXXXXX
14	760.0	29	XXXXXXXXXXXXXXXXXXXXXXXXXXXXX
15	780.0	34	XXXXXXXXXXXXXXXXXXXXXXXXXXXXXXXXXX
16	1000.	36	XXXXXXXXXXXXXXXXXXXXXXXXXXXXXXXXXXXX
17	1020.	33	XXXXXXXXXXXXXXXXXXXXXXXXXXXXXXXXX
18	1040.	32	XXXXXXXXXXXXXXXXXXXXXXXXXXXXXXXX
19	1060.	19	XXXXXXXXXXXXXXXXXX
20	1080.	25	XXXXXXXXXXXXXXXXXXXXXXXXX
21	1100.	20	XXXXXXXXXXXXXXXXXXXX
22	1120.	25	XXXXXXXXXXXXXXXXXXXXXXXXX
23	1140.	20	XXXXXXXXXXXXXXXXXXXX
24	1160.	13	XXXXXXXXXXXXX
25	1180.	16	XXXXXXXXXXXXXXXX
26	1200.	16	XXXXXXXXXXXXXXXX
27	1220.	7	XXXXXXX
28	1240.	5	XXXXX
29	1260.	1	X
30	1280.	4	XXXX
31	1300.	0	
32	1320.	0	
33	1340.	0	
34	1360.	0	
35	1380.	0	
36	1400.	0	
37	1420.	0	
38	1440.	0	
39	1460.	0	
40	1480.	0	
41	1500.	0	
42	1520.	0	
43	1540.	0	
44	1560.	0	
45	1580.	0	
46	1600.	0	
47	1620.	0	
48	1640.	0	
49	1660.	0	
50	1680.	0	

VOLTS

686 ENTRIES + 1 UNDERFLOW + 0 OVERFLOW = 687 TOTAL ENTRIES

MEAN: 962.4 STANDARD DEVIATION: 136.1 PRECISION: 0.1415 (SANS LES DEBORDEMENTS)

FIG 5.2(a)-

HISTOGRAMME 7 ARG(11)

1=TRUE, // 17=FALS,Corner Tube //

T4.1 HV2 PAS DE 1

1	700.0	0	
2	720.0	0	
3	740.0	1	X
4	760.0	4	XXXX
5	780.0	15	XXXXXXXXXXXXXXX
6	800.0	18	XXXXXXXXXXXXXXXXXX
7	820.0	24	XXXXXXXXXXXXXXXXXXXXXXXX
8	840.0	23	XXXXXXXXXXXXXXXXXXXXXXX
9	860.0	28	XXXXXXXXXXXXXXXXXXXXXXXXXXXX
10	880.0	21	XXXXXXXXXXXXXXXXXXXX
11	700.0	32	XXXXXXXXXXXXXXXXXXXXXXXXXXXXXXXX
12	920.0	25	XXXXXXXXXXXXXXXXXXXXXXXXX
13	940.0	27	XXXXXXXXXXXXXXXXXXXXXXXXXXX
14	960.0	26	XXXXXXXXXXXXXXXXXXXXXXXXXX
15	980.0	31	XXXXXXXXXXXXXXXXXXXXXXXXXXXXXXX
16	1000.	32	XXXXXXXXXXXXXXXXXXXXXXXXXXXXXXXX
17	1020.	32	XXXXXXXXXXXXXXXXXXXXXXXXXXXXXXXX
18	1040.	26	XXXXXXXXXXXXXXXXXXXXXXXXXX
19	1060.	23	XXXXXXXXXXXXXXXXXXXXXXX
20	1080.	30	XXXXXXXXXXXXXXXXXXXXXXXXXXXXXX
21	1100.	31	XXXXXXXXXXXXXXXXXXXXXXXXXXXXXXX
22	1120.	35	XXXXXXXXXXXXXXXXXXXXXXXXXXXXXXXXXXX
23	1140.	21	XXXXXXXXXXXXXXXXXXXX
24	1160.	23	XXXXXXXXXXXXXXXXXXXXXXX
25	1180.	19	XXXXXXXXXXXXXXXXXXX
26	1200.	18	XXXXXXXXXXXXXXXXXX
27	1220.	16	XXXXXXXXXXXXXXXX
28	1240.	23	XXXXXXXXXXXXXXXXXXXXXXX
29	1260.	18	XXXXXXXXXXXXXXXXXX
30	1280.	12	XXXXXXXXXXXX
31	1300.	12	XXXXXXXXXXXX
32	1320.	11	XXXXXXXXXXX
33	1340.	16	XXXXXXXXXXXXXXXX
34	1360.	5	XXXXX
35	1380.	4	XXXX
36	1400.	1	X
37	1420.	4	XXXX
38	1440.	0	
39	1460.	0	
40	1480.	0	
41	1500.	0	
42	1520.	0	
43	1540.	0	
44	1560.	0	
45	1580.	0	
46	1600.	0	
47	1620.	0	
48	1640.	0	
49	1660.	0	
50	1680.	0	

VOLTS

Fig. 5.2(6)

687 ENTRIES + 0 UNDERFLOW + 0 OVERFLOW = 687 TOTAL ENTRIES

MEAN: 1054. STANDARD DEVIATION: 157.7 PRECISION: 0.1496 (SANS LES DEBORDEMENTS)

```
HISTOGRAMME   8  ARG( 12)

   1=TRUE,                        // 17=FALS,Corner Tube          //

   T4.1 HV3                                                  PAS DE    1

   1      700.0          0
   2      720.0          0
   3      740.0          0
   4      760.0          0
   5      780.0          0
   6      800.0          1   X
   7      820.0          4   XXXX
   8      840.0         11   XXXXXXXXXXX
   9      860.0         14   XXXXXXXXXXXXX
  10      880.0         19   XXXXXXXXXXXXXXXXXX
  11      900.0         25   XXXXXXXXXXXXXXXXXXXXXXXXX
  12      920.0         17   XXXXXXXXXXXXXXXX
  13      940.0         26   XXXXXXXXXXXXXXXXXXXXXXXXXX
  14      960.0         16   XXXXXXXXXXXXXXXX
  15      980.0         35   XXXXXXXXXXXXXXXXXXXXXXXXXXXXXXXXXXX
  16     1000.          17   XXXXXXXXXXXXXXXX
  17     1020.          23   XXXXXXXXXXXXXXXXXXXXXX
  18     1040.          27   XXXXXXXXXXXXXXXXXXXXXXXXXX
  19     1060.          25   XXXXXXXXXXXXXXXXXXXXXXXX
  20     1080.          27   XXXXXXXXXXXXXXXXXXXXXXXXXX
  21     1100.          25   XXXXXXXXXXXXXXXXXXXXXXXX
  22     1120.          28   XXXXXXXXXXXXXXXXXXXXXXXXXXX
  23     1140.          21   XXXXXXXXXXXXXXXXXXXX
  24     1160.          24   XXXXXXXXXXXXXXXXXXXXXXX
  25     1180.          17   XXXXXXXXXXXXXXXX
  26     1200.          26   XXXXXXXXXXXXXXXXXXXXXXXXX
  27     1220.          36   XXXXXXXXXXXXXXXXXXXXXXXXXXXXXXXXXXX
  28     1240.          22   XXXXXXXXXXXXXXXXXXXXX
  29     1260.          20   XXXXXXXXXXXXXXXXXXX
  30     1280.          20   XXXXXXXXXXXXXXXXXXX
  31     1300.          12   XXXXXXXXXXXX
  32     1320.          19   XXXXXXXXXXXXXXXXXXX
  33     1340.          12   XXXXXXXXXXXX
  34     1360.          19   XXXXXXXXXXXXXXXXXXX
  35     1380.          16   XXXXXXXXXXXXXXXX
  36     1400.          16   XXXXXXXXXXXXXXXX
  37     1420.          10   XXXXXXXXXX
  38     1440.          10   XXXXXXXXXX
  39     1460.          14   XXXXXXXXXXXXXX
  40     1480.           4   XXXX
  41     1500.          14   XXXXXXXXXXXXXX
  42     1520.           6   XXXXXX
  43     1540.           2   XX
  44     1560.           3   XXX
  45     1580.           4   XXXX
  46     1600.          0
  47     1620.          0
  48     1640.          0
  49     1660.          0
  50     1680.          0

   687 ENTRIES  +        0 UNDERFLOW  +        0 OVERFLOW   =        687 TOTAL ENTRIES

   MEAN:   1158.       STANDARD DEVIATION:   183.7       PRECISION:  0.1587          (SANS LES DEBORDEMENTS)
```

VOLTS

FIG. 5.2(c)

HISTOGRAMME 9 ARG(206)

1=TRUE, // 17=FALS,Corner Tube //

T4.1 N12 PAS DE 1

1	5.000	0	
2	5.200	0	
3	5.400	1	X
4	5.600	0	
5	5.800	0	
6	6.000	5	XXXXX
7	6.200	11	XXXXXXXXXXX
8	6.400	22	XXXXXXXXXXXXXXXXXXXXX
9	6.600	32	XXXXXXXXXXXXXXXXXXXXXXXXXXXXXXXX
10	6.800	44	XXXXXXXXXXXXXXXXXXXXXXXXXXXXXXXXXXXXXXXXXXXX
11	7.000	47	XXXXXXXXXXXXXXXXXXXXXXXXXXXXXXXXXXXXXXXXXXXXXXX
12	7.200	74	XXXXXXXXXXXXXXXXXXXXXXXXXXXXXXXXXXXXXXXXXXXXXXXXXXXXXXXXXXXXXXXXXXXXXXXXXXXXXXX
13	7.400	66	XXXXXXXXXXXXXXXXXXXXXXXXXXXXXXXXXXXXXXXXXXXXXXXXXXXXXXXXXXXXXXXXXX
14	7.600	58	XXXXXXXXXXXXXXXXXXXXXXXXXXXXXXXXXXXXXXXXXXXXXXXXXXXXXXX
15	7.800	69	XXXXXXXXXXXXXXXXXXXXXXXXXXXXXXXXXXXXXXXXXXXXXXXXXXXXXXXXXXXXXXXXXXXXXX
16	8.000	57	XXXXXXXXXXXXXXXXXXXXXXXXXXXXXXXXXXXXXXXXXXXXXXXXXXXXXX
17	8.200	74	XXXXXXXXXXXXXXXXXXXXXXXXXXXXXXXXXXXXXXXXXXXXXXXXXXXXXXXXXXXXXXXXXXXXXXXXXXXXXXX
18	8.400	46	XXXXXXXXXXXXXXXXXXXXXXXXXXXXXXXXXXXXXXXXXX
19	8.600	31	XXXXXXXXXXXXXXXXXXXXXXXXXXXXXXX
20	8.800	26	XXXXXXXXXXXXXXXXXXXXXXXXXX
21	9.000	15	XXXXXXXXXXXXXXX
22	9.200	5	XXXXX
23	9.400	4	XXXX
24	9.600	0	
25	9.800	0	
26	10.00	0	
27	10.20	0	
28	10.40	0	
29	10.60	0	
30	10.80	0	

M12

687 ENTRIES + 0 UNDERFLOW + 0 OVERFLOW = 687 TOTAL ENTRIES

MEAN: 7.741 STANDARD DEVIATION: 0.7130 PRECISION: 0.9210E-01 (SANS LES DEBORDEMENTS)

FIG. 5.3(a)

```
HISTOGRA      10  ARG(207)

  1=TRUE,                        // 17=FALS,Corner Tube          //

  T4.1 N23                                                  PAS DE    1

  1      5.000          0
  2      5.200          0
  3      5.400          0
  4      5.600          3   XXX
  5      5.800          6   XXXXXX
  6      6.000         19   XXXXXXXXXXXXXXXXXX
  7      6.200         21   XXXXXXXXXXXXXXXXXXXX
  8      6.400         34   XXXXXXXXXXXXXXXXXXXXXXXXXXXXXXXX
  9      6.600         37   XXXXXXXXXXXXXXXXXXXXXXXXXXXXXXXXXXX
 10      6.800         44   XXXXXXXXXXXXXXXXXXXXXXXXXXXXXXXXXXXXXXXX
 11      7.000         57   XXXXXXXXXXXXXXXXXXXXXXXXXXXXXXXXXXXXXXXXXXXXXXXXXXX
 12      7.200         62   XXXXXXXXXXXXXXXXXXXXXXXXXXXXXXXXXXXXXXXXXXXXXXXXXXXXX
 13      7.400         63   XXXXXXXXXXXXXXXXXXXXXXXXXXXXXXXXXXXXXXXXXXXXXXXXXXXXXX
 14      7.600         59   XXXXXXXXXXXXXXXXXXXXXXXXXXXXXXXXXXXXXXXXXXXXXXXXXXXX
 15      7.800         69   XXXXXXXXXXXXXXXXXXXXXXXXXXXXXXXXXXXXXXXXXXXXXXXXXXXXXXXXXXXXXXXXXXXXX
 16      8.000         44   XXXXXXXXXXXXXXXXXXXXXXXXXXXXXXXXXXXXXXXX
 17      8.200         55   XXXXXXXXXXXXXXXXXXXXXXXXXXXXXXXXXXXXXXXXXXXXXXXX
 18      8.400         45   XXXXXXXXXXXXXXXXXXXXXXXXXXXXXXXXXXXXXXXX
 19      8.600         25   XXXXXXXXXXXXXXXXXXXXXXX
 20      8.800         23   XXXXXXXXXXXXXXXXXXXXX
 21      9.000         14   XXXXXXXXXXXXXX
 22      9.200          5   XXXXX
 23      9.400          1   X
 24      9.600          0
 25      9.800          1   X
 26      10.00          0
 27      10.20          0
 28      10.40          0
 29      10.60          0
 30      10.80          0

    687 ENTRIES  +        0 UNDERFLOW  +        0 OVERFLOW   =        687 TOTAL ENTRIES

    MEAN:   7.592      STANDARD DEVIATION:  0.7842      PRECISION:  0.1033          (SANS LES DEBORDEMENTS)
```

N23

FIG. 5.3(b)

HISTOGRAMME 11 ARG(222)

1=TRUE, // 17=FALS,Corner Tube //

T4.1 ALOG10(DKI1) PAS DE 2

1	-2.000	1	X
2	-1.800	0	
3	-1.600	2	X
4	-1.400	5	XXX
5	-1.200	10	XXXXX
6	-1.000	35	XXXXXXXXXXXXXXXXX
7	-0.8000	49	XXXXXXXXXXXXXXXXXXXXXXXX
8	-0.6000	69	XXXXXXXXXXXXXXXXXXXXXXXXXXXXXXXXX
9	-0.4000	127	XXXXXXXXXXXXXXXXXXXXXXXXXXXXXXXXXXXXXXXXXXXXXXXXXXXXXXXX
10	-0.2000	159	XXXXXXXXXXXXXXXXXXXXXXXXXXXXXXXXXXXXXXXXXXXXXXXXXXXXXXXXXXXXXXXXXXXXXXXXXXXXXXXX
11	0.0000E+00	85	XXXXXXXXXXXXXXXXXXXXXXXXXXXXXXXXXXXXXXX
12	0.2000	72	XXXXXXXXXXXXXXXXXXXXXXXXXXXXXXXXX
13	0.4000	54	XXXXXXXXXXXXXXXXXXXXXXXXXX
14	0.6000	17	XXXXXXXXX
15	0.8000	1	X
16	1.000	0	
17	1.200	0	
18	1.400	0	
19	1.600	0	
20	1.800	0	
21	2.000	0	
22	2.200	0	
23	2.400	0	
24	2.600	0	
25	2.800	0	
26	3.000	0	
27	3.200	0	
28	3.400	0	
29	3.600	0	
30	3.800	0	

log (I DARK)

686 ENTRIES + 1 UNDERFLOW + 0 OVERFLOW = 687 TOTAL ENTRIES

MEAN: -0.1597 STANDARD DEVIATION: 0.4260 PRECISION: -2.667 (SANS LES DEBORDEMENTS)

FIG. 5.4(a)

HISTOGR E 12 ARG(223)

1=TRUE, // 17=FALS,Corner Tube //

T4.1 ALOG10(DKI2) PAS DE 3

1	-2.000	1	
2	-1.800	0	
3	-1.600	0	
4	-1.400	1	
5	-1.200	3	X
6	-1.000	9	XXX
7	-0.8000	24	XXXXXXXX
8	-0.6000	46	XXXXXXXXXXXXXX
9	-0.4000	73	XXXXXXXXXXXXXXXXXXXXXXX
10	-0.2000	140	XXXXXXXXXXXXXXXXXXXXXXXXXXXXXXXXXXXXXXXXXXXX
11	0.0000E+00	161	XXXXXXXXXXXXXXXXXXXXXXXXXXXXXXXXXXXXXXXXXXXXXXXXXXXXXXXX
12	0.2000	71	XXXXXXXXXXXXXXXXXXXXXX
13	0.4000	75	XXXXXXXXXXXXXXXXXXXXXXX
14	0.6000	43	XXXXXXXXXXXXX
15	0.8000	38	XXXXXXXXXXXX
16	1.000	1	
17	1.200	0	
18	1.400	0	
19	1.600	0	
20	1.800	0	
21	2.000	0	
22	2.200	0	
23	2.400	0	
24	2.600	0	
25	2.800	0	
26	3.000	0	
27	3.200	0	
28	3.400	0	
29	3.600	0	
30	3.800	0	

log (I dark)

686 ENTRIES + 1 UNDERFLOW + 0 OVERFLOW = 687 TOTAL ENTRIES

MEAN: 0.6985E-01 STANDARD DEVIATION: 0.4229 PRECISION: 6.054 (SANS LES DEBORDEMENTS)

Fig. 5.4 (6)

HISTOGRAMME 13 ARG(224)

1=TRUE, // 17=FALS,Corner Tube //

T4.1 ALOG10(DKI3) PAS DE 3

1	-2.000	0	
2	-1.800	0	
3	-1.600	0	
4	-1.400	0	
5	-1.200	0	
6	-1.000	4	X
7	-0.8000	5	XX
8	-0.6000	17	XXXXXX
9	-0.4000	34	XXXXXXXXXX
10	-0.2000	72	XXXXXXXXXXXXXXXXXXXXXX
11	0.0000E+00	117	XXXXXXXXXXXXXXXXXXXXXXXXXXXXXXXXXXXX
12	0.2000	172	XXXXXXXXXXXXXXXXXXXXXXXXXXXXXXXXXXXXXXXXXXXXXXXXXXXXXXX
13	0.4000	83	XXXXXXXXXXXXXXXXXXXXXXXX
14	0.6000	55	XXXXXXXXXXXXXXXX
15	0.8000	76	XXXXXXXXXXXXXXXXXXXXXX
16	1.000	41	XXXXXXXXXXXX
17	1.200	11	XXXX
18	1.400	0	
19	1.600	0	
20	1.800	0	
21	2.000	0	
22	2.200	0	
23	2.400	0	
24	2.600	0	
25	2.800	0	
26	3.000	0	
27	3.200	0	
28	3.400	0	
29	3.600	0	
30	3.800	0	

$\log(I_{DARK})$

687 ENTRIES + 0 UNDERFLOW + 0 OVERFLOW = 687 TOTAL ENTRIES

MEAN: 0.3434 STANDARD DEVIATION: 0.4248 PRECISION: 1.237 (SANS LES DEBORDEMENTS)

FIG. 5.4(c)

```
HISTOGRA     17  ARG(203)

   1=TRUE,                        // 17=FALS,Corner Tube          //  81=FALS,Dummy Big Gain Uncer //

   T4.1 Av. Gn. (*10E5)                                          PAS DE    2

    1     0.0000E+00        0
    2      1.000            0
    3      2.000            0
    4      3.000            1   X
    5      4.000            6   XXX
    6      5.000           28   XXXXXXXXXXXXX
    7      6.000           77   XXXXXXXXXXXXXXXXXXXXXXXXXXXXXXXXXXXXXXXXX
    8      7.000           96   XXXXXXXXXXXXXXXXXXXXXXXXXXXXXXXXXXXXXXXXXXXXXXXX
    9      8.000           92   XXXXXXXXXXXXXXXXXXXXXXXXXXXXXXXXXXXXXXXXXXXXXXXX
   10      9.000           70   XXXXXXXXXXXXXXXXXXXXXXXXXXXXXXXXXX
   11     10.00            65   XXXXXXXXXXXXXXXXXXXXXXXXXXXXXXXXX
   12     11.00            34   XXXXXXXXXXXXXXXXX
   13     12.00            20   XXXXXXXXXX
   14     13.00            13   XXXXXXX
   15     14.00            14   XXXXXXX
   16     15.00            10   XXXXX
   17     16.00            11   XXXXXX
   18     17.00             4   XX
   19     18.00             2   X
   20     19.00             0
   21     20.00             2   X
   22     21.00             2   X
   23     22.00             0
   24     23.00             2   X
   25     24.00             0
   26     25.00             0
   27     26.00             0
   28     27.00             0
   29     28.00             4   XX
   30     29.00             2   X

      555 ENTRIES  +      125 UNDERFLOW  +        7 OVERFLOW   =        687 TOTAL ENTRIES

      MEAN:   9.537       STANDARD DEVIATION:   3.580       PRECISION:  0.3754            (SANS LES DEBORDEMENTS)
```

GAIN (x 10^5)

FIG. 5,5

HISTOGRAMME 14 ARG(332)

1=TRUE, // 17=FALS,Corner Tube //

T4.1 Corr. PH(5) PAS DE 2

1	0.0000E+00	0	
2	10.00	0	
3	20.00	0	
4	30.00	0	
5	40.00	0	
6	50.00	0	
7	60.00	0	
8	70.00	0	
9	80.00	0	
10	90.00	0	
11	100.0	1	X
12	110.0	4	XX
13	120.0	9	XXXXX
14	130.0	17	XXXXXXXXX
15	140.0	31	XXXXXXXXXXXXXXX
16	150.0	58	XXXXXXXXXXXXXXXXXXXXXXXXXXXXX
17	160.0	72	XXXXXXXXXXXXXXXXXXXXXXXXXXXXXXXXXX
18	170.0	80	XXXXXXXXXXXXXXXXXXXXXXXXXXXXXXXXXXXXXX
19	180.0	80	XXXXXXXXXXXXXXXXXXXXXXXXXXXXXXXXXXXXXX
20	190.0	63	XXXXXXXXXXXXXXXXXXXXXXXXXXXXXXX
21	200.0	74	XXXXXXXXXXXXXXXXXXXXXXXXXXXXXXXXXX
22	210.0	53	XXXXXXXXXXXXXXXXXXXXXXXXX
23	220.0	45	XXXXXXXXXXXXXXXXXXXXX
24	230.0	33	XXXXXXXXXXXXXXXX
25	240.0	18	XXXXXXXXX
26	250.0	12	XXXXXX
27	260.0	7	XXXX
28	270.0	3	XX
29	280.0	3	XX
30	290.0	4	XX
31	300.0	2	X
32	310.0	0	
33	320.0	1	X
34	330.0	0	
35	340.0	0	
36	350.0	0	
37	360.0	0	
38	370.0	0	
39	380.0	0	
40	390.0	0	

Pulse Height (pC)

670 ENTRIES + 0 UNDERFLOW + 17 OVERFLOW = 687 TOTAL ENTRIES

MEAN: 190.9 STANDARD DEVIATION: 33.75 PRECISION: 0.1767 (SANS LES DEBORDEMENTS)

Fig. 5.6

HISTOGRAMME 16 ARG(150)

1=TRUE, // 17=FALS,Corner Tube //

T4.1 CHI2 Linearity PAS DE 2

1	0.0000E+00	0	
2	0.2000	0	
3	0.4000	0	
4	0.6000	0	
5	0.8000	0	
6	1.000	0	
7	1.200	0	
8	1.400	0	
9	1.600	0	
10	1.800	3	XX
11	2.000	3	XX
12	2.200	9	XXXXX
13	2.400	10	XXXXX
14	2.600	39	XXXXXXXXXXXXXXXXXXX
15	2.800	54	XXXXXXXXXXXXXXXXXXXXXXXXXX
16	3.000	62	XXXXXXXXXXXXXXXXXXXXXXXXXXXXX
17	3.200	73	XXXXXXXXXXXXXXXXXXXXXXXXXXXXXXXXXX
18	3.400	73	XXXXXXXXXXXXXXXXXXXXXXXXXXXXXXXXXX
19	3.600	80	XXXXXXXXXXXXXXXXXXXXXXXXXXXXXXXXXXXXX
20	3.800	59	XXXXXXXXXXXXXXXXXXXXXXXXXXX
21	4.000	43	XXXXXXXXXXXXXXXXXXXX
22	4.200	45	XXXXXXXXXXXXXXXXXXXXX
23	4.400	31	XXXXXXXXXXXXXXX
24	4.600	26	XXXXXXXXXXXX
25	4.800	13	XXXXXXX
26	5.000	15	XXXXXXXX
27	5.200	12	XXXXXX
28	5.400	8	XXXX
29	5.600	5	XXX
30	5.800	3	XX
31	6.000	0	
32	6.200	1	X
33	6.400	0	
34	6.600	0	
35	6.800	2	X
36	7.000	3	XX
37	7.200	0	
38	7.400	2	X
39	7.600	1	X
40	7.800	0	
41	8.000	1	X
42	8.200	3	XX
43	8.400	0	
44	8.600	0	
45	8.800	1	X
46	9.000	1	X
47	9.200	1	X
48	9.400	1	X
49	9.600	0	
50	9.800	1	X

684 ENTRIES + 0 UNDERFLOW + 3 OVERFLOW = 687 TOTAL ENTRIES

MEAN: 3.804 STANDARD DEVIATION: 1.020 PRECISION: 0.2681 (SANS LES DEBORDEMENTS)

Fig. 5.7

ENGINEERING NOTE | CDF

SUBJECT: PHOTOMULTIPLIER BASE

NAME:

DATE: 25 MAR 83 | REVISION DATE:

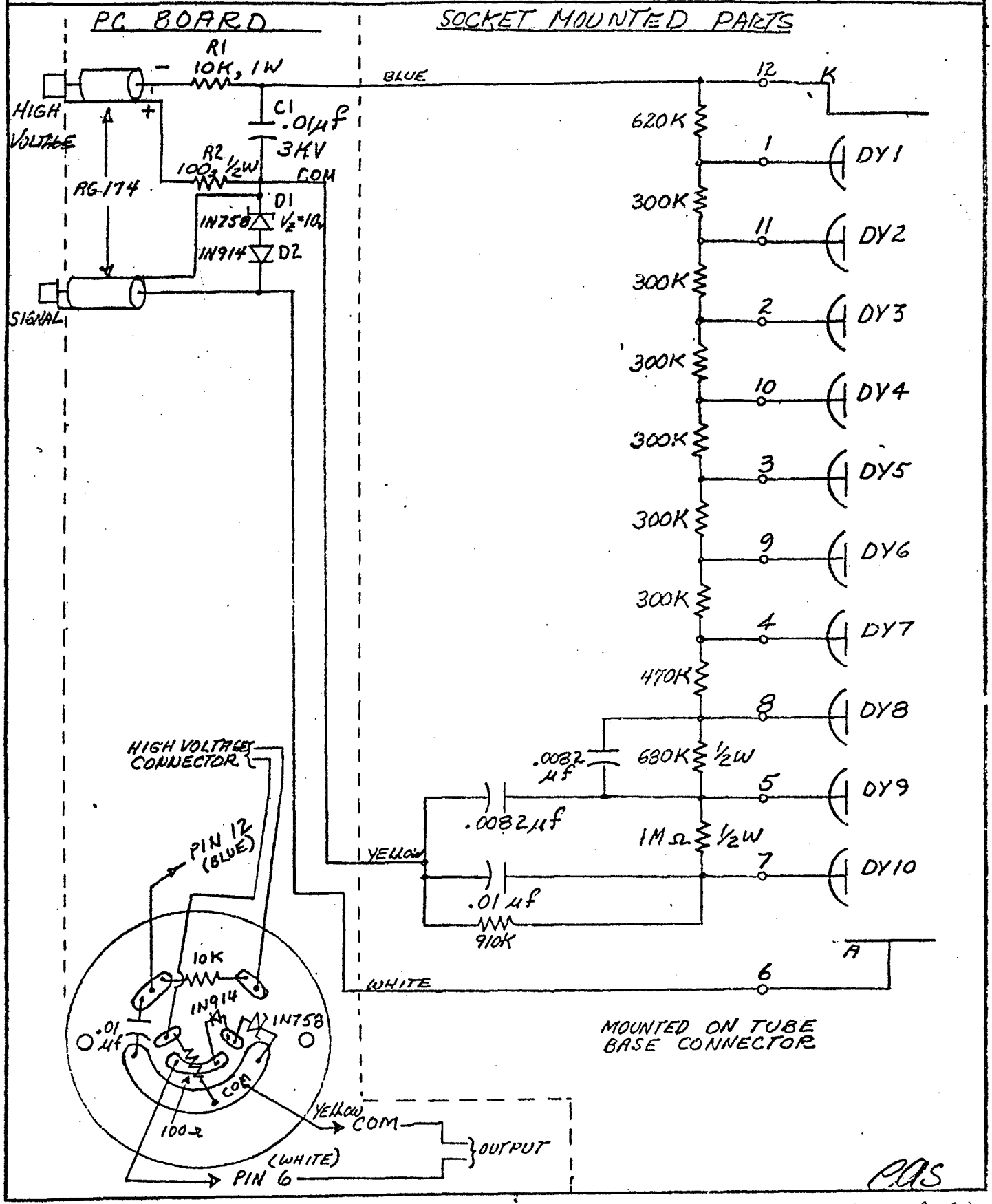

FIG. A1(a)

ENGINEERING NOTE

SUBJECT: PHOTOMULTIPLIER BASE

NAME:

DATE: 25 MAR 83

REVISION DATE:

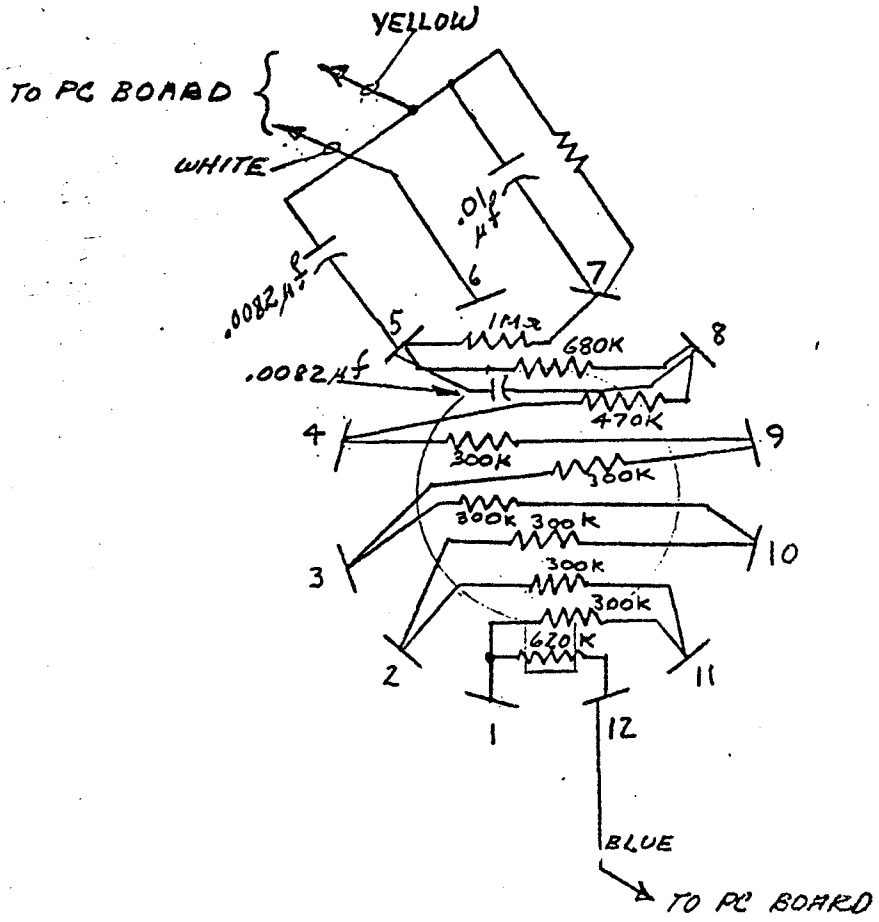

FIG A-1(b)

CABLE A: 20-conductor flat cable
CABLE B: " " " "
CABLE C: " " " "
CABLE D: 34- " " "
See: RU-CDF-PMT-7

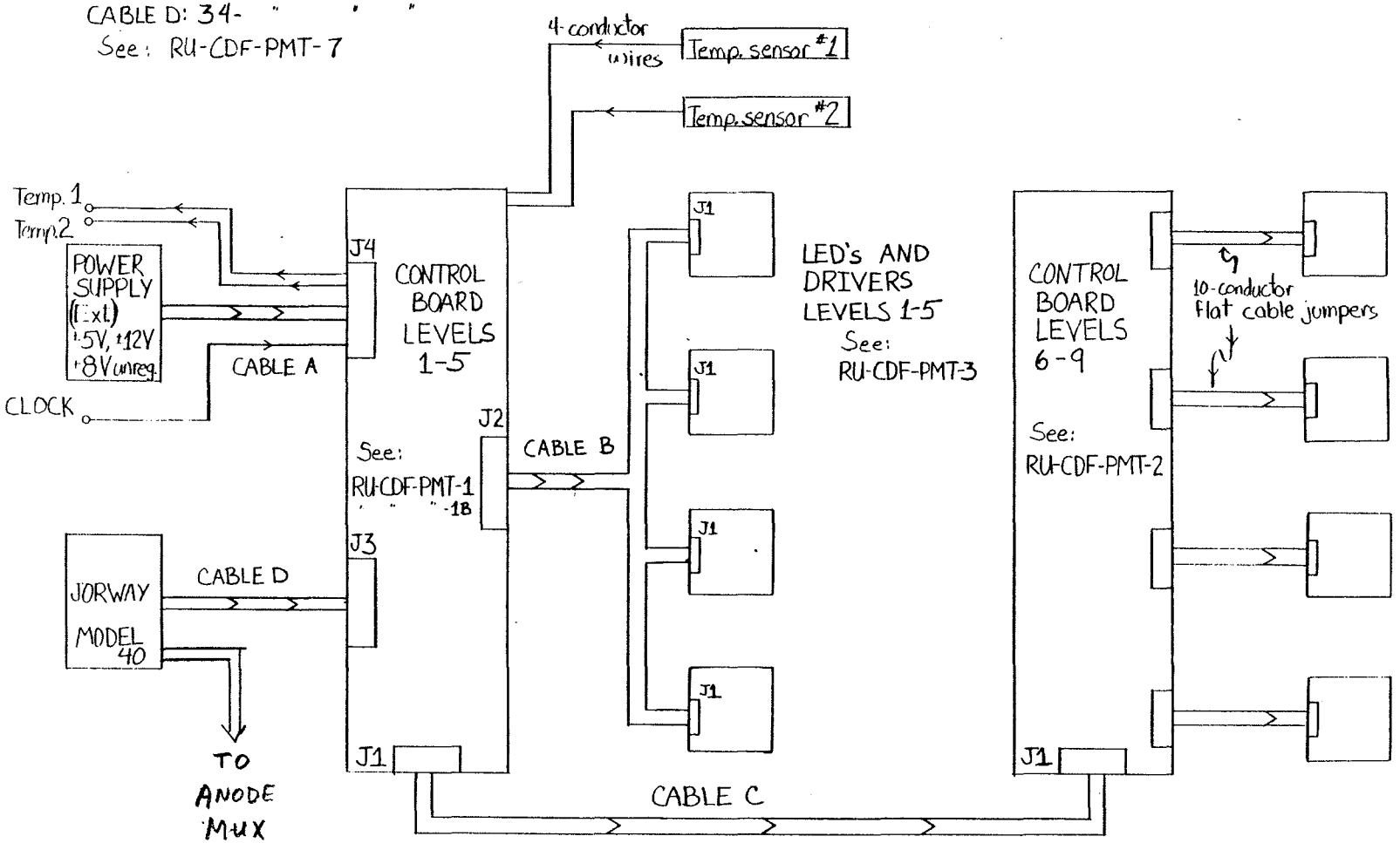

R.J.P. 08AUG84

RU-CDF-PMT-6

FIG. A-2(a)

CABLE A:

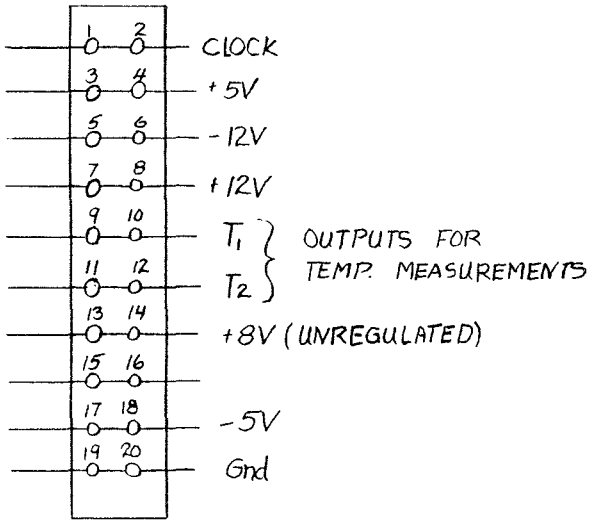

(FROM VOLTAGE BOX)

CABLE B:

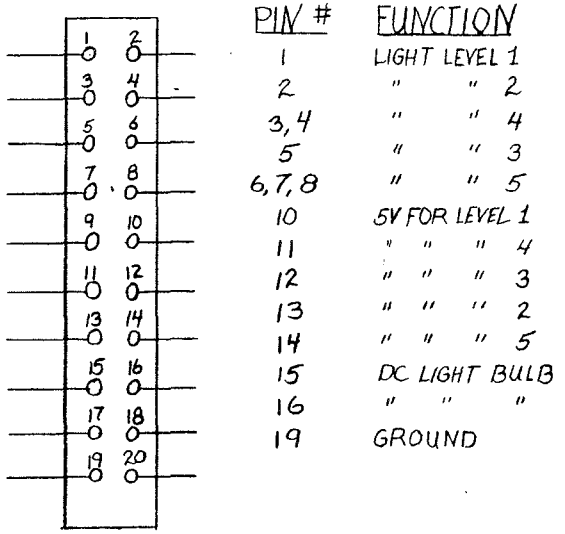

PIN #	FUNCTION
1	LIGHT LEVEL 1
2	" " 2
3, 4	" " 4
5	" " 3
6, 7, 8	" " 5
10	5V FOR LEVEL 1
11	" " " 4
12	" " " 3
13	" " " 2
14	" " " 5
15	DC LIGHT BULB
16	" " "
19	GROUND

(TO LED BOARD, LEVELS 1-5)

CABLE C:

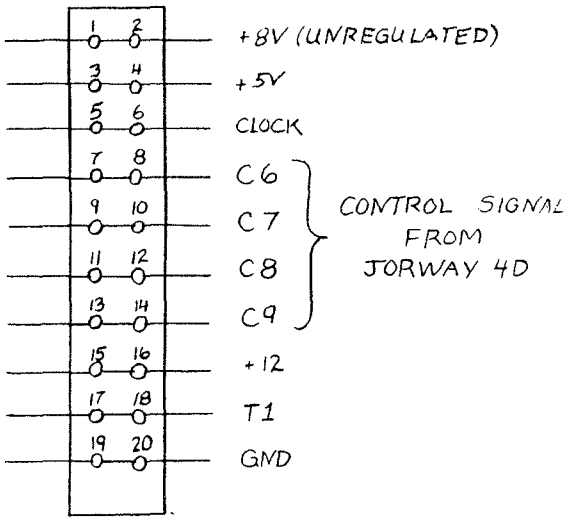

(TO CONTROL BOARD IN FRONT OF PMT)

A.S.P.
25 JUL 84

RU-CDF-PMT-7

Fig. A-2(b)

JORWAY 40-2 W/SPECIAL CONNECTORS

34-PIN 3M TYPE 3431

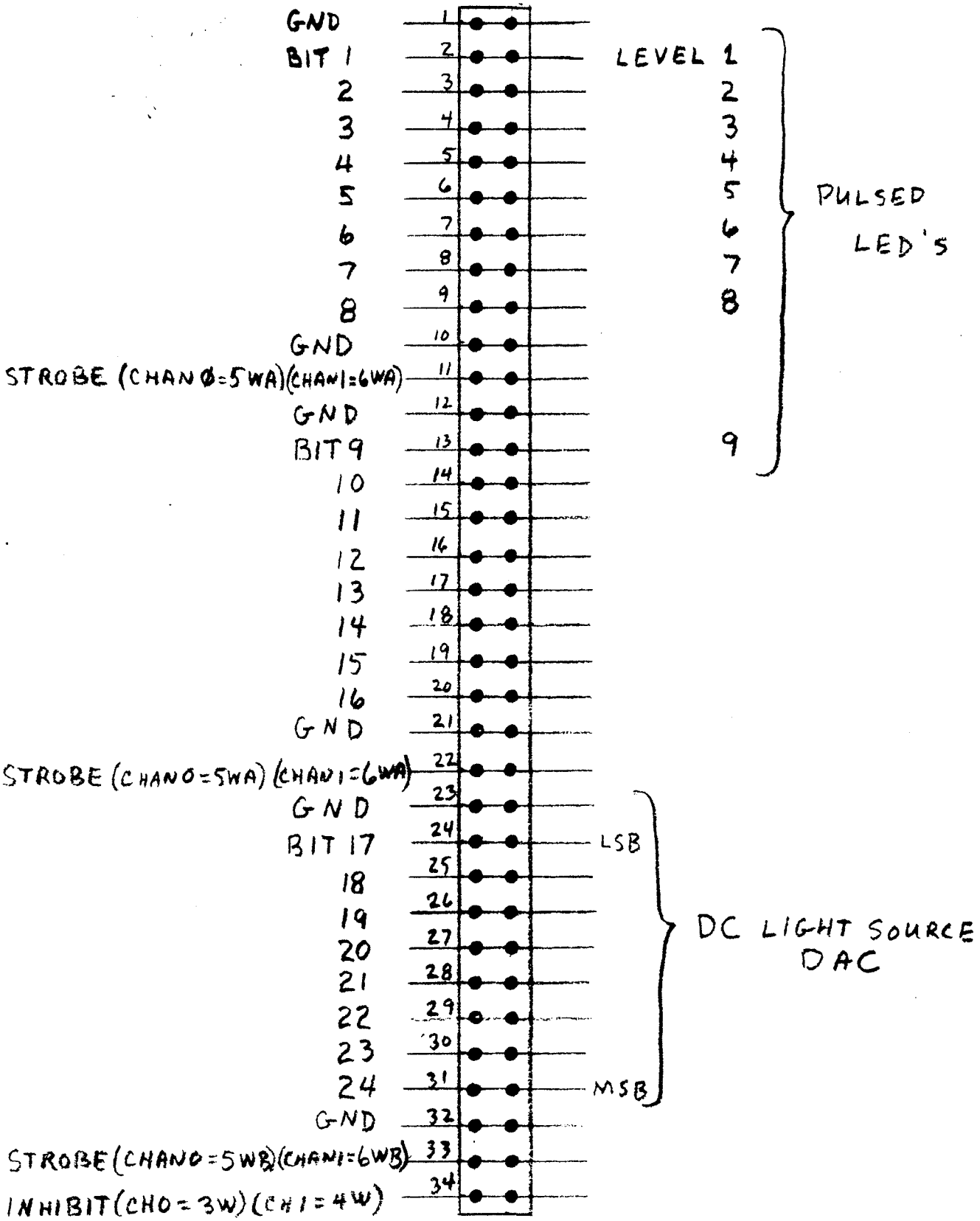

FIG. A-2(c)

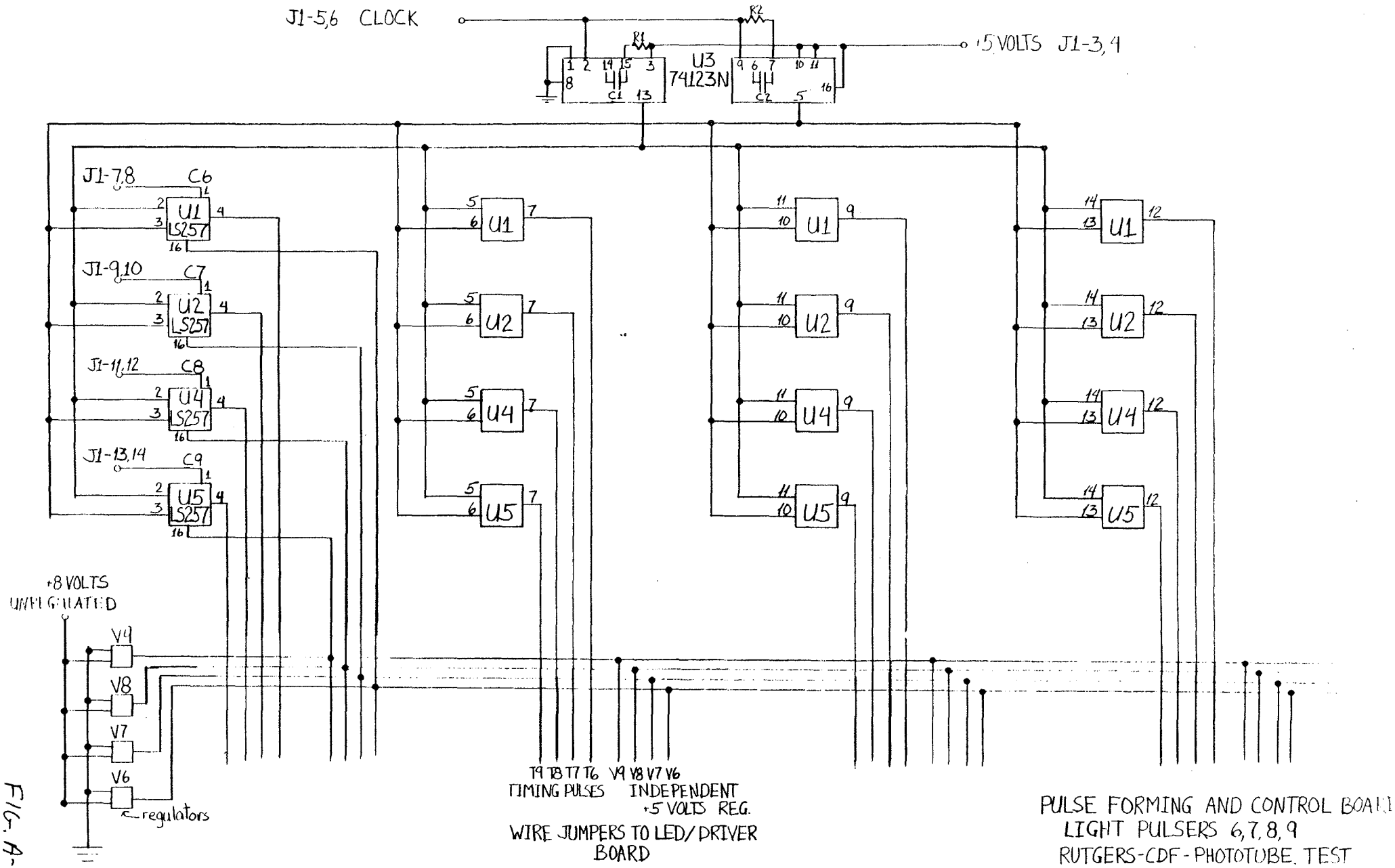
J1-5,6 CLOCK
R2
R1
+5 VOLTS J1-3,4
U3
74123N
J1-7,8
C6
U1
LS257
J1-9,10
C7
U2
LS257
J1-11,12
C8
U4
LS257
J1-13,14
C9
U5
LS257
+8 VOLTS
UNREGULATED
V9
V8
V7
V6
regulators
T9 T8 T7 T6 V9 V8 V7 V6
TIMING PULSES
INDEPENDENT
+5 VOLTS REG.
WIRE JUMPERS TO LED/DRIVER
BOARD
(TYPICAL)
PULSE FORMING AND CONTROL BOARD
LIGHT PULSERS 6,7,8,9
RUTGERS-CDF-PHOTOTUBE TEST
RU-CDF-PMT-2A

FIG. A-3(a)

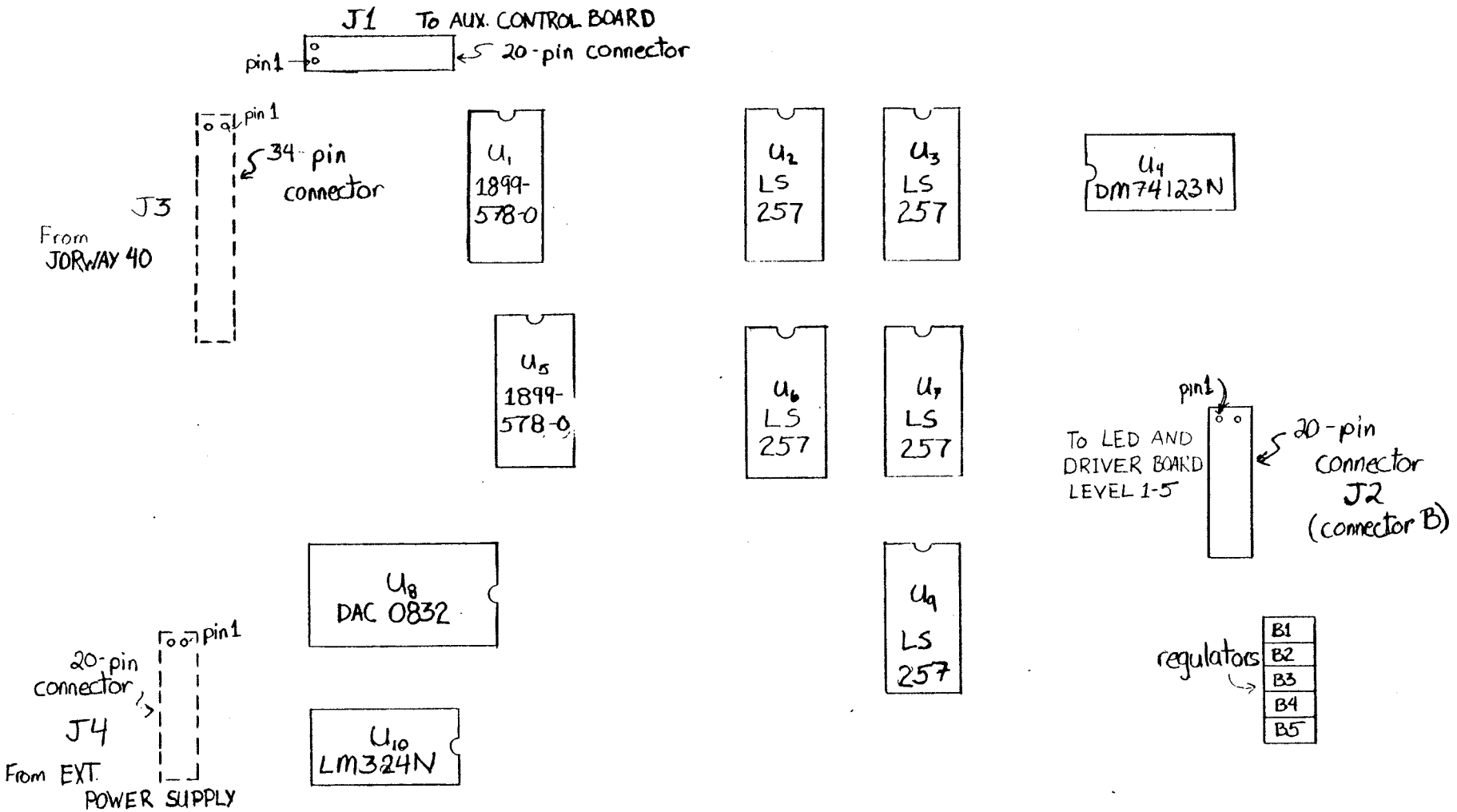

RU-CDF PMT CHAMBER CONTROL BOARD

RJP 8/2/84
RU-CDF-PMT-1

FIG. 4-3(b)

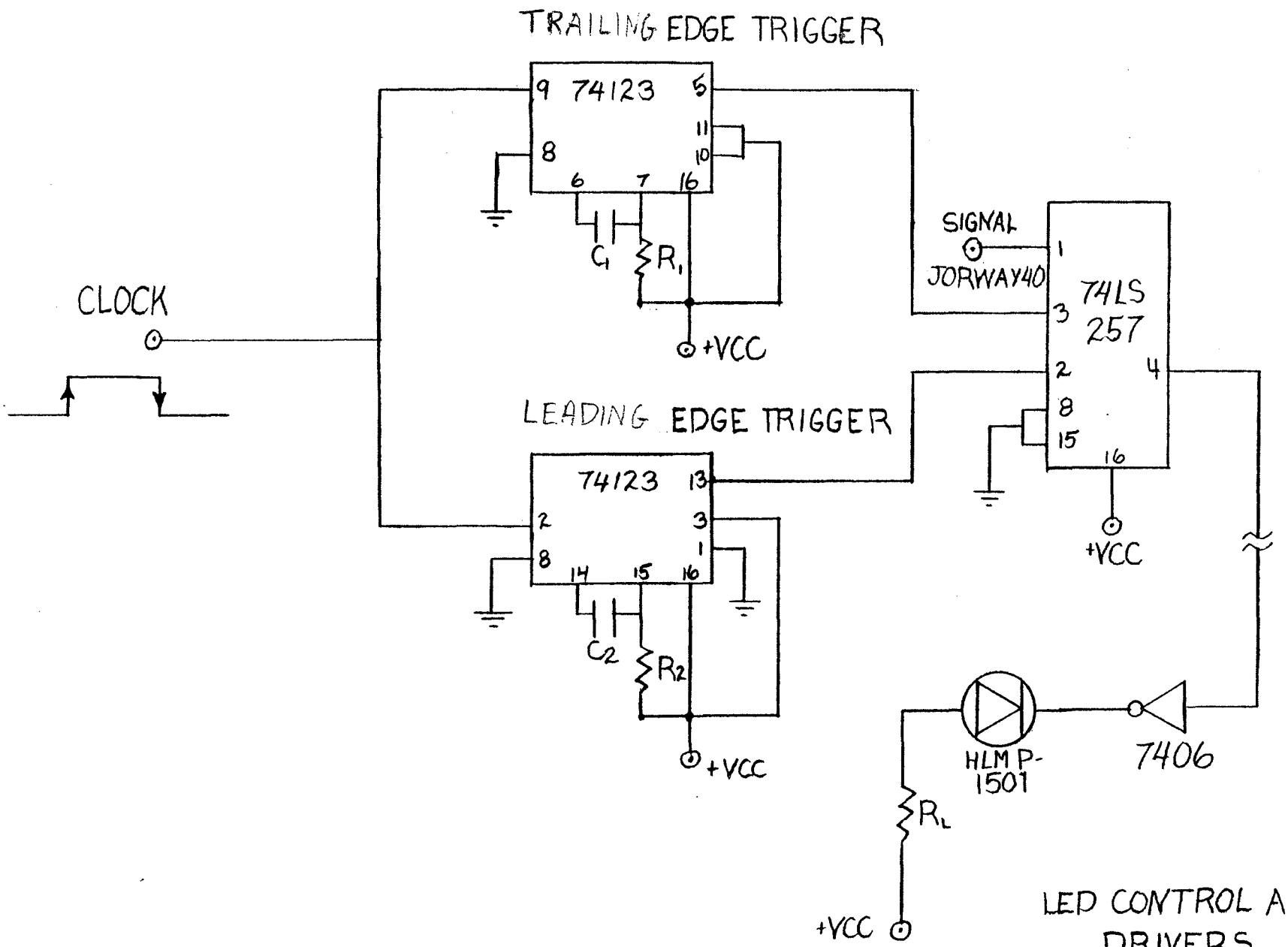

LED CONTROL AND
DRIVERS
A S P
1 AUG 1984

FIG. A-3(e)

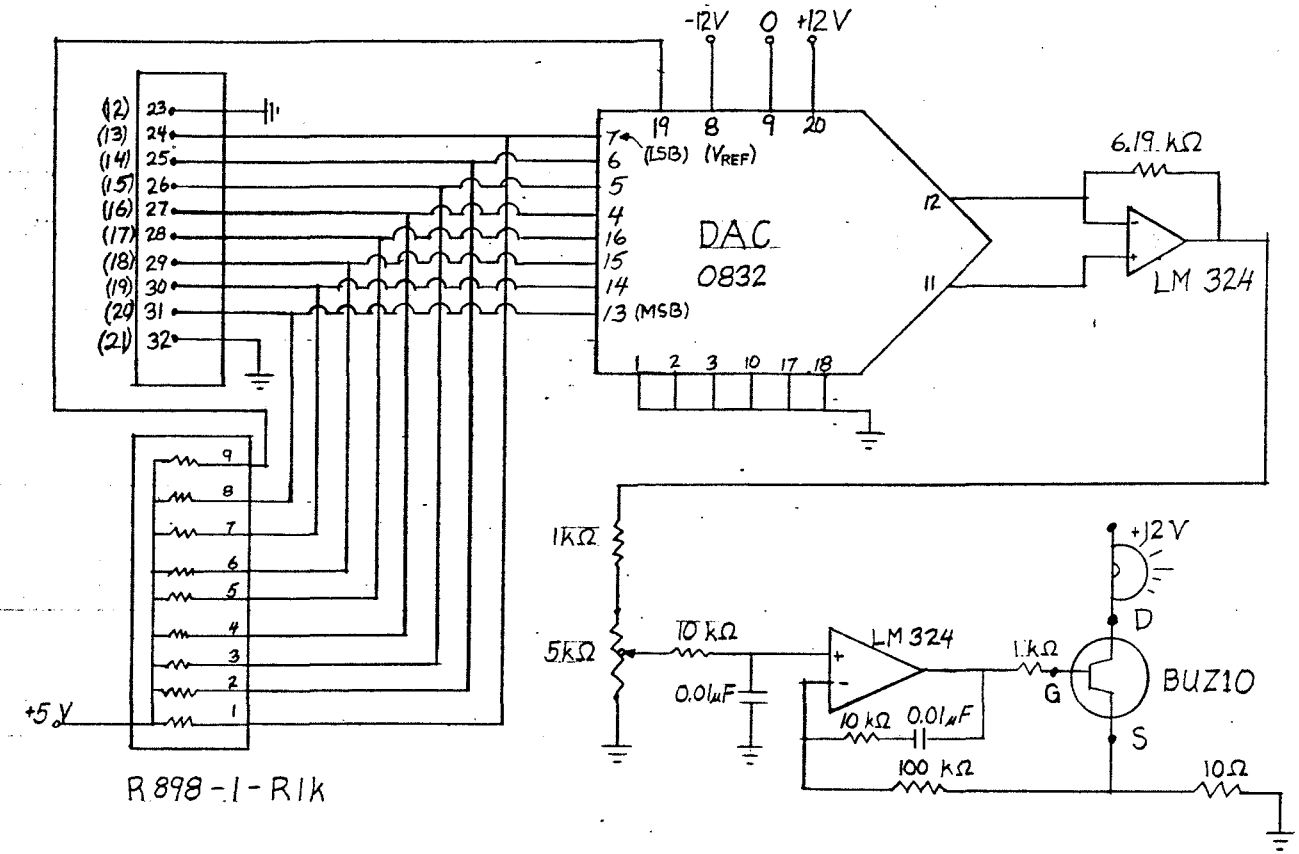

DC LIGHT SOURCE		
SCALE:	APPROVED BY:	DRAWN BY A.S.P.
DATE: 25 JUL 84		REVISED
RUTGERS - CDF - PHOTOTUBE TESTING		
RU-CDF-PMT-1C		DRAWING NUMBER

Fig. A-3(d)

A8

National Semiconductor

MICRO-DAC™ DAC0830/0831/0832
8-Bit μP Compatible, Double-Buffered D to A Converters

General Description

The DAC0830 is an advanced CMOS/Si-Cr 8-bit multiplying DAC designed to interface directly with the 8080, 8048, 8085, Z-80, and other popular microprocessors. A deposited silicon-chromium R-2R resistor ladder network divides the reference current and provides the circuit with excellent temperature tracking characteristics (0.05% of Full Scale Range maximum linearity error over temperature). The circuit uses CMOS current switches and control logic to achieve low power consumption and low output leakage current errors. Special circuitry provides TTL logic input voltage level compatibility.

Double buffering allows these DACs to output a voltage corresponding to one digital word while holding the next digital word. This permits the simultaneous updating of any number of DACs.

The DAC0830 series are the 8-bit members of a family of microprocessor-compatible DAC's (MICRO-DAC's™). For applications demanding higher resolution, the DAC1000 series (10-bits) and the DAC1208 and DAC1230 (12-bits) are available alternatives.

Micro-Dac is a trademark of National Semiconductor Corp.

Features

- Double-buffered, single-buffered or flow-through digital data inputs
- Easy interchange and pin-compatible with 12-bit DAC1230 series
- Direct interface to all popular microprocessors
- Linearity specified with zero and full scale adjust only—NOT BEST STRAIGHT LINE FIT.
- Works with ±10V reference-full 4-quadrant multiplication
- Can be used in the voltage switching mode
- Logic inputs which meet TTL voltage level specs (1.4V logic threshold)
- Operates "STAND ALONE" (without μP) if desired

Key Specifications

■ Current settling time	1 μs
■ Resolution	8-bits
■ Linearity (guaranteed over temp.)	8, 9, or 10 bits
■ Gain Tempco	0.0002% FS/°C
■ Low power dissipation	20 mW
■ Single power supply	5 to 15 V_{DC}

Typical Application

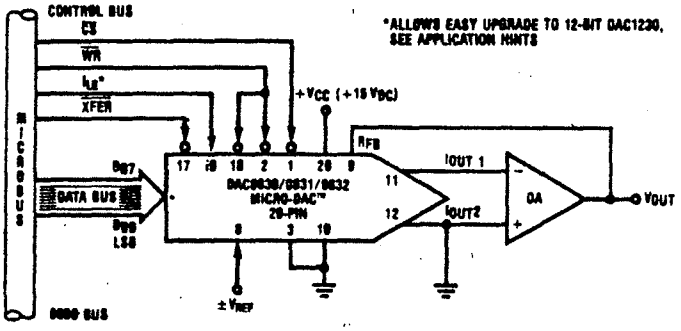

Pin Configuration Top View

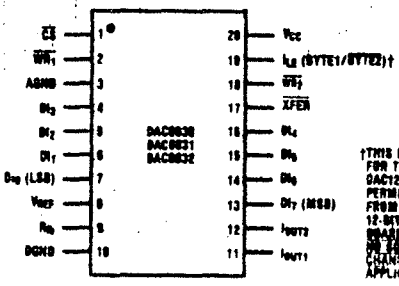

†THIS IS NECESSARY FOR THE 12-BIT DAC1230 SERIES TO PERMIT INTERCHANGING FROM AN 8-BIT TO A 12-BIT DAC WITH NO PC BOARD CHANGES AND NO SOFTWARE CHANGES. SEE APPLICATIONS SECTION.

8

FIG A-3(e)

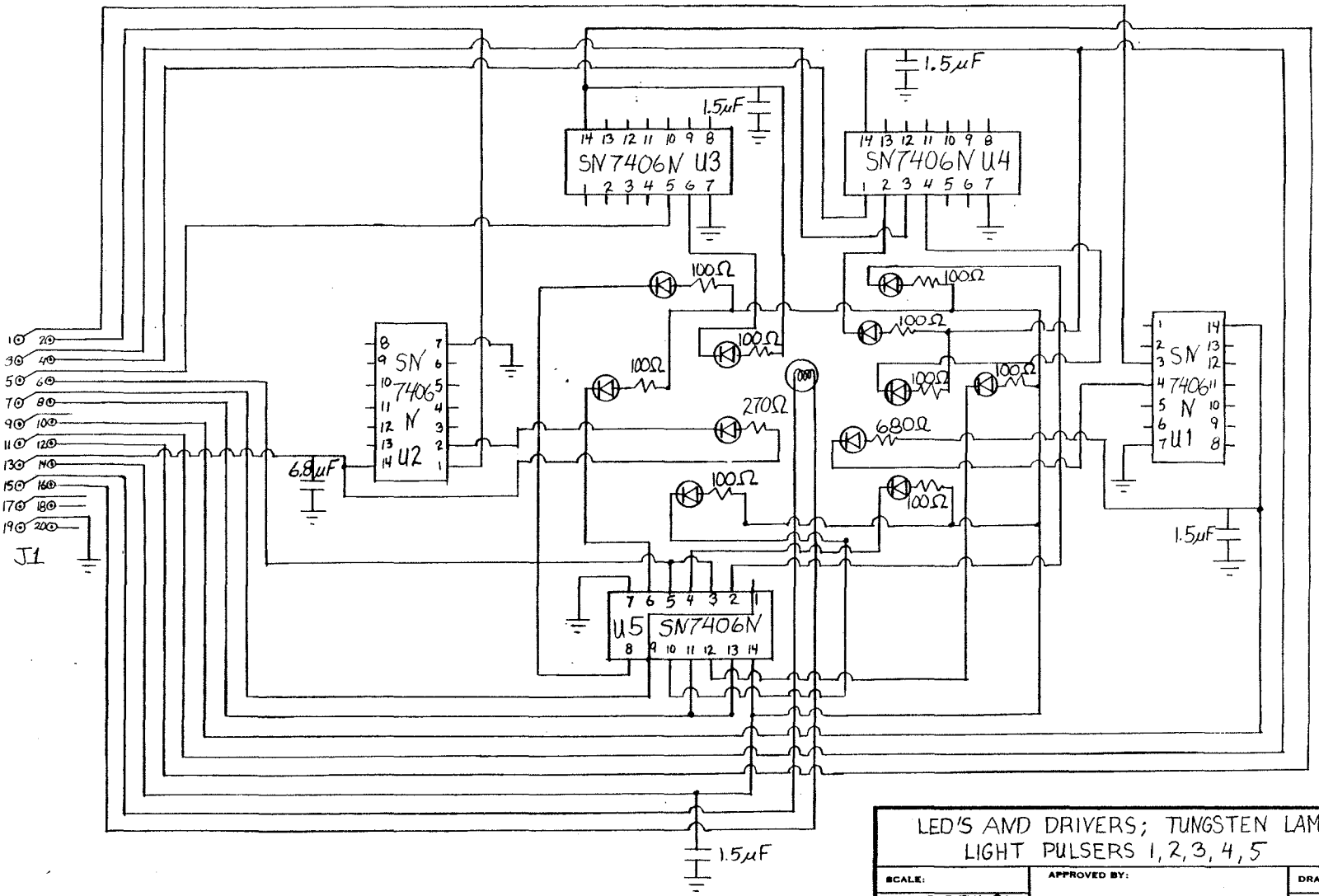

LED'S AND DRIVERS; TUNGSTEN LAMP
LIGHT PULSERS 1, 2, 3, 4, 5

SCALE:	APPROVED BY:	DRAWN BY A.S.P.
DATE: 27JUL 84		REVISED

RUTGERS - CDF - PHOTOTUBE TESTING

DRAWING NUMBER
RU-CDF-PMT-3

Fig. A-4

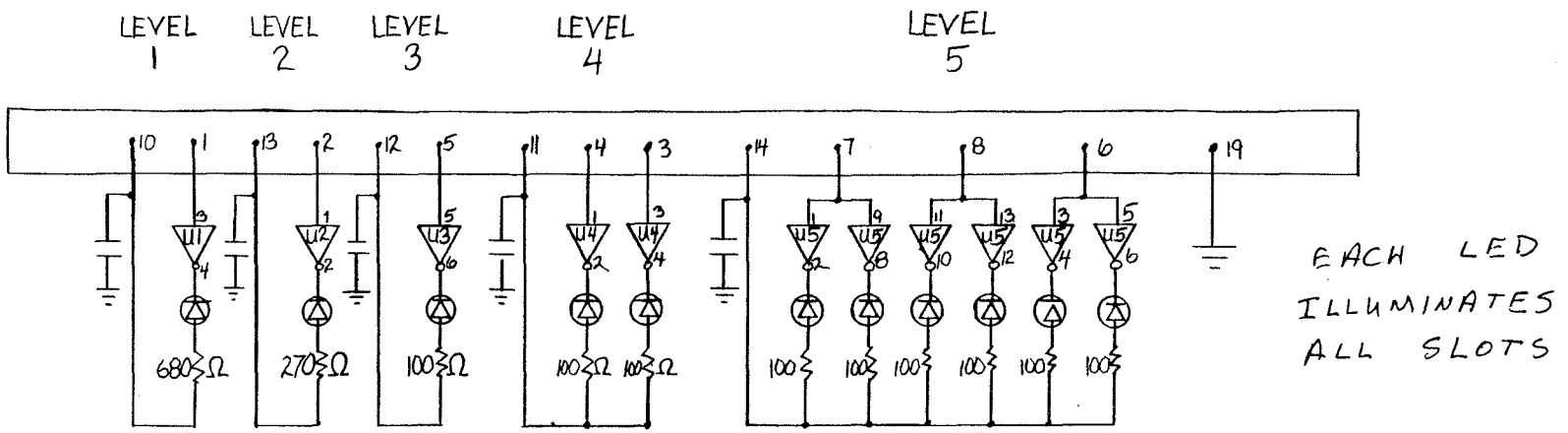

EACH LED ILLUMINATES ALL SLOTS

LEVEL 6 (SIMILAR FOR 7, 8 9)

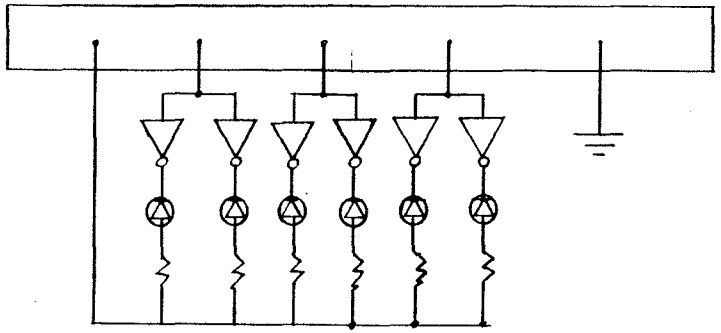

EACH LED ILLUMINATES ONLY ONE SLOT

LED'S AND DRIVERS		
30 JUL 84		ASP
RUTGERS - CDF - PHOTOTUBE TESTS		
RU-CDF-PMT-5		1

FIG. A-5

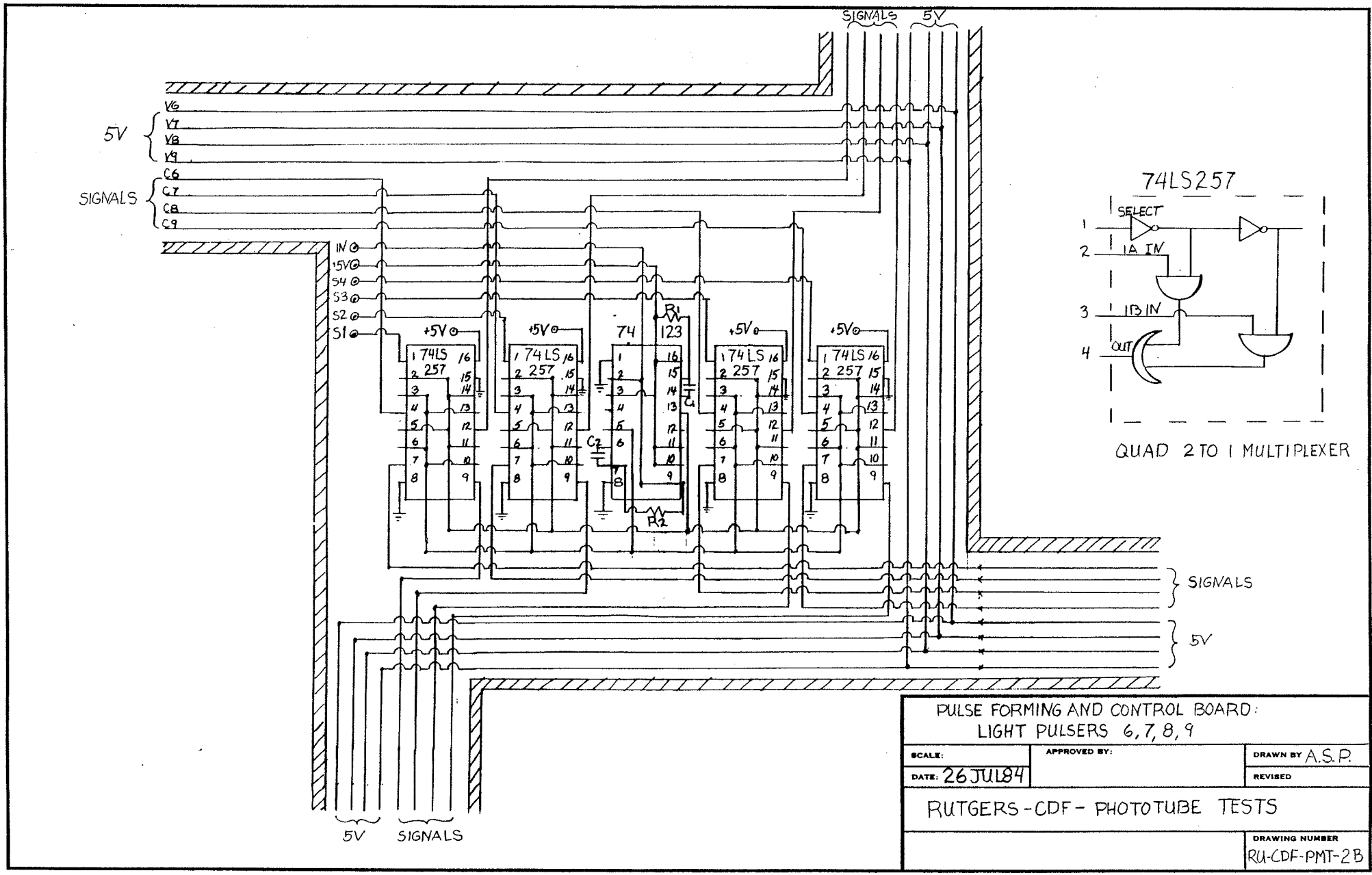

FIG. A-2

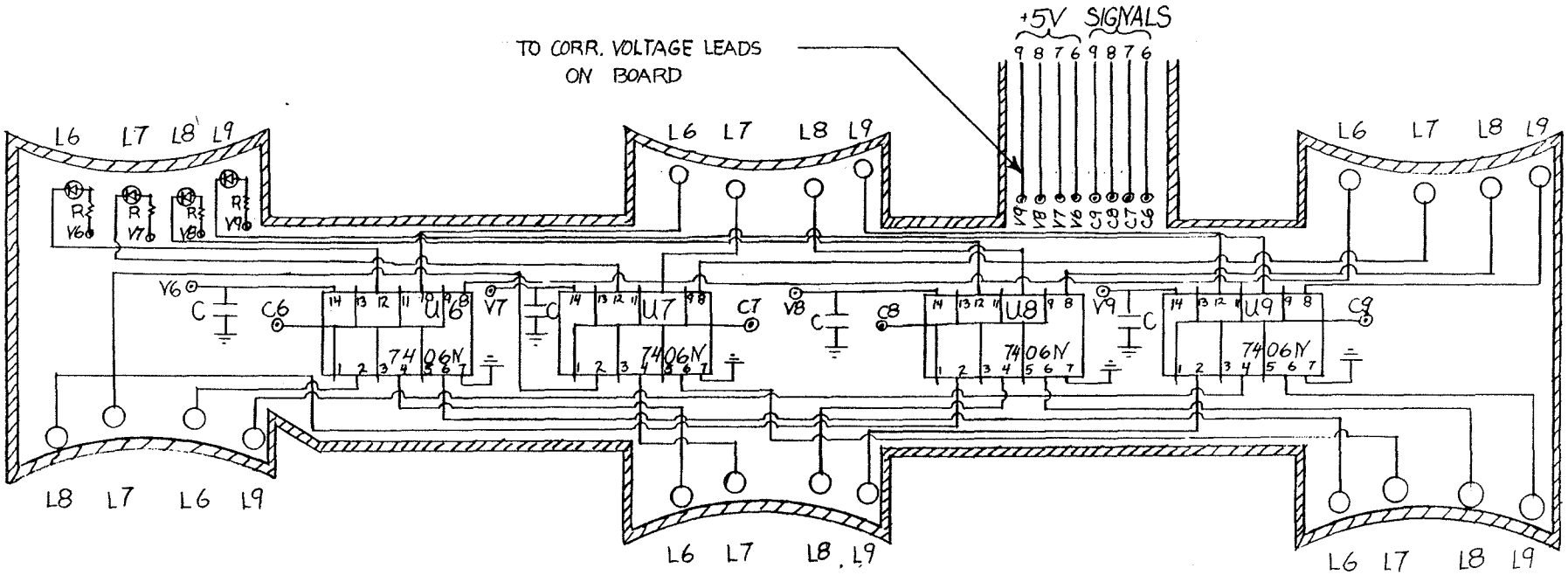

ALL RESISTORS ARE 100 Ω
ALL CAPACITORS ARE F

LED'S AND DRIVERS
LIGHT PULSERS 6, 7, 8, 9

SCALE:	APPROVED BY:	DRAWN BY A.S.P.
DATE: 25 JUL 84		REVISED

RUTGERS - CDF - PHOTOTUBE TESTS

DRAWING NUMBER
RU-CDF-PMT-4

FIG. A-7

TEMPERATURE SENSOR FOR CDF PHOTOTUBE TESTS

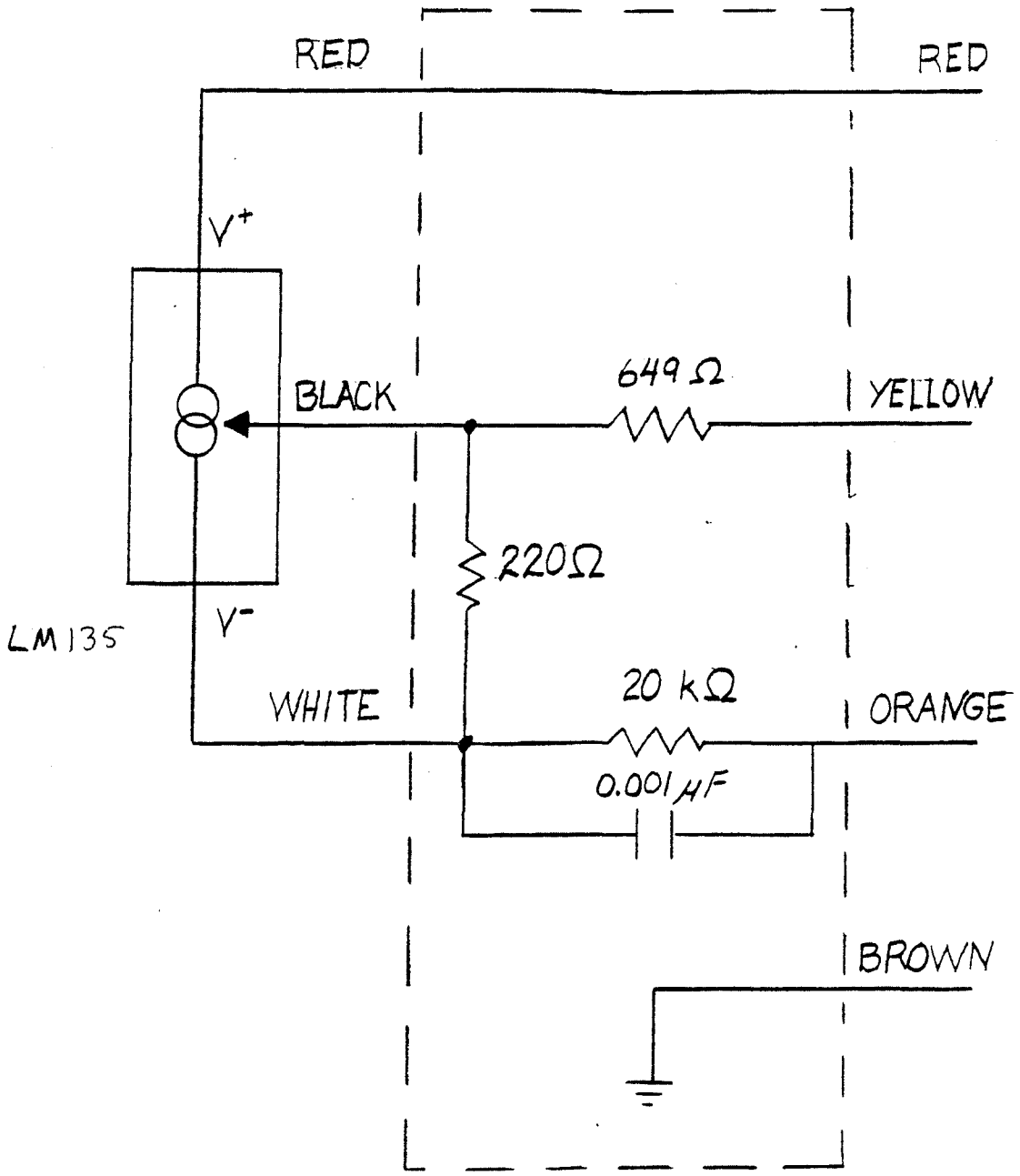

FIG. A-8(a)

National Semiconductor

LM135/LM235/LM335, LM135A/LM235A/LM335A Precision Temperature Sensors

General Description

The LM135 series are precision, easily-calibrated, integrated circuit temperature sensors. Operating as a 2-terminal zener, the LM135 has a breakdown voltage directly proportional to absolute temperature at +10 mV/°K. With less than 1Ω dynamic impedance the device operates over a current range of 400 μA to 5 mA with virtually no change in performance. When calibrated at 25°C the LM135 has typically less than 1°C error over a 100°C temperature range. Unlike other sensors the LM135 has a linear output.

Applications for the LM135 include almost any type of temperature sensing over a −55°C to +150°C temperature range. The low impedance and linear output make interfacing to readout or control circuitry especially easy.

The LM135 operates over a −55°C to +150°C temperature range while the LM235 operates over a −40°C to +125°C temperature range. The LM335 operates from −40°C to +100°C. The LM135/LM235/LM335 are available packaged in hermetic TO-46 transistor packages while the LM335 is also available in plastic TO-92 packages.

Features

- Directly calibrated in °Kelvin
- 1°C initial accuracy available
- Operates from 400 μA to 5 mA
- Less than 1Ω dynamic impedance
- Easily calibrated
- Wide operating temperature range
- 200°C overrange
- Low cost

Schematic Diagram

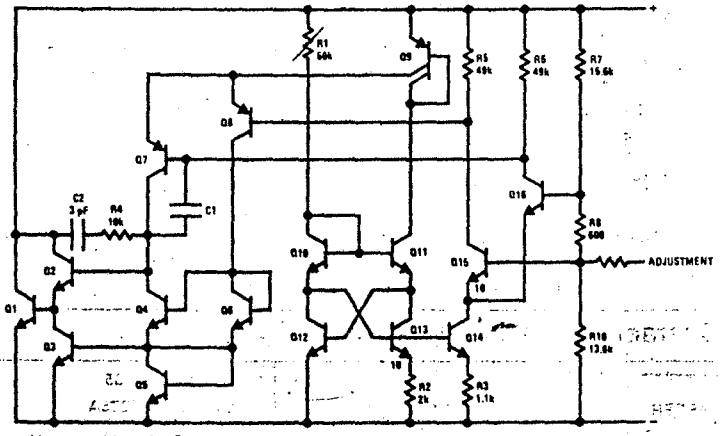

Typical Applications

Basic Temperature Sensor

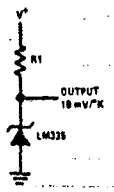

Calibrated Sensor

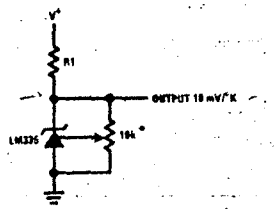

*Calibrate for 2.982V at 25°C

Wide Operating Supply

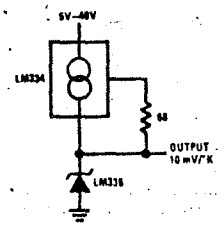

FIG. A-8(b)

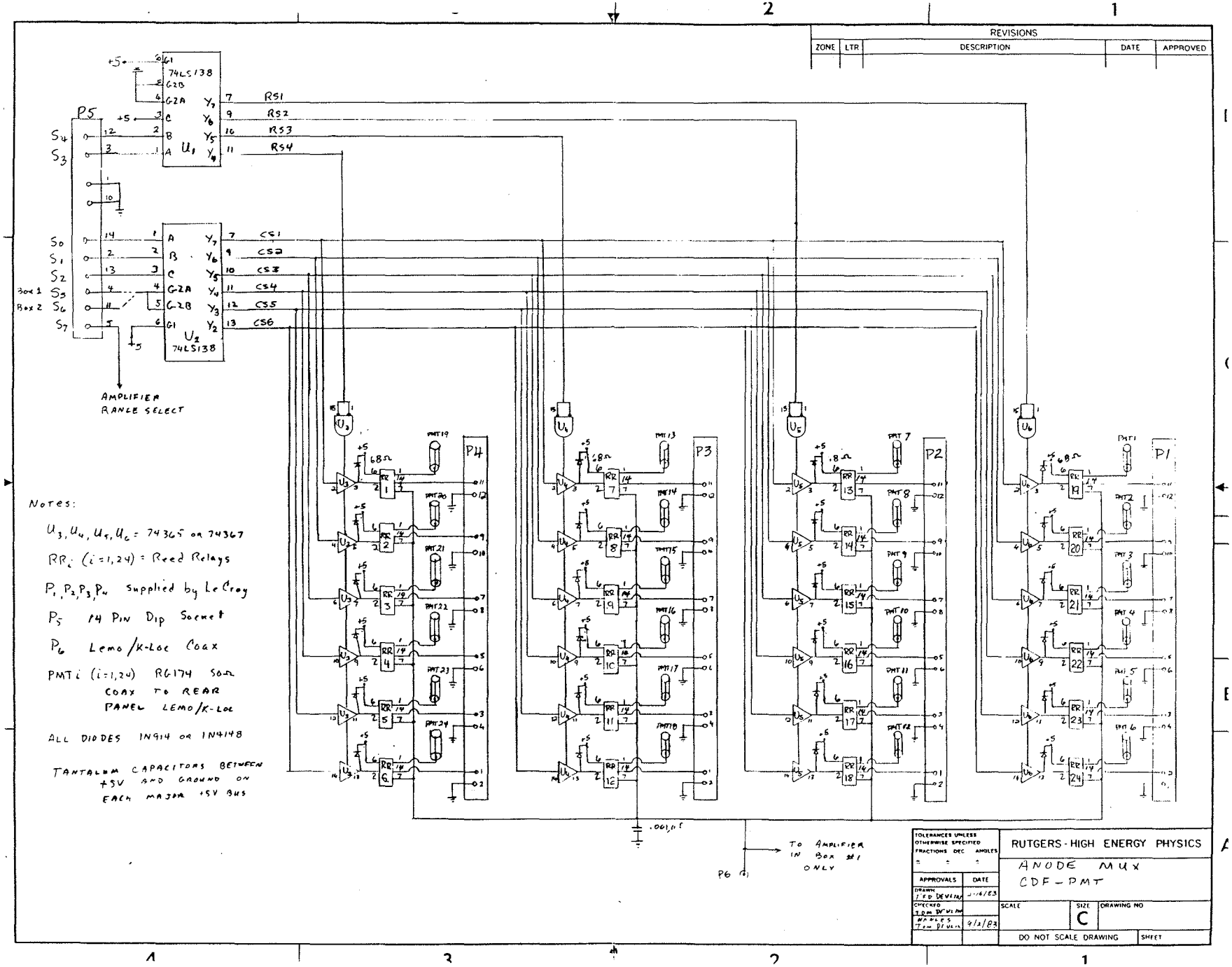
REVISIONS
ZONE | LTR | DESCRIPTION | DATE | APPROVED
74LS138
P5
RS1
RS2
RS3
RS4
CS1
CS2
CS3
CS4
CS5
CS6
AMPLIFIER RANGE SELECT
P4
P3
P2
P1
.068Ω
.001μF
TO AMPLIFIER IN BOX #1 ONLY
P6
Notes:
U3, U4, U5, U6 = 74365 or 74367
RRi (i=1,24) = Reed Relays
P1, P2, P3, P4 Supplied by LeCroy
P5 14 Pin Dip Socket
P6 Lemo/K-Loc Coax
PMTi (i=1,24) RG174 50Ω COAX TO REAR PANEL LEMO/K-LOC
ALL DIODES IN914 OR IN4148
TANTALUM CAPACITORS BETWEEN +5V AND GROUND ON EACH MAJOR +5V BUS
TOLERANCES UNLESS OTHERWISE SPECIFIED
RUTGERS - HIGH ENERGY PHYSICS
ANODE MUX
CDF - PMT
APPROVALS | DATE
SCALE
SIZE C
DRAWING NO
DO NOT SCALE DRAWING
SHEET

Fig A9 (a)

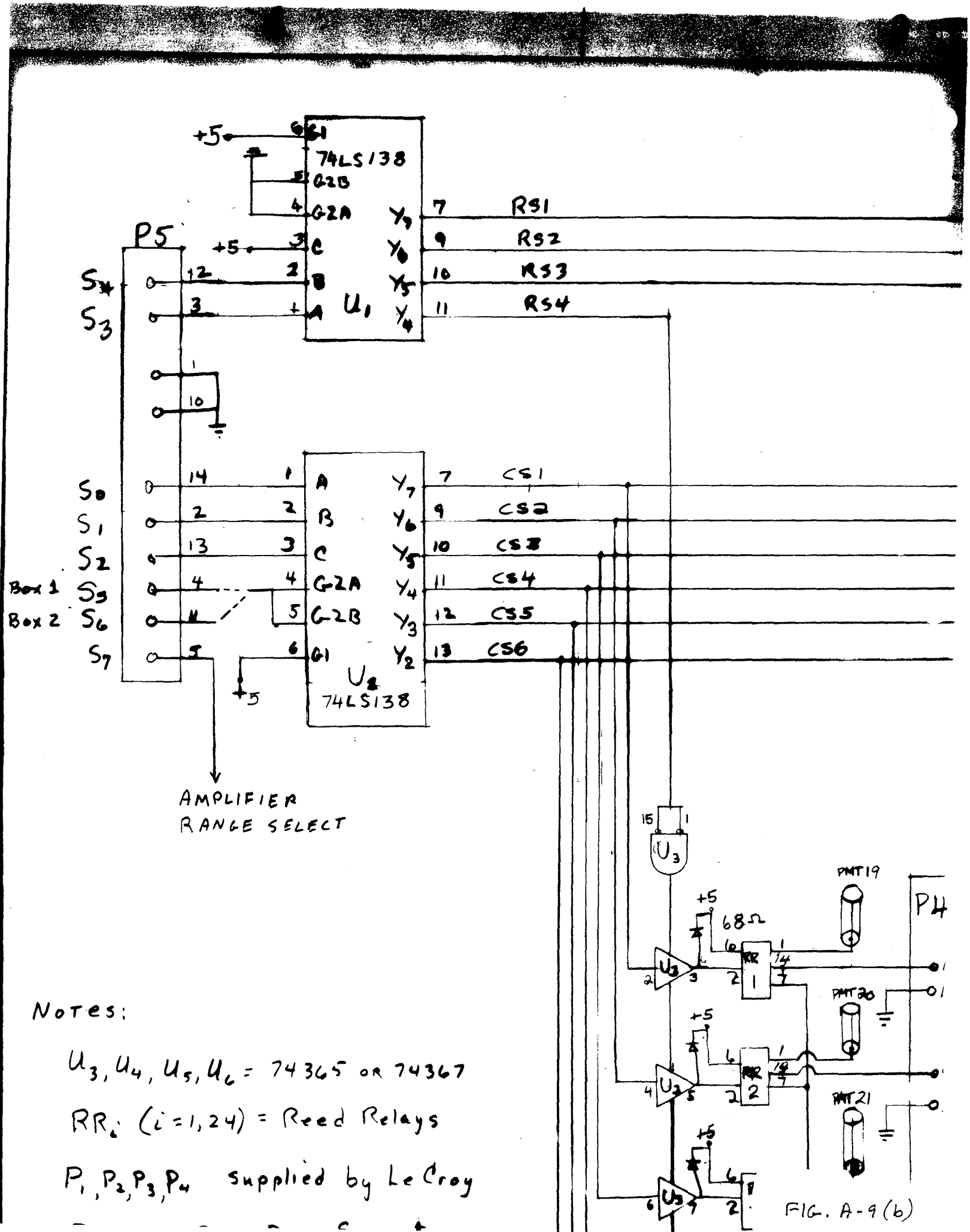

Notes:

U_3, U_4, U_5, U_6 = 74365 or 74367

RR_i $(i = 1, 24)$ = Reed Relays

P_1, P_2, P_3, P_4 supplied by LeCroy

FIG. A-9(b)

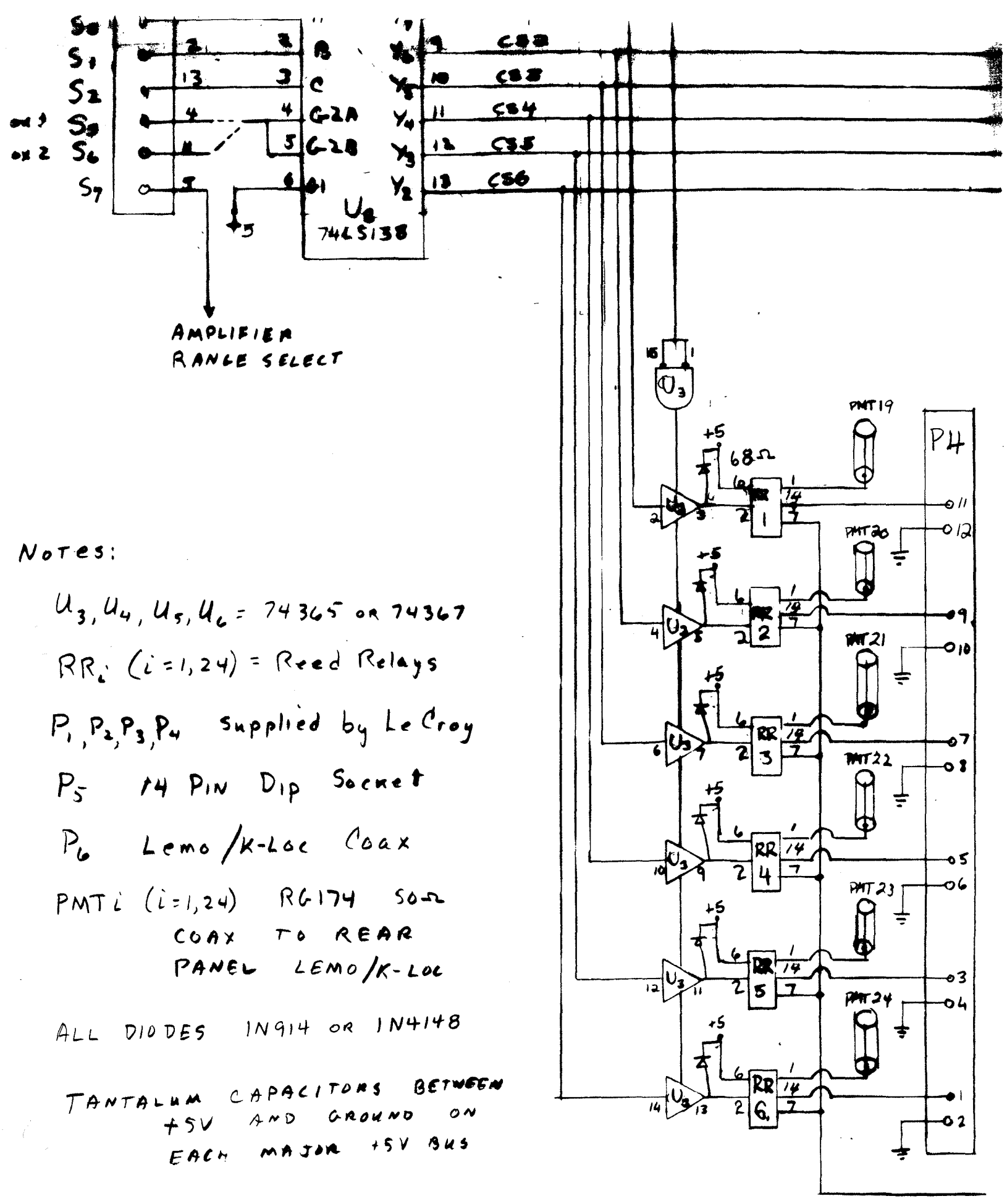

NOTES:

U_3, U_4, U_5, U_6 = 74365 or 74367

RR_i $(i = 1, 24)$ = Reed Relays

P_1, P_2, P_3, P_4 supplied by LeCroy

P_5 14 Pin Dip Socket

P_6 Lemo/K-Loc Coax

PMT i $(i = 1, 24)$ RG174 50Ω
COAX TO REAR
PANEL LEMO/K-LOC

ALL DIODES 1N914 OR 1N4148

TANTALUM CAPACITORS BETWEEN
+5V AND GROUND ON
EACH MAJOR +5V BUS

FIG. A-9(c)

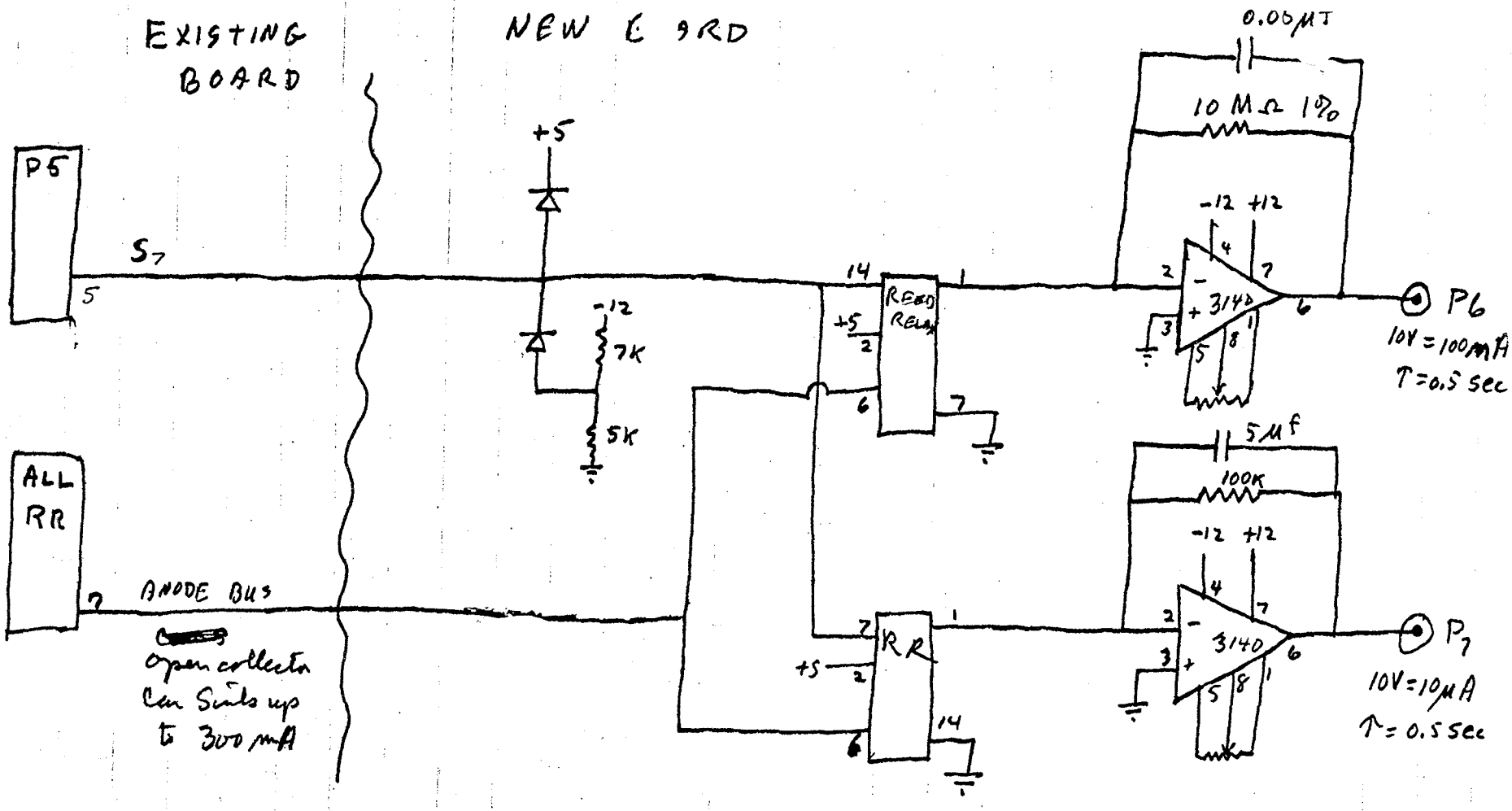

NANO-AMMETER FOR ANODE MUX

T. DEVLIN
22 MAR 83

FIG. A-10